7-12-2014

POLY(N-ISOPROPYL ACRYLAMIDE)-COATED SURFACES: INVESTIGATION OF CYTOTOXICITY WITH MAMMALIAN CELLS AND THE MECHANISM OF CELL DETACHMENT

Marta Cooperstein

Marta A Cooperstein
Candidate

Chemical and Nuclear Engineering
Department

This dissertation is approved, and it is acceptable in quality and form for publication:

Approved by the Dissertation Committee:

Heather Canavan, Chairperson

Eva Chi

Diane Lidke

Dimiter Petsev

POLY(*N*-ISOPROPYL ACRYLAMIDE)-COATED SURFACES: INVESTIGATION OF CYTOTOXICITY WITH MAMMALIAN CELLS AND THE MECHANISM OF CELL DETACHMENT

by

MARTA A. COOPERSTEIN

B.S. Chemical Engineering, University of New Mexico, 2009

DISSERTATION

Submitted in Partial Fulfillment of the
Requirements for the Degree of

Doctor of Philosophy
Engineering

The University of New Mexico
Albuquerque, New Mexico

May, 2014

ACKNOWLEDGMENTS

First and foremost, I would like to thank my advisor and Dissertation committee chair, Prof. Heather Canavan, for her tremendous support and guidance throughout my undergraduate and graduate studies. I am grateful for her patience and help while I was pregnant with each of my boys. She made it possible for me to have children and be in graduate school. I appreciate her sense of humor and honesty, and the fact that I could always be honest with her. Working in her lab was a great experience and I couldn't have asked for a better advisor. Thank you.

I would like to thank my Dissertation committee members, Prof. Eva Chi, Prof. Diane Lidke, and Prof. Dimiter Petsev for serving as my committee members and for providing the guidance to complete this work.

I also would like to thank everyone who helped me with experiments, taught me how to use laboratory equipment, or simply took their time to discuss aspects of my research with me. I would like to acknowledge Jamie Reed and Adrianne Lucero for introducing me to the lab and teaching me everything I needed to know to start my research. I wanted to thank Linnea Ista for confocal microscopy training and Laura Pawlikowski for showing me everything I needed to know about the plasma reactor. I wanted to thank Prof. Jim Freyer for helpful discussions about cytotoxicity testing and training on the Coulter counter, and Jacqueline De Lora, for teaching me about growth curves and plating efficiency. Thank you to Phanindhar Shivapooja for introducing me to atom transfer polymerization, and to Dan Graham for pNIPAM cartoons. I also would like to thank Prof. Elizabeth Dirk for her generous donation of 3T3 cells and for allowing

me to use her group's Schlenk line setup. Finally, I would like to thank Dirk lab group members, Matt Rush, Kirsten Cicotte, and Kent Coombs, for their help with the setup of my polymerization reactions and helpful discussions.

I wanted to thank all of my lab group members, past and present, for helpful discussions and assistance, and especially Colin Sillerud, Blake Bluestein, and Lyndsay Stapleton. I also wanted to acknowledge everyone who helped me acquire data for my research: Gerry Hammer at NESAC/BIO at the University of Washington (NIBIB grant EB-0020271) and Kateryna Artyushkova at UNM for XPS data acquisition, as well as Fei Li from the Chemistry Department at the University of New Mexico for size exclusion chromatography data.

I would like to acknowledge funding that made this work possible: the National Science Foundation Partnership for Research and Education in Materials (PREM, DMR-0611616), the National Science Foundation Graduate Research Fellowship Program (NSF GRFP), Center for Biomedical Engineering (CBME), 3M, and Small Grant-in-Aid for Research (RAC grant, proposal # 10-11).

Most importantly, I wanted to thank my family. I wanted to thank my parents for not being scared of letting me go. Thanks to you I am where I am right now. I was blessed with parents that were open-minded and supportive for my crazy ideas, was it going to Germany after high school instead of going to college, or moving to the United States. You have always loved me and believed in me, and for that I will be forever grateful. Finally, I would like to thank my husband, Noah. He is the reason I am graduating with a PhD in Engineering. He made me believe in myself, helped me realize

how much I love science, and gave me unending love and support throughout my studies. Thank you.

POLY(*N*-ISOPROPYL ACRYLAMIDE)-COATED SURFACES: INVESTIGATION OF CYTOTOXICITY WITH MAMMALIAN CELLS AND THE MECHANISM OF CELL DETACHMENT

by

Marta A. Cooperstein

B.S., Chemical Engineering, University of New Mexico, 2009
Ph.D., Chemical Engineering, University of New Mexico, 2014

ABSTRACT

With the increase in life expectancy and with growing numbers of an aging population, there is a rising need worldwide for replacement tissues and organs. One way to address this growing need is through engineered tissues, such as those generated from stimulus-responsive polymers. Stimulus-responsive polymers undergo a physical or chemical change when a stimulus is applied. One such material is poly(*N*-isopropyl acrylamide), (pNIPAM), which undergoes a conformation change in a physiologically relevant temperature range to release intact mammalian cell monolayers capable of being used to engineer tissues. Two factors currently limit the use of cell sheets for this purpose: 1) although the NIPAM monomer is toxic, it is unclear (and highly contested) whether its polymerized form is toxic as well; 2) there is little understanding of the mechanism of how cells detach from pNIPAM, and whether the (possibly) cytotoxic polymer would be transferred to implanted engineered tissues.

In this work, we present an investigation of the cytotoxicity of pNIPAM-grafted surfaces, as well as an investigation of the mechanism of cell detachment from pNIPAM. The cytotoxicity of substrates prepared using several polymerization and deposition techniques are evaluated using appropriate cytotoxicity tests (MTS, Live/Dead, plating efficiency). Endothelial, epithelial, smooth muscle, and fibroblast cells were used for the cytotoxicity testing. The mechanism of cell detachment from pNIPAM was investigated using endothelial cells and surfaces synthesized via surface-initiated atom transfer radical polymerization. The detachment experiments were performed at various temperatures with and without an ATP inhibitor. In addition, fluorescent pNIPAM surfaces were generated to determine if any pNIPAM is removed with the detached cells.

We find that cell sheets obtained by detachment from pNIPAM films will be suitable for use in engineered tissues, provided that the pNIPAM films that the cells were obtained from are themselves robust (i.e., grafted, covalently linked, or similar). We also find that the cell detachment from pNIPAM is mostly a passive process, and that no pNIPAM is removed from the surfaces during the detachment. Our results therefore provide an important step to clearing the hurdles presently obstructing the generation of engineering tissues from pNIPAM films.

TABLE OF CONTENTS

LIST OF FIGURES

LIST OF TABLES

CHAPTER 1: INTRODUCTION

1.1 Tissue engineering

With the increase in life expectancy and with growing numbers of an aging population, there is a rising need worldwide for replacement tissues and organs. According to the American Heart Association, coronary heart disease caused ~ 1 of every 6 deaths in the United States in 2010. Roughly every 34 seconds one American has a coronary event, and the number of cardiovascular operations increased by 28% from 2000 to 2010 in the United States.[1] Also, just in the US, close to 500,000 burn victims receive medical treatment annually. Out of those victims, 30% exceed 10% of total body area burned, and 10% have above 30% of their total body area burned. The areas of the body frequently affected are face, hands, and feet.[2]

Burn victims need new skin to cover and heal large surface areas of their bodies. Frequently, the only rescue for cardiac patients is a bypass graft. Figure 1.1 shows a schematic of a bypass graft. Here, an occlusion is bypassed by grafting a new vessel, above and below the occluded vessel. Ideally, one would use a blood vessel or a skin patch (in case of burn victims) from a different part of the patient's body. However, there is a limited supply of such autologous material, and synthetic materials, while more readily available, can cause immunoresponse and transplant rejection. There is a need for alternative techniques to donor tissue and organ transplantation.[3]

Figure 1.1 Schematic of a bypass graft. Image adapted from http://www.drparaskevas.com/img/4-bypass-graft.png.

One solution to this problem is tissue engineering. There are several approaches to tissue engineering: nonbiodegradable synthetic grafts, collagen gels, biodegradable synthetic polymer scaffolds, acelullar techniques, and cell sheet engineering.[3] Nonbiodegradable synthetic grafts have been successfully employed as a replacement for large diameter vessels. However, they cannot be used in a place of small diameter vessels, due to their thrombogenic properties. To avert this problem, synthetic grafts seeded with endothelial cells, which have anti-thrombogenic properties, have been developed. However, a synthetic graft cannot be remodeled by the cells when required by the environment, which provides a serious limitation.[3] A more adjustable model is provided by collagen gels. While this type of scaffold offers environment that allows for cell growth, proliferation and adaptation, it is not strong enough to withstand regular physiological pressure.[4] Scaffolds that are synthesized from biodegradable polymers

such as polyglycolic acid provide more support for the cells. They do not pose the same problems as synthetic scaffolds, since they are biodegradable. However, it is extremely difficult to determine appropriate culture conditions for generation of a construct with required physiological and morphological characteristics using this method.[5, 6] A different approach to repairing injured tissues and organs is an acelullar approach. Here, a noncellular construct (for example small intestinal submucosa) is implanted into the injured area, where it attracts cells from the native tissue.[7] However, the way cells migrate to such a material as well as how to manipulate such a material to attract the cells is still poorly understood.[3]

Finally, there is "cell sheet engineering," a term coined by Okano et al.[8, 9] Here, cells harvested from the patient can be grown on a suitable substrate to form cell sheets, which then can be layered to form a tissue, which then are transplanted into the patients. There are several advantages to this technique. This method eliminates the need of finding a donor and taking immunosuppressing drugs to prevent rejection of the transplant. It also allows engineering of a needed amount of tissue. This is especially important for burn victims with large affected body surface areas, or patients who do not have any organs fit for transplantation (e.g. blood vessels). However, to be able to engineer such tissues, one needs a suitable substrate. For example, the substrate should allow for culture of various types of cells into cell sheets. It should not alter cell function or kill the cells (i.e. biocompatible substrate), and it should provide for non-invasive harvest of these cell sheets. To fabricate such a substrate, scientists turned to stimuli-responsive polymers, with special attention for one of them: thermoresponsive poly(*N*-isopropyl acrylamide).

1.2 Stimuli-responsive polymers and poly(*N*-isopropyl acrylamide)

Stimuli-responsive polymers are polymers that undergo a physical or chemical change when a stimulus is applied. There are three types of stimuli: physical, chemical, and biological.[10] Physical stimuli (e.g. light, temperature or magnetic field) modify chain dynamics (e.g. the energy level of the polymer/solvent system). Chemical stimuli (pH, ionic strength) modify molecular interactions between polymer chains or between polymer and solvent molecules. Finally, biological stimuli include enzymes and receptors.[10] There have been several reviews of stimuli-responsive polymers, and their applications include biotechnology (tissue engineering), medicine (e.g. drug delivery systems), and generation of smart textiles.[10-15] Table 1.1 lists common stimuli and their corresponding stimuli-responsive polymers.

Table 1.1 Examples of common stimuli and stimuli-responsive polymers.

TYPE OF STIMULUS	STIMULI-RESPONSIVE POLYMER	USE
Physical (Temperature)	Poly(*N*-isopropyl acrylamide), poly(*N*,*N*-diethylacrylamide), poly(*N*-vinylcaprolactam), poly(2-hydroxyethylvinylether)[11, 16]	Tissue engineering, drug release, tissue adhesion prevention
Physical (Electric potential)	Sulphonated-polystyrene[10], polythiophene[15]	Drug release, cancer chemotherapy
Chemical (pH)	Chitosan, poly(acrylic acid), poly(methacrylic acid), copolymers of acrylic acid and 2-vinylpyridine[10, 11, 16]	Drug release and controlled delivery
Biological (Glucose)	Copolymerized 2-hydroxyethyl methacrylate and *N*,*N*-dimethyl aminoethyl methacrylate immobilized with glucose oxidase[11]	Self-regulated insulin delivery

There is a special interest in thermoresponsive polymers in the field of tissue engineering.[13, 16, 17] Thermoresponsive polymers can be divided into two groups: those that exhibit upper critical solution temperature (UCST) transitions and those with lower critical solution temperature (LCST) transitions. Upper critical solution temperature polymers become soluble in their solvent when the system is above a specific temperature (the UCST). Poly(uracilacrylate) and poly(*N*-acryloylglycinamide) are examples of such polymers.[18] Lower critical solution temperature polymers become soluble in their solvent at temperatures below a specific temperature (the LCST). Among the most common LCST polymers are poly(*N*-vinyl caprolactam), poly(vinyl methyl ether), and poly(*N*-isopropyl acrylamide).[14, 16] Poly(*N*-isopropyl acrylamide) (pNIPAM), the structure of which is shown in Figure 1.2, is the focus of this work.

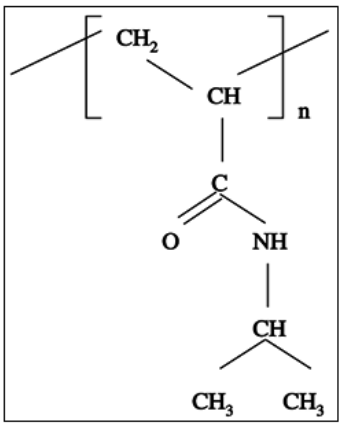

Figure 1.2 Chemical structure of poly(*N*-isopropyl acrylamide).

1.2.1 Properties of poly(*N*-isopropyl acrylamide)

Poly(*N*-isopropyl acrylamide) (pNIPAM) is a thermoresponsive polymer widely used in bioengineering applications. Although there are many polymers that respond to a stimulus such as temperature, pH, light, or magnetic field,[11] pNIPAM is of special

interest due to the phase change it undergoes in a physiologically relevant temperature range, that leads to cell/protein release. PNIPAM has an LCST of ~32^{o}C. Above its LCST, pNIPAM is relatively hydrophobic. When grafted to a surface, it takes a globular, packed conformation. Below the LCST, the polymer is hydrated, and its chains become more extended (see Figure 1.3).[19] Mammalian cells can be easily cultured on pNIPAM at 38^{o}C (body temperature, and therefore the temperature at which cells are cultured in an incubator). When the temperature is lowered to below pNIPAM's LCST, the polymer's chains extend and cells detach in intact sheets (see Figure 1.3 A and B).[20, 21]

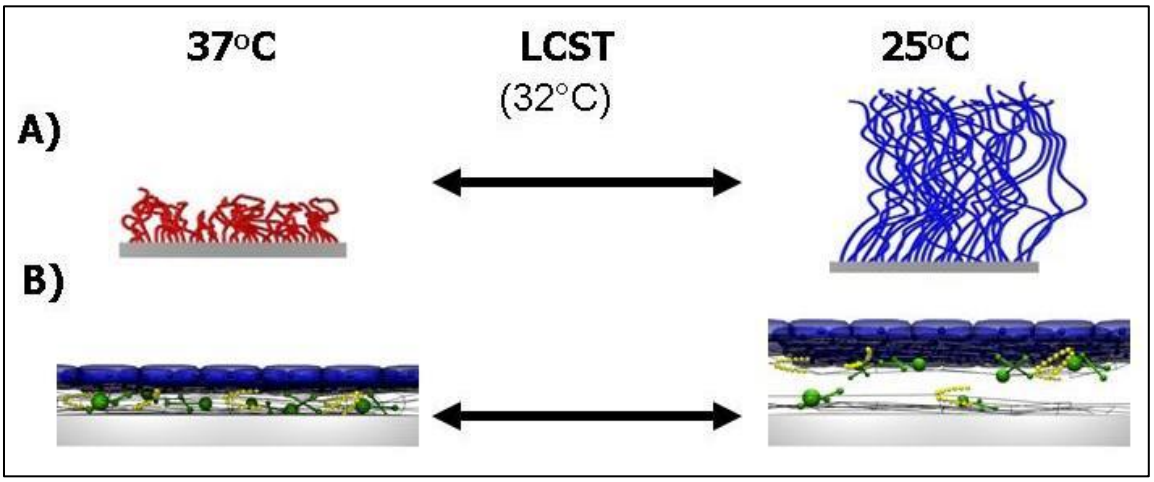

Figure 1.3 Schematic of pNIPAM tethered on a substrate above its LCST (left), and below its LCST (right).

Since cell sheet detachment using pNIPAM preserves the cell sheet and its extracellular matrix, [22, 23] this detachment method may be preferred to enzymatic digestion or mechanical scraping. A detached cell sheet can be transferred to another surface and cultured for further use.[9, 17, 24-27] The non-destructive release of cells opens up a wide range of applications, including the use of pNIPAM for tissue engineering, for controlling bioadhesion and bioadsorption, and for manipulation of

microorganisms. These uses are summarized in our Feature Article in *Langmuir* and in Chapter 3 of this dissertation.[17]

1.2.2 Applications of pNIPAM

Due to its conformation change around the physiological temperature, pNIPAM has been used in various areas of research. The most popular use of pNIPAM is for generation of thermoresponsive surfaces and for cell culture.[13, 17] Chapter 3 of this dissertation reviews the many ways pNIPAM has been used for research with mammalian cells. Among these methods are tissue engineering, manipulation of microorganisms, and biofouling.[17]

However, pNIPAM is of interest not only for use with mammalian cells. It has also been used for research with textiles,[14, 28] drug delivery,[29-31] and protein-ligand interactions.[32] The goal of using pNIPAM in textiles is to make fabrics that can be used as an interface between the environment and the body. Such fabrics could modulate thermal and molecular exchange and could also be used to release various products to the body, such as cosmetics, nutrients, or medications.[14, 28] PNIPAM has been successfully grafted onto fabrics such as non-woven cotton cellulose or polypropylene, resulting in fabrics that have acquired pNIPAM's thermoresponsive behavior.[14] These fabrics experience radical permeation change below and above the LCST of pNIPAM, and have shown to acquire temperature-sensitive vapor permeability and water absorbance.[14, 28]

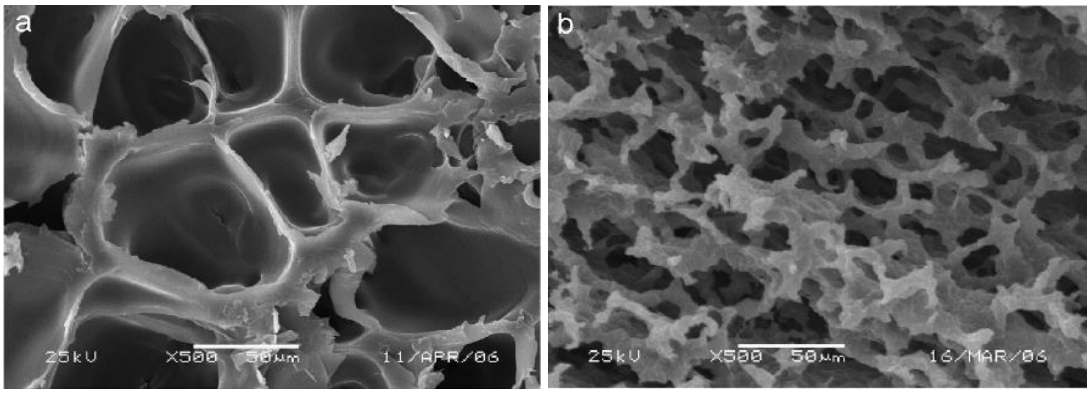

Figure 1.4 A PNIPAM hydrogel swells below its LCST (a), and shrinks above its LCST (b). Image adapted from Ref. [33]

There is also great deal of research into using pNIPAM for drug delivery. The most common form of pNIPAM used for this application is a hydrogel.[30, 31] However, there are also reports of pNIPAM micelles.[29] Whatever the form of delivery, the methods used to release a medication are similar, and are based around pNIPAM's response to a change of the temperature of the environment. Figure 1.4 shows a structure of a pNIPAM hydrogel below (a) and above (b) of pNIPAM's LCST. When loaded with a drug, the pNIPAM delivery vehicle will shrink when the temperature is raised to above its LCST (as seen in Figure 1.4 b), which will result in release of the drug. Copolymerization of pNIPAM with another stimuli-responsive polymer is often employed to produce sensitivity to an additional stimulus, such as pH, which can be useful when introducing drug delivery systems into different parts of the body.[29-31]

PNIPAM has also been used for applications such as affinity separations or protein – ligand interactions.[32] When conjugated with streptavidin, pNIPAM allowed normal binding of biotin to streptavidin below the polymer's LCST, however, when the temperature was raised, the binding site was blocked by the collapsed polymer, inhibiting

the binding. Such control of binding could be used in applications such as the control of enzyme reaction rates or biosensor activity.[32]

1.3 Cell sheet engineering using pNIPAM

Thermoresponsive polymers have been widely used as a substrate for engineering cell sheets. Their unique properties allow the cell sheets to detach from the surface while retaining most of their extracellular matrix proteins.[34-40] Over the years, many different types of cells and substrates have been investigated, as have the methods of grafting pNIPAM to surfaces. Among the different cell types to be detached as cell sheets are bovine aortic endothelial cells (BAECs), Madin-Darby canine kidney (MDCK) cells, pluripotent C2C12 cells, cardiac myocytes, fibroblasts, urothelial cells, epithelial cells, keratinocytes, hepatocytes, chondrocytes, preosteoblastic cell lines, as well as mesenchymal stem cells.[16, 41-44] A review of methods used to create pNIPAM substrates for bioengineering can be found in the article by da Silva et al.[13]

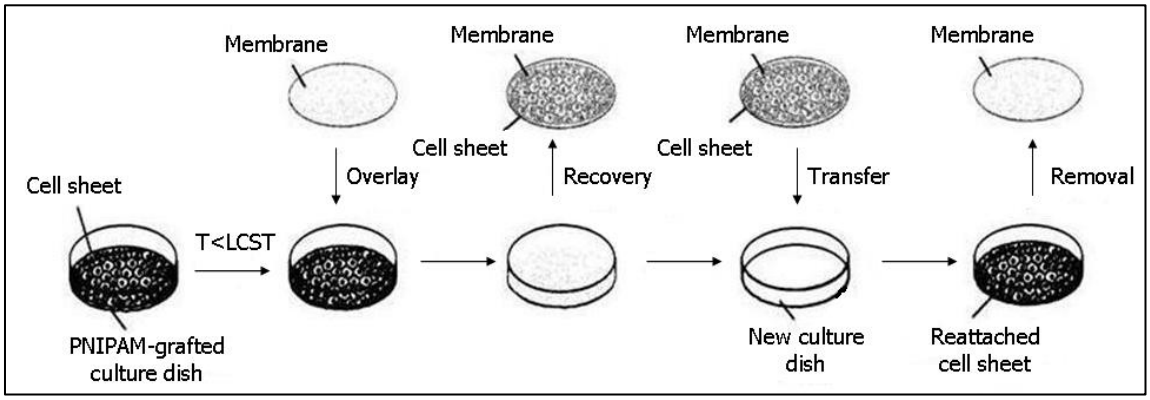

Figure 1.5 Schematic of cell sheet engineering using a pNIPAM-grafted dish. Image adapted from Ref.[40].

Figure 1.5 shows a method of removing cell sheets from thermoresponsive surfaces. This method has been used with some modifications by most groups using

thermoresponsive dishes for cell detachment. First, a tissue culture dish (i.e., tissue culture polystyrene (TCPS), or a glass slide) is grafted with pNIPAM. Cells are seeded and cultured on the pNIPAM-grafted dish at 37^{o}C until they reach confluence. When the cells form a confluent cell monolayer, they are ready for detachment. The temperature of the culture is decreased, usually by changing the medium that the cells were growing in with a medium below the LCST of pNIPAM, and incubating the cells at that temperature. Most studies report incubating the cells at room temperature (~20^{o}C); however, some researchers performed cell detachment at 10^{o}C or even at 4^{o}C.[27, 45, 46] In the next step, a membrane, such as poly(vinylidene difluoride) (PVDF), chitin, or gelatin is overlaid over the confluent cell sheet in the dish (i.e., becomes a superstrate). The membrane is used to prevent cell sheets from shrinking and folding after detachment. The membrane attaches to the apical surface of the cells. Tweezers are used to remove the membrane with the cell sheet attached to it from the pNIPAM-grafted dish. The detached cell sheet can then be transferred to another dish. Upon adding medium to the new dish, the membrane detaches, leaving an intact cell sheet. The detachment can also be achieved without using a membrane. However, the detached cell sheets may shrink and/or fold, and the detachment process will require more time to allow the cell sheets to detach from the surface without any mechanical help.

Figure 1.6 demonstrates the appearance of a cell sheet after the detachment from a thermoresponsive dish without the use of a membrane. Image A shows an urothelial cell sheet before the detachment. Image B shows the same cell sheet after the detachment. An unsupported detached cell sheet does not remain flat: it is wrinkled and slightly folded.

Using a membrane superstrate during detachment helps maintain its orientation and prevents wrinkling.

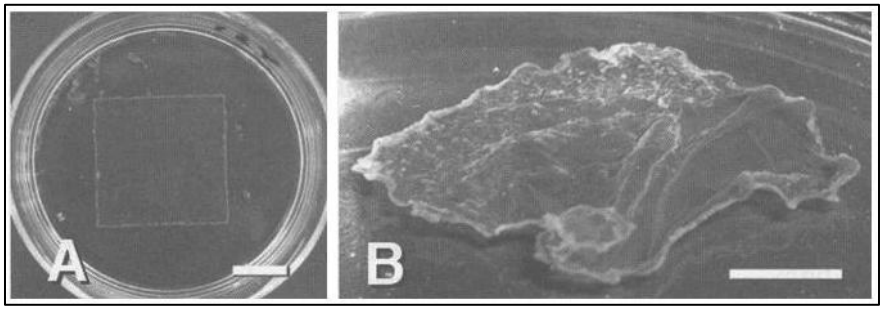

Figure 1.6 Urothelial cell sheet: A) Cell sheet cultured at 37^{o}C on a pNIPAM-grafted tissue culture dish; B) Cell sheet after detachment by lowering the temperature to 20^{o}C. Bars are 1 cm. Image adapted from Ref. [47].

Several different tissue-resembling constructs have been created in vitro using some variation of the above described method, e.g., using myoblasts, chondrocytes, or corneal sheets.[26, 48-52] These constructs were then transplanted into living organisms. They successfully adhered to and incorporated into the native tissue. A more detailed description of these experimentations follows in Chapter 3.

1.4 Cytotoxicity of pNIPAM

The ability to reversibly adhere cells and biomolecules has made pNIPAM one of the most popular stimulus-responsive polymers for research.[11, 12] There is currently a great deal of research regarding the development of engineered tissues or devices using pNIPAM.[8, 9, 15, 17, 53] Many of these devices will ultimately be used on humans. However, there has been relatively little conclusive research regarding the extent of its cytotoxicity or biocompatibility.[54-60]

The assessment of the relative biocompatibility and cytotoxicity of surfaces coated with pNIPAM is a crucial step in the development of devices based on the technology. The Internal Organization of Standardization (ISO) requires extensive testing of medical devices, with in vitro cytotoxicity being one of the required assessments.[61] It has previously been demonstrated that the NIPAM monomer is toxic.[62] There are conflicting opinions, however, as to whether the polymerized form of NIPAM (pNIPAM) is toxic.

One reason for this conflict is because there are very few publications (<15 studies),[54-60, 63-68] that explore the cytotoxicity of pNIPAM. In addition, it should be noted that none of the studies are comprehensive. Instead, they focus on isolated cell lines (e.g., only fibroblasts,[59] smooth muscle cells,[69] or endothelial cells[60]), and employ different methods of cytotoxicity testing (e.g., morphologic observations,[56] concentration gradients,[54] or direct contact test[55]). While some of the studies examine pNIPAM without any additives, others concern copolymers of pNIPAM,[69] or other forms such as hydrogels[55] or nanoparticles[57] that are composed not only of pNIPAM but also of other compounds. These copolymers are known to affect NIPAM's properties such as LCST;[70] therefore it is likely that their inclusion would also contribute to the cytotoxicity, or even be the sole source of cytotoxicity of the composite product. In total, only seven of these studies investigate the cytotoxicity of pure pNIPAM unaltered with addition of copolymers.[54-60] Furthermore, of these studies, not one investigated more than a single polymerization technique, although various polymerization and deposition techniques are used to generate pNIPAM surfaces for cell sheet engineering. Different polymerizing techniques and deposition methods result in

surfaces with varying topographies, different chain lengths of the polymer attached to the surface, etc. The technique most commonly used in these cytotoxicity studies was free radical polymerization. In addition, these studies examined different forms of pNIPAM, such as pNIPAM hydrogels,[55] pNIPAM nanoparticles,[56, 57] or pNIPAM in solution.[54, 58-60] Table 1.2 summarizes these seven studies.

Table 1.2: Summary of previous studies on the cytotoxicity of pNIPAM.[54-60]

	VIHOLA ET AL.[54]	**PANAYIOTOU AND FREITAG [55]**	**WADAJKAR ET AL. [56]**	**NAHA ET AL. [57]**	**XU ET AL. [58]**	**MORTISEN ET AL. [59]**	**LI ET AL. [60]**
Formulation tested	NIPAM, pNIPAM in solution	pNIPAM hydrogels	NIPAM, pNIPAM nanoparticles	pNIPAM nanoparticles	pNIPAM in solution	pNIPAM and its degradation products in solution	pNIPAM in solution
Polymerization method	Free radical polymerization	Free radical polymerization	Free radical polymerization	Free radical polymerization	Commercial pNIPAM	Free radical polymerization	?
Cells used	Human carcinoma cells	Jurkat cells (human T-cell leukemia cells)	Human micro-vascular endothelial cells (EC), 3T3 fibroblasts, human aortic smooth muscle cells (SMC)	Keratinocytes, primary adenocarcinoma colon cells	Human embryonic kidney cells	hTERT-BJ1 fibroblasts	Human vein endothelial cells
Temperature	Room and body T	Body T	Body T	Body T	Body T	Body T	Body T
Time exposure	3h, 12h	6h	6, 24, 48, 96h	24, 48, 72, 96h	24h	24, 48h	48h
Concentration gradient	Yes	No	Yes	Yes	Yes	Yes	Yes
Extracts	No	No	No	No	No	No	No
Direct contact	No	0.5cm^3 hydrogel	No	No	No	No	No
Morphology observations	No	Yes	Yes	No	No	No	No
Cytotoxicity assays used	MTT, LDH	Trypan blue	MTS	Alamar Blue uptake, Alkaline Comet	MTT	Alamar Blue	MTT
Results	- lower viability at lower pNIPAM concentrations - higher viability at room T than at body T after 3h - decreased viability at 12h at room and body T	- no significant decrease in viability - cells grown with hydrogels were less numerous with changed morphology	- different effect on viability depending on cell type -decrease in survival for ECs at 5mg/mL and above	- no significant cytotoxicity found	- lower viability at higher pNIPAM concentrations	- lower viability at lower pNIPAM concentrations	- lower viability at lower pNIPAM concentrations

To achieve cell detachment from pNIPAM, or to obtain another result, such as swelling or deswelling of a pNIPAM hydrogel, the temperature of the system must be changed. It is possible that the cytotoxicity of the polymer varies at these two temperatures. It is thus critical to investigate the cytotoxicity of pNIPAM not only at body temperature, but also at a temperature below pNIPAM's LCST. Only one of the seven studies investigated the cytotoxicity of pNIPAM above and below its LCST.[54] This study showed that there is a difference in cellular viability below and above the LCST of the polymer.

The remaining six studies came to contradictory conclusions including no significant cytotoxicity found,[57] different cell viability depending on cell type,[56] lower cell viability in the presence of lower concentrations of pNIPAM,[54, 59, 60] and lower cell viability in the presence of higher pNIPAM concentrations.[58] None of these studies investigated the effects of growing cells directly on pNIPAM-coated surfaces or the effect of pNIPAM fragments that may leach out of the surface into the cell culture medium.

There is no consensus between the existing studies on cytotoxicity of pNIPAM (see Table 1.2). The results of these previous studies are contradictive and inconclusive. Therefore, a comprehensive study of pNIPAM cytotoxicity is necessary. Such a study must take into account the various conditions under which cells are cultured with pNIPAM (such as temperature above and below LCST of pNIPAM). It must also examine more than one polymerization and deposition technique (e.g., free radical polymerization and plasma polymerization). It is also imperative to test pNIPAM's

cytotoxicity with a number of relevant cell types to rule out cell type dependent cytotoxicity.

1.5 Mechanism of cell detachment from pNIPAM

In addition to its influence on future engineered tissues, a comprehensive cytotoxicity study could also yield important information for the study of the mechanism of cellular detachment from pNIPAM films. Cells will not attach to a cytotoxic surface as readily as they attach to a non-cytotoxic surface. Conversely, cells will detach from cytotoxic surfaces more easily than from non-cytotoxic surfaces.[71]

The mechanism of cell detachment is the least understood aspect of cell sheet engineering using temperature-responsive surfaces. It is also the least studied one. There have only been a few studies on the mechanism of cell detachment from pNIPAM. Out of over 200 papers reviewed prior to writing our manuscript on pNIPAM and its applications,[17] we found that ~ 5% of publications discussed the mechanism.

The most extensive study of the mechanism of cell detachment was performed by Okano et al.[72-74] In this work, a two-step process was proposed. The first proposed step is a passive phase, where the cell detachment is induced by the hydration of the substrate's chains caused by the temperature drop. The second proposed step is an active phase, where cells themselves undergo shape changes (cell rounding, as shown in Figure 1.7 B in the third image) due to metabolic processes to achieve detachment. Figure 1.7 shows rat hepatocytes detaching from a pNIPAM-grafted surface. The first panel in part A shows single cells attached to the surface. The cells are flat and spread, which is their normal morphology. In the second panel, the cells' morphology is less spread, and rounder. The detachment continues to the fourth panel, in which the cells no longer have

a spread and flattened morphology. The cells detached from the surface, which causes them to be out of focus, appearing bright in phase-contrast microscope. The cartoons in panel B (below the microscopy images) are schematic depictions of the shape changes that cells undergo in each panel.

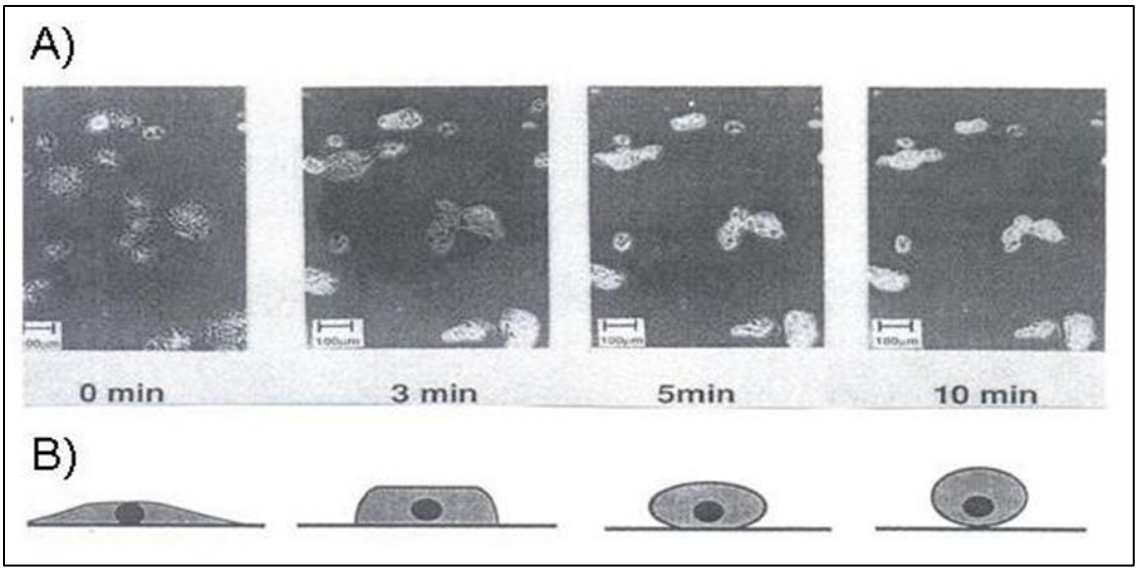

Figure 1.7 Phase contrast micrographs (bottom row) and a schematic representation (top row) of a mechanism of cell sheet detachment from pNIPAM-coated surfaces. Bars are 100 μm. Cells are hepatocytes. Image adapted from Okano et al., 1995.

The passive phase of the detachment was proposed to be induced by the temperature drop and hydration of pNIPAM chains, effecting initial detachment. This initial detachment stimulates the active phase (shape change) which the authors proposed to be coordinated by cell metabolic processes. The researchers' evidence for the role of cellular metabolism in the detachment process was supported by observing less detachment at lower temperatures (4 and 10 ^{o}C), at which suppressed cell metabolism was observed. Further evidence for the role of cellular metabolism in detachment came from the observation that less detachment was also observed when sodium azide, which

inhibits ATP generation, was added. This suggests that metabolic activity is an important factor for cell detachment from pNIPAM.[72]

Yamato et al. found that the hydration of pNIPAM chains itself failed to detach fibronectin from fibronectin-preadsorbed pNIPAM-surfaces. Based on their observations of hepatocytes' detachment from pNIPAM surfaces, they concluded that the active step is based on cellular activity. There are two types of cellular activity: chemical (degradation of matrix components by matrix metalloproteinases, and covalently crosslinking by transglutaminase), and physical (the cytoskeleton tensile forces). The researchers found that the crosslinking of fibronectin was negligible and the activity of matrix metalloproteinase was suppressed in the serum. However, when cytoskeletal dynamics were preserved, the cytoskeleton tensile forces caused cell rounding and detachment. The researchers concluded that physical, and not chemical cellular activity needs to accompany the hydration of pNIPAM chains for cells to fully detach.[73]

Another study found that inhibition of tyrosine phosphorylation suppressed cell detachment as well. Since tyrosine phosphorylation is involved in integrin-mediated signaling, it was proposed that cell detachment involves already existing proteins, and does not require formation of new proteins. The authors also found that inhibition of actin polymerization and stabilization of F-actin slowed cell detachment, which indicates that cell detachment may involve actin dynamics.[74]

The mechanism of cell detachment from pNIPAM-grafted surfaces was also investigated through observations of collagen type IV.[75] Immunofluorescence study of this protein revealed that relatively little collagen was left on the dish from the center of each cell, with more collagen left on the dish from the cells' edges. This pattern may

suggest a two-step mechanism of cell detachment. In the first step, cells actively detach from the ECM on the cell edges only. This step is followed by a complete detachment of the rest of the cell from the surface, with the ECM attached to the cells.

More recently, Chen et al. investigated the dynamics of cellular detachment from pNIPAM-coated surfaces using atomic force microscopy as well as fluorescence microscopy.[76] In their study, they compared surfaces with various polymerization times, as well as surfaces coating with a layer of collagen of varying thicknesses. They found that the initial rate of cell detachment increases with the increasing polymerization time (i.e. larger thickness of pNIPAM surfaces), and cell detachment decreases with a thicker collagen coating. They also stained actin, a cytoskeletal protein, in their cells, and performed fluorescent imaging on cells growing on pNIPAM-coated surfaces of different polymerization times, as well as on cells growing on pNIPAM surfaces that were coated with collagen. Cells were fixed immediately prior to detachment (i.e. at the regular cell culture temperature, 37^{o}C), as well as after 30 minutes of incubation below the LCST (at 18^{o}C). Figure 1.8 shows fluorescence images of a cell growing on a pNIPAM-coated surface right before detachment (left) and after 30 minutes at lower temperature. They discovered that actin concentration on the periphery of the cell after 30 minutes below the LCST of pNIPAM varies with different polymerization times as well as with collagen coating.

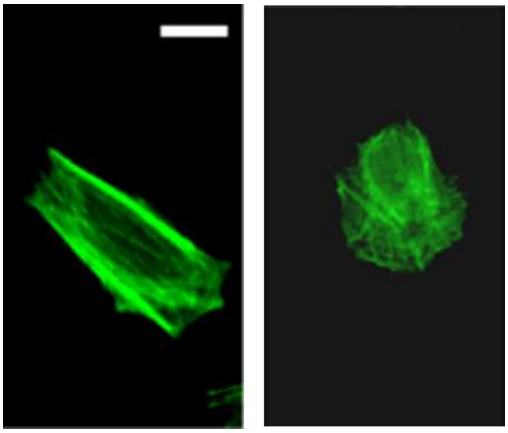

Figure 1.8 Fluorescent images of smooth muscle cells attached to a pNIPAM-coated surface (left) and 30 minutes after incubation at 18^{o}C (right) with actin stained in green. The scale bar represents 1 μm. Image adapted from Chen at al.[76]

The mechanism of cell detachment from pNIPAM was investigated using bovine aortic endothelial cells (BAECs), hepatocytes, retinal pigment epithelium cells, and Madin-Darby canine kidney (MDCK) cells.[36, 40, 72-75, 77] For MDCKs, the detachment from the surfaces varied depending on the age of the culture (no detachment for cells cultured for three weeks or less).[40] Several studies tested the temperature at which the detachment is the most efficient. Okano et al. concluded that the best cell detachment was achieved at room temperature with less cell detachment at lower temperatures (4, 10^{o}C), which they attributed to suppressed cell metabolism.[72] However, a number of studies performed successful cell sheet detachment from pNIPAM-grafted surfaces at lower temperatures (4 and 10^{o}C).[27, 45, 46, 78, 79] In our previous work, we compared cell detachment at different temperatures (37^{o}C, 25^{o}C, and 4^{o}C) and found that the fastest cell release occurred at 4^{o}C in serum-free medium.[27] This result contradicts the conclusion from Okano et al. that cells detach from pNIPAM-grafted surfaces the fastest at 25^{o}C.[72] In contrast to these two studies, Wang et al. found that the highest detachment of fibroblast cells from pNIPAM-coated surfaces was

achieved at ~15^{o}C. At 10^{o}C and 4^{o}C, less cell detachment was observed, which the authors contributed to suppressed cell metabolism at these temperatures.[80]

No clear picture of what happens to cells during the detachment from pNIPAM currently exists. In order to build engineered tissues, we need to understand how the detachment process works, and prove that the cytotoxic polymer is not released with the tissue. The optimization of the process involves choosing the right conditions for detachment, such as the appropriate medium and temperature. Further investigation into the mechanism of cell detachment at lower temperatures and research using different types of cells needs to be performed to apply the proposed mechanism to all cell types. An understanding of the exact mechanism of cell detachment from a temperature-responsive surface will be invaluable in developing better methods of engineering and detaching intact cell sheets.

1.6 Summary

In this work, we present a thorough investigation of pNIPAM's cytotoxicity, as well as the mechanism of cell detachment from this thermoresponsive polymer. Chapter 2 gives an overview of all experimental and analytical techniques used to complete this work. A review of pNIPAM's various applications with mammalian cells can be found in Chapter 3. We designed a comprehensive study of the cytotoxicity of NIPAM, pNIPAM, and pNIPAM-coated surfaces, which is described in detail in Chapter 4. To test the mechanism of cell detachment from pNIPAM-coated surfaces, we performed experiments at various temperatures and conditions, with and without an ATP inhibitor, utilizing light microscopy (described in Chapter 5). Fluorescent pNIPAM-coated surfaces were used for the investigation of pNIPAM-cell interface to determine if any

fragments of the polymer are removed with the cells during cell detachment (described in Chapter 6). Table 1.3 shows organization of chapters and outlines the studies described in this work, including important experimental detail and journal in which this work was published (if applicable). Final conclusions and future directions for this work are outlined in Chapter 7.

Table 1.3 Chapter organization and overview of studies presented in this work.

Chapter #	**Chapter title**	**PNIPAM formulation used**	**Cell type used**	**Published in**
3	Biological cell detachment from poly(*N*-isopropyl acrylamide) and its applications	N/A	N/A	*Langmuir*
4	Assessment of cytotoxicity of *N*-isopropyl acrylamide and poly(*N*-isopropyl acrylamide)-coated surfaces	NIPAM, cpNIPAM, frpNIPAM, spNIPAM, ppNIPAM	Endothelial, epithelial, fibroblast, smooth muscle cells	*Biointerphases*
5	Mechanism of cell detachment from pNIPAM-coated surfaces	atrpNIPAM	Endothelial cells	To be published in *Langmuir*
6	Investigation of pNIPAM/cell interface	atrpNIPAM	Endothelial cells	To be published in *Langmuir*
7	Conclusions and future directions	N/A	N/A	

CHAPTER 2: EXPERIMENTAL METHODS

2.1 Surface preparation

Cell culture was performed on round glass cover slips (Ted Pella Inc., Redding, CA), while surface analysis was performed on silicon chips (Silitec, Salem, OR). Silicon wafers were cut into 1cm x 1cm squares for X-ray photoelectron spectroscopy (XPS), and 0.8cm x 3cm rectangles for goniometry. The Si chips were cleaned in an ultrasonic cleaner from VWR International (West Chester, PA) twice in each of the following solutions for 5 minutes: dichloromethane, acetone, and methanol (Honeywell Burdick & Jackson, Deer Park, TX). Glass cover slips were cleaned for 30 min with an acid wash, a 1:1 solution by volume of methanol and hydrochloric acid (Honeywell Burdick & Jackson, Deer Park, TX), rinsed with deionized water, and dried with nitrogen. Both types of surfaces were placed under nitrogen in a Petri dish sealed with Parafilm and stored in a desiccator for future experiments.

2.2 Polymerization of NIPAM

Several different polymerization and deposition methods were used for experiments outlined in this work. PNIPAM films were generated using vapor-phase plasma polymerization of NIPAM (ppNIPAM) and atom transfer radical polymerization (ATRP), as well as spin-coating of cpNIPAM/tetraethyl orthosilicate sol gel (spNIPAM), spin-coating of cpNIPAM dissolved in isopropanol (cpNIPAM/IPA), and spin-coating of frpNIPAM, also dissolved in isopropanol (frpNIPAM/IPA). These techniques alone account for the majority of the ongoing research in this area (~90%).[81] Figure 2.1

shows all techniques used to synthesize pNIPAM and generate pNIPAM-coated surfaces for experiments performed in this work.

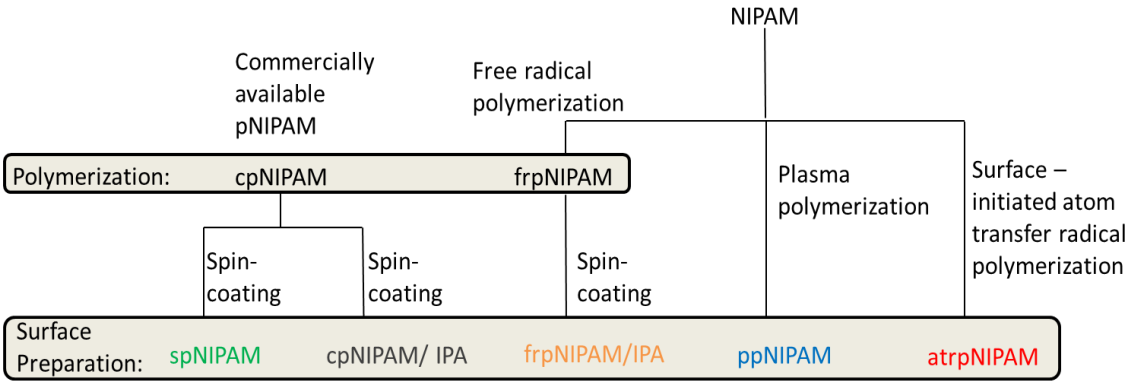

Figure 2.1 Overview of all polymerization and surface preparation techniques used in this work.

2.2.1 Free radical polymerization

Free radical polymerization of NIPAM was adapted from Vihola et al.[54] Briefly, 133 mmol of the NIPAM monomer (99%, Acros Organics, Geel, Belgium) was dissolved in 55 mL of dioxane (99.8%, anhydrous, Sigma Aldrich, St. Louis, MO). The polymerization solution was degassed with nitrogen and heated to 70^{o}C. Once the desired temperature was reached, the solution of initiator [AIBN (0.1%, 0.133 mmol, Sigma Aldrich, St. Louis, MO) in 5 mL of dioxane] was added to the polymerization solution. The reaction was allowed to proceed for 18 hours. After 18 hours, the polymerization solution was cooled to room temperature and the polymer was precipitated into excess cold diethyl either (99.5%, extra dry, Acros Organics, Geel, Belgium) twice. The resulting powder was dried in a vacuum oven overnight.

2.2.2 Surface-initiated atom transfer radical polymerization

Covalently bounded, reproducible pNIPAM surfaces, (atrpNIPAM), were generated using surface-initiated atom transfer radical polymerization (ATRP). ATRP has the advantage over other techniques (such as plasma polymerization and spin coating) in that it allows control over the degree of polymerization. The polymer thickness is controlled by polymerization time, with longer polymerization times resulting in a thicker polymer layer. Figure 2.2 shows the relationship between polymerization time and the thickness of pNIPAM coating for the polymerization method used in this work. It has been reported that cells easily attach and detach from pNIPAM surfaces generated using electron beam irradiation of a thickness of approximately 20 nm.[82] For plasma polymerization and sol gel deposition, the thickness of 60 nm or larger still allowed cell attachment and detachment.[83, 84] For this study, we performed polymerizations for 5, 10, 15, and 30 minutes (dashed lines on Figure 2.2), which correspond to surface thicknesses less than or equal to 20 nm (the 5-15 minutes time points), as well as larger than 20 nm (30 minutes time point).

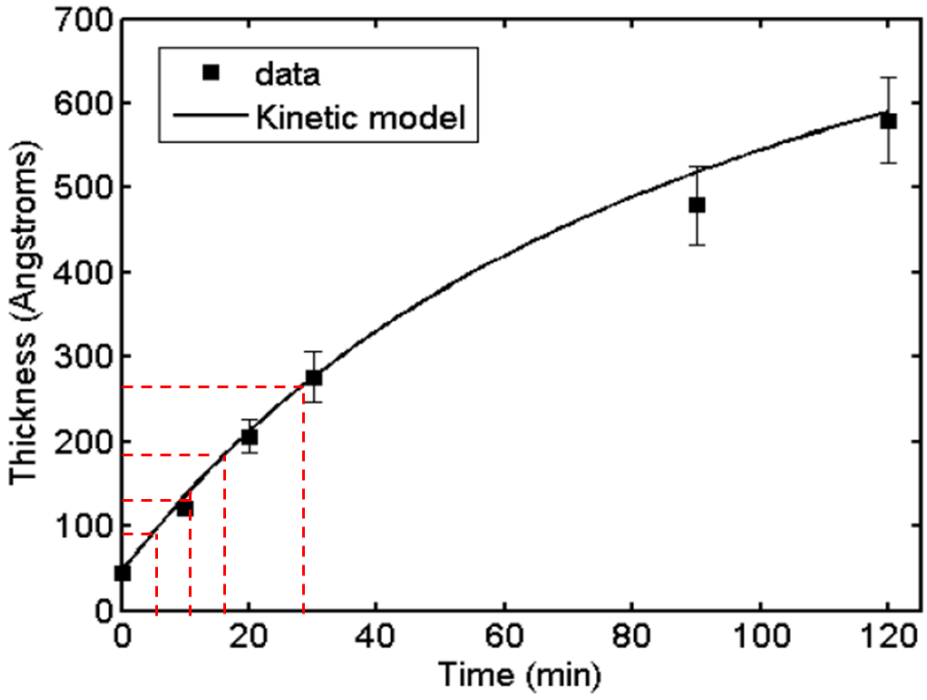

Figure 2.2 Degree of polymerization (thickness of pNIPAM coating) vs. time for ATRP reaction of pNIPAM. Dashed lines show polymerization times used in this work and corresponding coating thicknesses. Image adapted from Andrzejewski.[85]

Figure 2.3 illustrates basic steps used to complete ATRP of NIPAM. Round glass coverslips (for cell culture) and Si chips (for XPS and goniometry) are prepared as described in section 2.1.1. These surfaces were then cleaned with sulfuric acid (EMD Chemicals, Gibbstown, NJ) for 30 minutes. The hydroxylated surfaces were then exposed to the initiator, 3-(trimethoxysilylpropyl)-2-bromo-2-methylpropionate (Gelest, Inc., Morrisville, PA), dissolved in toluene (Honeywell Burdick & Jackson, Deer Park, TX), at the concentration of 100 µL in 50 mL of toluene (step A in Figure 2.3). NIPAM monomer (10g) was dissolved in water/methanol mixture (50 mL, 1:1 by weight). The metal catalyst, cooper (I) bromide, 14 mg (Sigma Aldrich, St. Louis, MO), and the ligand, N,N,N',N'',N''-pentamethyldiethylenetriamine, 60 µL (Sigma Aldrich, St.Louis,

MO), were added to the NIPAM solution (step B in Figure 2.3). The solution was then purged with nitrogen. In a separate flask, glass cover slips and Si chips were purged with nitrogen. The solution with the reactants was then added to the flask with slides and the reaction was allowed to proceed for a desired amount of time. Figure 2.3 C shows the resulting pNIPAM-coated surface. The number of repeated polymer units ("n" in Figure 2.3 C) is proportional to the duration of the polymerization reaction.

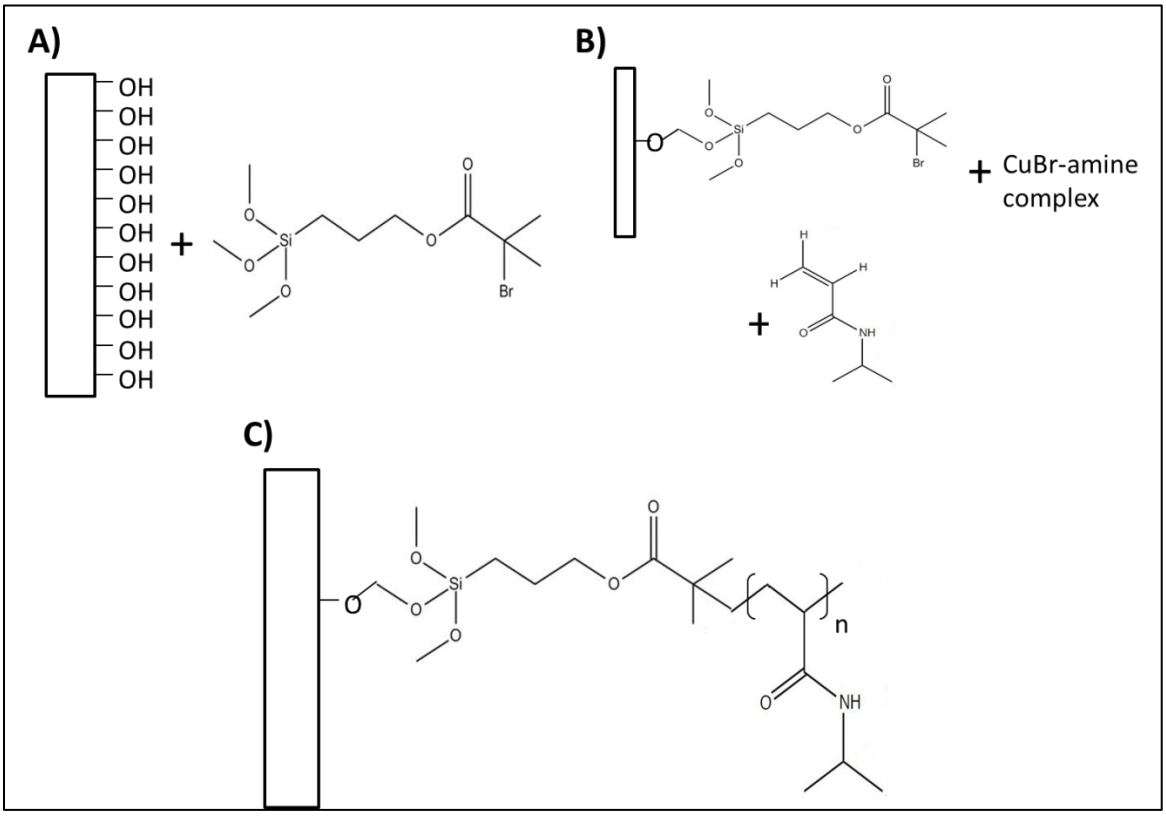

Figure 2.3 Basic steps of atom transfer radical polymerization of NIPAM: A) surface initiation, B) reactants, C) final product. Image adapted from Andrzejewski.[85]

2.2.3 Surface-initiated atom transfer polymerization with a fluorescent molecule

Fluorescent pNIPAM-coated surfaces, (atrpNIPAM-5AF), were generated using surface initiated atom transfer polymerization. To generate fluorescence, 0.05 molar % of 5-acrylamidofluorescein (synthesized in the lab from 5-aminofluorescein, Sigma Aldrich, St. Louis, MO) was added to the polymerization solution and the polymerization proceeded as described in previous section.

2.2.4 Plasma polymerization

Deposition of polymers onto surfaces by vapor-phase plasma polymerization has become a popular method due to its many advantages.[23, 86] Surfaces generated by plasma polymerization are sterile and uniform. The thickness of the film can be controlled by adjusting the conditions at which the polymerization is performed (such as wattage and time). This method does not require a solvent, and can be used with substrates of various types and geometries. While relatively expensive to build (~ $35,000), this method is fairly quick and capable of coating several surfaces at once.

Plasma polymerization for experiments presented in this dissertation was performed in a reactor chamber fabricated to our design specifications by Scientific Glass (Albuquerque, NM) following a method previously described.[83] Figure 2.4 shows a schematic of the plasma reactor built in our laboratory. The glass chamber is connected to two copper electrodes. Flow of gasses into the chamber is controlled by mass flow controllers. A vacuum pump is used to create vacuum inside of the chamber. The monomer is placed in a monomer flask and submersed in a warm water bath (at the

temperature > 70^{o}C for the NIPAM monomer) and heated until it goes into the vapor phase.

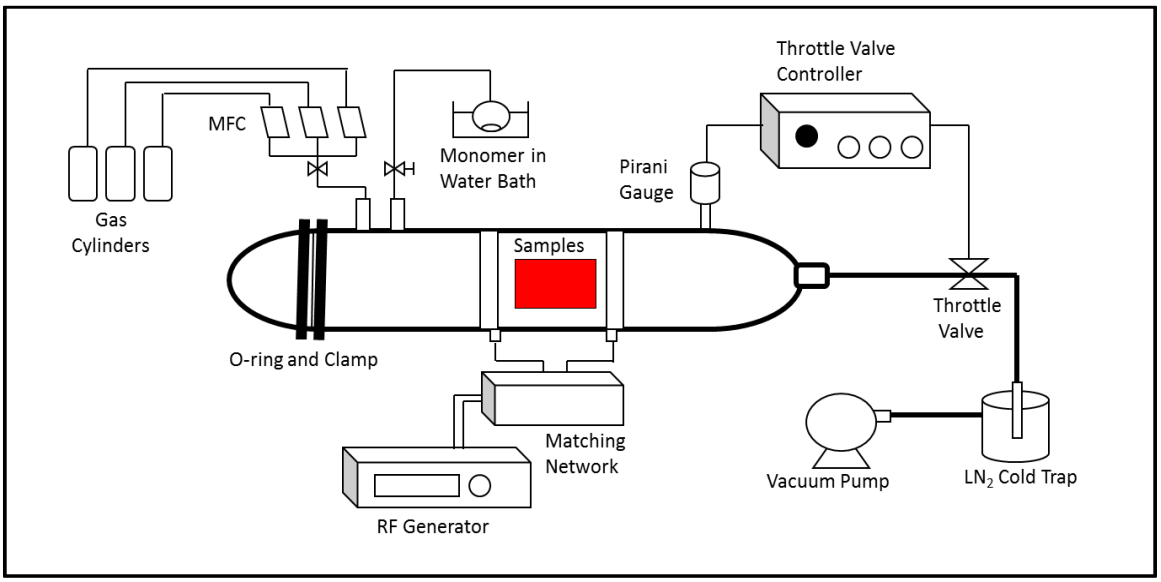

Figure 2.4 Schematic of UNM plasma reactor design.

To spark a plasma in the chamber, the two 2.5 cm copper electrodes were connected to a Dressler (Stolberg, Germany) matching network and Cesar radio frequency (rf) power generator from Advanced Energy (Fort Collins, CO). Argon etching (40 W, 2 min) and methane adhesion-promoting layer (80 W, 5 min) were performed before pNIPAM deposition. During pNIPAM deposition, the power setting of the rf generator was slowly decreased from 100 W to 0 W (100 W for 5 minutes, 10 W for 5 minutes, 5 W for 5 minutes, 1 W for 10 minutes, followed by 10 minutes at 0 W). Lower power results in smaller degree of fragmentation of the monomer. The higher power at the beginning of the deposition was used to build a foundation with a more fragmented and cross-linked film. The pressure was maintained at 140 mT. After the samples were

removed from the reactor chamber, they were rinsed with cold deionized water to remove any uncross-linked monomer, dried with nitrogen, placed in a Petri dish and sealed with Parafilm under nitrogen. The ppNIPAM surfaces were then stored in a desiccator at room temperature for further experiments.[87]

2.3 Deposition of pNIPAM

2.3.1 Sol-gel pNIPAM solution preparation and deposition

Solution preparation using sol-gel (spNIPAM) was performed following a method developed in our laboratory and previously described.[27] Briefly, 35 mg of pNIPAM, 5 mL of deionized water, and 200 μL of hydrochloric acid were mixed and a weight percentage of pNIPAM was determined. In a separate container, 250 μL of TEOS solution (1 wt% TEOS : 3.8 ethanol : 1.1 water : 0.0005 HCl), 43 μL of deionized water, and 600 μL of ethanol were mixed and weighted. The appropriate amount of the pNIPAM solution was calculated and added to achieve the final weight percentage of pNIPAM of 0.35%.

100-250 μL of the spNIPAM solution was evenly distributed onto clean glass cover slips and Si chips placed on a spin coater, model 100 spinner from Brewer Science, Inc. (Rolla, MO). The surfaces were spun at 2000 rpm for 60 seconds. The surfaces were stored under nitrogen in a Parafilm covered Petri dish until used for cell culture or surface analysis.

2.3.2 Deposition of frpNIPAM and cpNIPAM

FrpNIPAM or cpNIPAM were dissolved in isopropanol to achieve 1% of pNIPAM by weight. The solutions were the spun onto surfaces in the same manner as the spNIPAM surfaces.

2.4 Analysis methods

2.4.1 Nuclear magnetic resonance

Nuclear magnetic resonance (NMR) spectroscopy was used to confirm successful polymerization of frpNIPAM and cpNIPAM. NMR gives information about the number of magnetically different atoms of one type. For this study, H NMR was used. H NMR allows determining the number of each of the distinct types of hydrogen nuclei in the molecule, as well as obtaining information regarding the immediate environment of each type of hydrogen. Therefore, NMR can be used to confirm or establish the structure of the investigated compound.

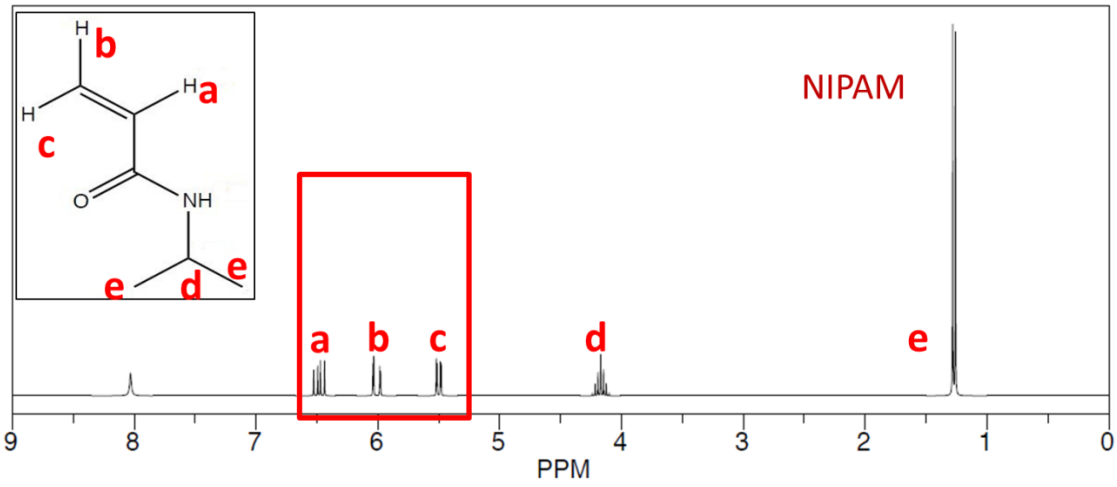

Figure 2.5 Predicted NMR spectrum of NIPAM monomer. Inset shows chemical structure of the NIPAM monomer. Hydrogens bound to alkenes are indicated as “a”, “b”, and “c” in the inset and spectrum.

Figure 2.5 shows the predicted NMR spectrum of NIPAM monomer and the chemical structure of the monomer. In the red box are the hydrogens that are present in

the monomer. These peaks should disappear from the spectrum of the polymer, as the polymer should not have any double bonded carbons.

The NMR spectra of frpNIPAM and cpNIPAM were obtained using an Avance III NMR spectrometer (Bruker, Billerica, MA). It is a 300 MHz, standard bore, nanobay instrument. Spectra were obtained on a 5 mm broadband/proton probe, at room temperature, using CDCl3 as a solvent.

2.4.2 Size exclusion chromatography

FrpNIPAM was analyzed with size exclusion chromatography (SEC) to determine the molecular weight of this polymer and its polydispersity index. SEC is used to separate the molecules of interest by size (molecular weight). Figure 2.6 illustrates how this method is performed. The polymer is dissolved in a solvent and injected into a column containing a stationary phase. The stationary phase is composed of small beads with a network of uniform pores. Small polymer chains can penetrate this network, while larger chains will not be able to enter it. As a result, it will take longer for smaller molecules to travel through the column than for larger molecules. Therefore, larger molecules will elute first, followed by smaller molecules.

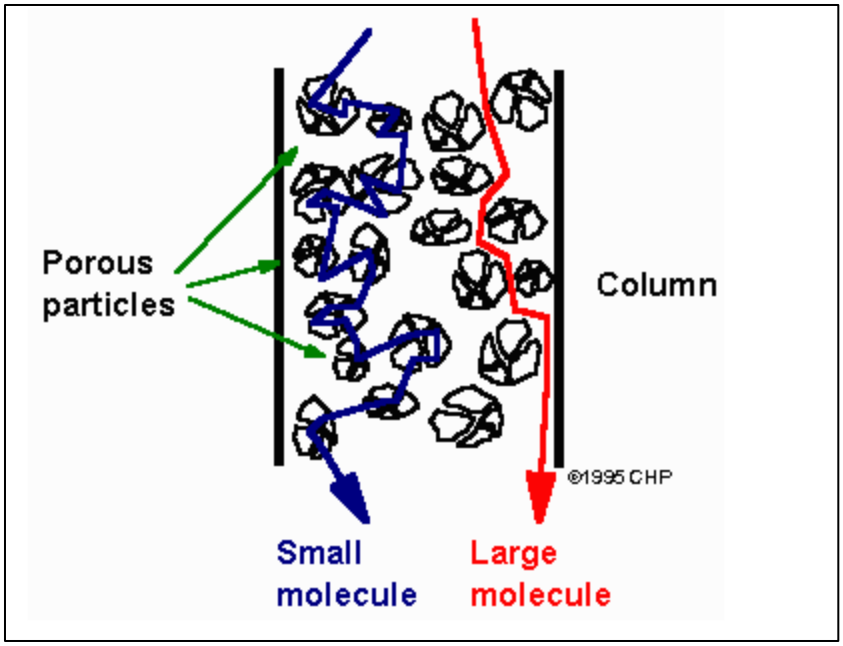

Figure 2.6 Schematic of the principle behind size exclusion chromatography. Image adapted from http://www.files.chem.vt.edu/chem-ed/sep/lc/size-exc.html.

SEC analysis on frpNIPAM was performed in chloroform with 0.5% (v/v) triethylamine (1 mL/min) using a Waters Breeze system equipped with a 2707 autosampler, a 1515 isocratic HPLC pump and a 2414 refractive index detector. Two styragel columns (Polymer Laboratories; 5 μm Mix-C), which were kept in a column heater at 35 °C, were used for separation. The columns were calibrated with polystyrene standards (Varian).

2.4.3 Goniometry

As previously mentioned, pNIPAM is a thermoresponsive polymer, with a conformation change at ~32^{o}C.[16, 19] Below this temperature, pNIPAM is hydrophilic. It becomes relatively hydrophobic when the temperature is raised to above 32^{o}C. Contact angle measurements can be used to determine if pNIPAM retained its thermoresponsive

behavior after deposition onto a surface. Above the LCST, at body temperature, the contact angles should be larger than below the LCST, at room temperature.[16, 27]

For goniometry measurements, pNIPAM was deposited onto silicon chips. Contact angles were taken on these pNIPAM-coated Si surfaces. Uncoated Si-surfaces were used as controls. The measurements were performed using an Advanced Goniometer model 300-UPG from ramé-Hart Instrument Co. (Mountain Lakes, NJ) with an environmental chamber. The inverted (captive) bubble method was used for the measurements.

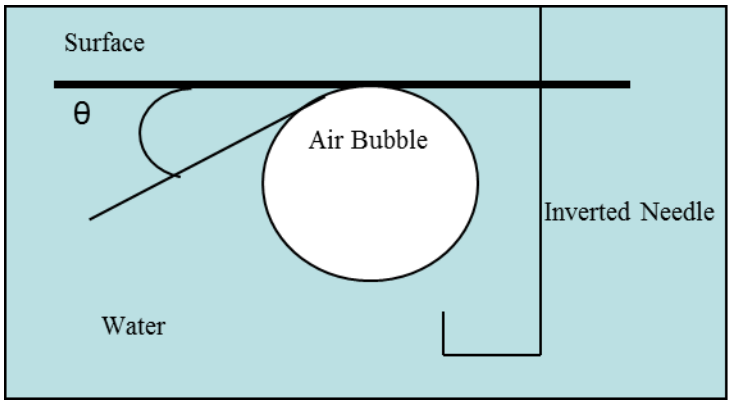

Figure 2.7 Illustration of contact angle measurements using captive bubble method.

Figure 2.7 depicts how captive bubble method works. The surface was placed facing down in a quartz cell filled with Millipore water (18 MΩ). Syringe with an inverted needle was used to place an air bubble on the surface. The angle between the surface and air bubble (θ in Figure 2.7) was measured using the DROPimage Standard program. Angles were obtained below the LCST, at room temperature (20^{o}C), and above the LCST, at body temperature (37^{o}C). The quartz cell was heated up to the body temperature using the Temp Controller model 100-500 connected to the environmental

chamber. The results were compared to contact angles obtained on control surfaces (uncoated surfaces should not demonstrate thermoresponse).

2.4.4 X-ray photoelectron spectroscopy

X-ray photoelectron spectroscopy (XPS), also known as electron spectroscopy for chemical analysis (ESCA), is a widely used method for obtaining elemental composition and molecular bonding environment of surfaces of interest. It is based on the photoelectric effect, where the transmission of energy from light photons to electrons results in the emission of the electrons without energy loss.

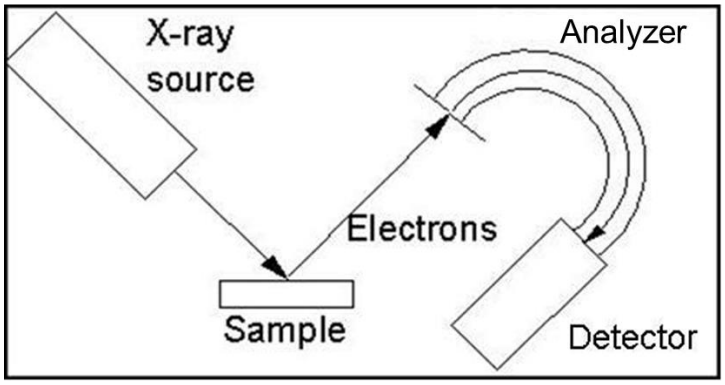

Figure 2.8 Schematic of a basic XPS experiment.

In a basic XPS experiment, as shown in Figure 2.8, X-rays are directed on the sample and are absorbed. Energy from the photons is transferred to electrons, which results in the ejection of core and valence electrons. All XPS experiments are performed in ultra-high vacuum, to ensure long inelastic mean free path for the emitted electrons. These electrons travel to the analyzer, and are counted in the detector. The energy of the electrons is related to the atomic and molecular environment from which they originated.

The number of electrons emitted is related to the concentration of the emitting atom in the sample. The energy measured by the detector is the kinetic energy of the electron.

$$E_B = h\nu - KE - \phi$$

- E_B – binding energy of the electron in the atom, calculated
- hν – energy of photons (Al Kα – 1486.6 eV)
- KE – kinetic energy of the emitted electron, measured in the XPS experiment
- Φ – work function (energy required to remove electron from the highest occupied energy level to vacuum level), known for a specific spectrometer

Figure 2.9 Calculation of binding energy in XPS experiment.

The binding energy is then calculated according to the equation in Figure 2.9. The photon energy (hν) is known and it is different depending on the source of X-rays. One of the common X-ray sources is Al Kα with photon energy of 1486.6 eV.[88] The work function is known for the specific spectrometer used. With the detected kinetic energy, the binding energy can be calculated and used to determine the identity of the emitting atom.

Survey spectra of the pNIPAM surfaces used in experiments described in this work were obtained at the National ESCA and Surface Analysis Center (NESAC/BIO) using Kratos Axis-Ultra DLD (Manchester, UK) and Surface Science Instruments S-probe spectrometers. Both instruments use monochromatized Al Kα X-rays, low-energy electron flood gun for charge neutralization, and were operated in low (10-9 Torr)

pressure. The analysis area was < 800 μm. Data analysis was carried out using the appropriate analysis programs (Casa XPS for most cases). The binding energy scales of the high resolution spectra were calibrated by assigning the most intense C1s high resolution peak a binding energy of 285.0 eV. A linear function was used to model the background.

Figure 2.10 shows typical survey and high resolution spectra of ppNIPAM. From the survey spectrum (Figure 2.10, top), we can obtain quantitative information regarding the elemental composition on the surface. In this case, the surface is predominantly composed of carbon, nitrogen, and oxygen, which is what we expect from surfaces coated with pNIPAM. This spectrum also allows us to determine relative atomic percentage of all the atoms detected. Carbon has the highest relative atomic percentage, as determined by the stoichiometry of the monomer (inset in Figure 2.10). The theoretical atomic composition of pNIPAM-coated surfaces is 75% carbon, and 12.5% of each oxygen and nitrogen.

The high resolution carbon spectrum (Figure 2.10, bottom) shows the molecular bonding environment of a single element (in this case, carbon). The peaks were assigned their corresponding bonding environment and labeled on the spectrum. The spectrum shows three major environments. The areas under the curves for each environment stand for the relative abundance for each bonding environment. For pNIPAM, we should predominantly see the C-C/C-H environment (66.7%), while the other two should be at ~ 16.7%.

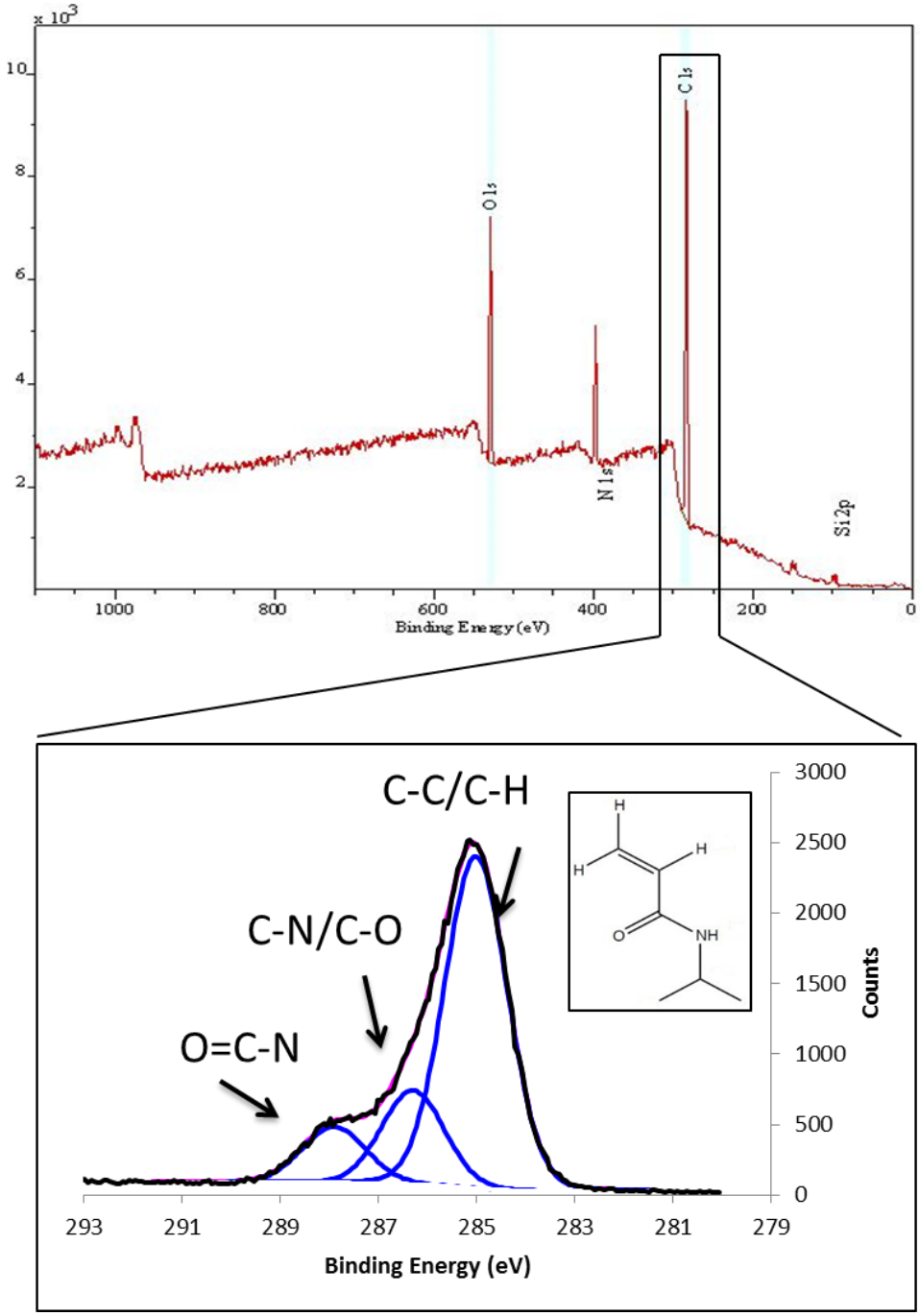

Figure 2.10 Survey (above) and high resolution C1s spectra (below) of ppNIPAM. The monomer structure demonstrates bonding environments detected by XPS.

2.5 Cell culture

2.5.1 Bovine aortic endothelial cells

Experiments with cells were performed with four different types of cells: endothelial cells, epithelial cells, smooth muscle cells, and fibroblast cells. Bovine aortic endothelial cells (BAECs) were purchased from Genlantis (San Diego, CA). BAEC cells were cultured according to previously established protocols. [27] Dulbecco's modified eagle's medium (DMEM, HyClone, Logan, UT), was supplemented with 10% fetal bovine serum (HyClone, Logan, UT), 1% penicillin/streptomycin (Gibco, Grand Island, NY), and 1% Minimum Essential Medium Non-Essential Amino Acids solution (MEM NEAA, Gibco, Grand Island, NY). Cells were incubated at 37^{o}C in a humid atmosphere with 5% CO_2. When confluent, the cells were washed with Dulbecco's phosphate buffered saline without calcium or magnesium (HyClone, Logan, UT). 0.25% trypsin/EDTA (Gibco, Grand Island, NY) was used to lift cells from cell culture flasks. Figure 2.11 shows BAECs cultured according to the described procedure.

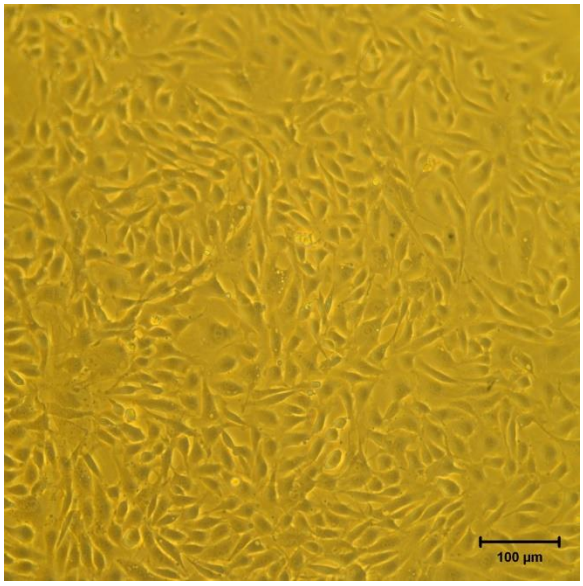

Figure 2.11 Bovine aortic endothelial cells (BAECS) cultured to confluence on tissue culture polystyrene (TCPS) at day 3.

2.5.2 Vero epithelial cells

Monkey kidney epithelial cells (Vero, CCL-81) were obtained from ATCC (Manassas, VA). Vero cells were cultured in Dulbecco's modified eagle's medium supplemented with 10% fetal bovine serum and 1% penicillin/streptomycin. Cells were incubated at 37^{o}C in a humid atmosphere with 5% CO_2. When confluent, the cells were washed with 0.25% trypsin/EDTA and lifted from cell culture flasks using 0.25% trypsin/EDTA. Figure 2.12 shows Veros cultured according to the described procedure.

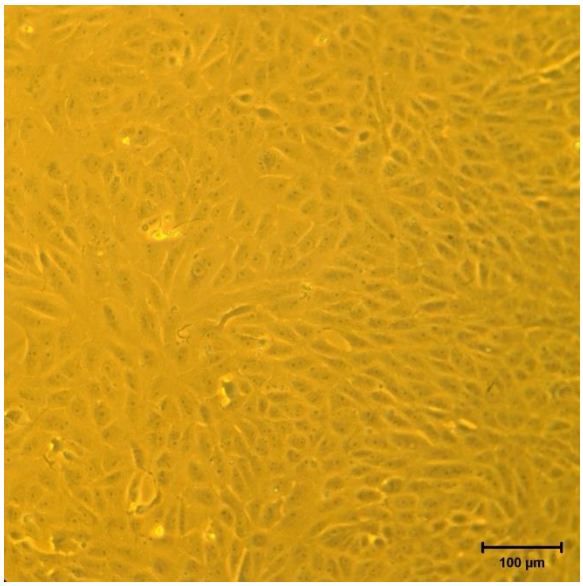

Figure 2.12 Vero cells cultured to confluence on TCPS at day 3.

2.5.3 Smooth muscle cells

Rat aorta smooth muscle cells (CRL-1444, SMCs), were obtained from ATCC (Manassas, VA). SMCs cells were cultured in Dulbecco's modified eagle's medium supplemented with 10% fetal bovine serum and 1% penicillin/streptomycin. Cells were incubated at 37^{o}C in a humid atmosphere with 5% CO_2. When confluent, the cells were

washed with 0.25% trypsin/EDTA and lifted from cell culture flasks using 0.25% trypsin/EDTA. Figure 2.13 shows SMCs cultured according to the described procedure.

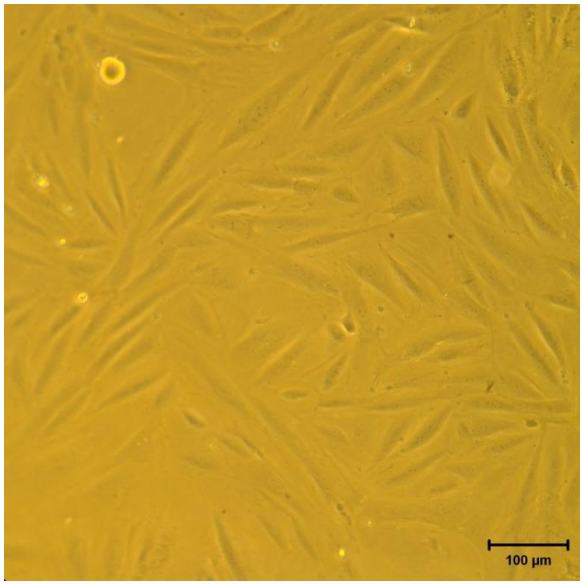

Figure 2.13 SMC cells cultured to confluence on TCPS at day 3.

2.5.4 3T3 fibroblast cells

Fibroblasts (MC3T3-E1, 3T3s) were a gift from Elizabeth Hedberg-Dirk. They were cultured in minimum essential medium with alpha modification (αMEM, HyClone, Logan, UT), supplemented with 10% FBS and 1% penicillin/streptomycin. Cells were incubated at 37^{o}C in a humid atmosphere with 5% CO_2. When confluent, the cells were washed with 0.25% trypsin/EDTA and lifted from cell culture flasks using 0.25% trypsin/EDTA. Figure 2.14 shows 3T3s cultured according to the described procedure.

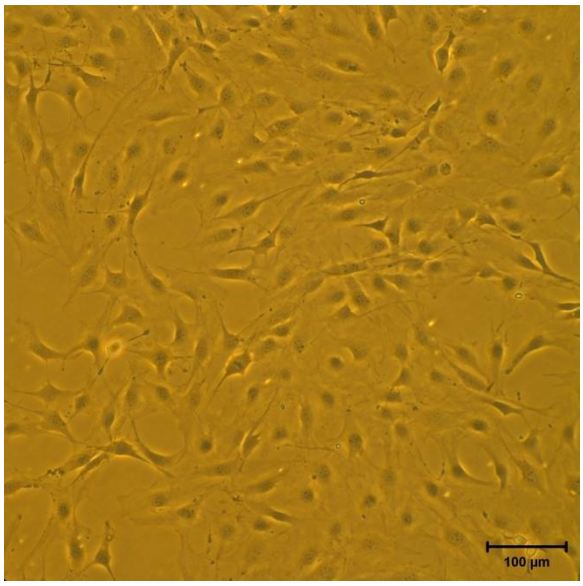

Figure 2.14 3T3 cells cultured to confluence on TCPS at day 3.

2.5.5 Cell detachment

Cell detachment was performed in cold media without added supplements. Cells were first cultured in regular cell culture media. To initiate detachment, the medium was replaced with cold non-supplemented medium. The well plates with cells in the cold medium were placed on a shaker table. The detachment was allowed to proceed for the desired amount of time (up to 2 hours) at room temperature.

2.6 Cytotoxicity testing

All cytotoxicity experiments (except for plating efficiency) were performed in 5% FBS media according to ISO standards.[61] Media without phenol red was used for experiments evaluated with the MTS assay, as the dye contributes to increased background absorbance.[89]

2.6.1 LIVE/DEAD assay

LIVE/DEAD viability kit was purchased from Invitrogen (Grand Island, NY). LIVE/DEAD assay is based on the integrity of the cellular membrane. The kit contains

two dyes: Calcein AM and Ethidium homodimer-1. Calcein AM is membrane-permeant. It is cleaved by esterases in live cells and fluoresces green. Ethidium homodimer-1 is membrane-impermeant. It labels nucleic acids in cells with damaged membrane, and fluoresces red. Therefore, live cells will be stained green with Calcein AM and dead cells will be stained red with Ethidium homodimer-1. Figure 2.15 shows cells stained with the LIVE/DEAD kit.

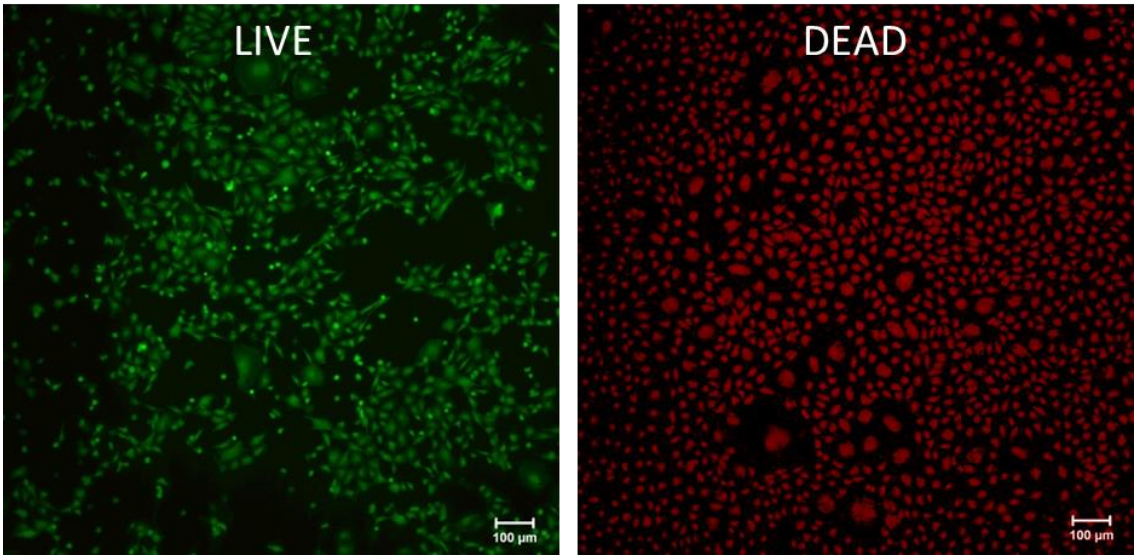

Figure 2.15 Bovine aortic endothelial cell stained with LIVE/DEAD assay. Cell stained green are live (left), cells stained red are dead (right).

The procedure for LIVE/DEAD assay was adapted from the procedure supplied by the manufacturer.[90] To create combined LIVE/DEAD solution, 1µL of the Calcein solution (to stain live cells) and 1 µL of the ethidium solution (to stain dead cells) were added per 1 mL of DPBS. Cells were seeded in well plates and cultured for the desired amount of time in the regular cell culture medium. To perform the assay, cells were first cleaned with DPBS. DPBS was then replaced with the dye solution and the well plates were left at room temperature for 1 hour. After 1 hour, the dye solution was replaced with

DPBS and imaged. Fluorescent images were taken on a Nikon Eclipse TS200F inverted microscope with an epi-fluorescence attachment (Nikon Instruments, Melville, NY) and a SPOT Insight color mosaic digital camera (Diagnostic Instruments, Sterling Heights, MI).

2.6.2 MTS assay

CellTiter 96® AQueous One Solution Cell Proliferation Assay (MTS assay) was obtained from Promega (Madison, WI). MTS assay tests metabolic activity of cells. It is based on cellular conversion of a tetrazolium salt (MTS) into a formazan product. The conversion occurs in the mitochondrium and results in the change of color of the solution (from yellow to dark brown/purple). Figure 2.16 shows an image of a well plate after MTS assay was performed. The wells with the fewest live cells are yellow, while wells with the most live cells are dark brown.

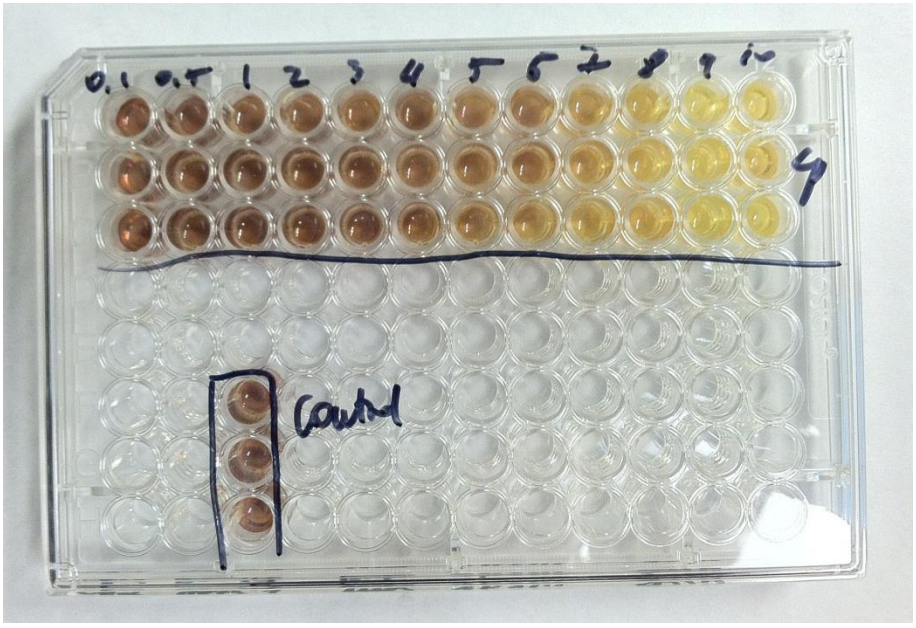

Figure 2.16 Photograph of a 96 well plate after MTS assay was performed for a concentration gradient experiment. The marking 0.1 to 10 denote concentrations of pNIPAM dissolved in cell culture media (μl/mL). "Control" stands for cell culture media without pNIPAM, and "cp" stands for cpNIPAM.

The procedure for MTS assay was adapted from the procedure supplied by the manufacturer.[89] Cells were seeded in well plates at the desired density and cultured in a regular cell culture media for 24 hours. The cell culture media was removed and replaced with the MTS solution (20 µL of MTS test solution per 100 µL of media). The well plates were then wrapped in aluminum foil and left in the incubator for 3 hours. After 3 hours, the assay was read at 490 nm in a plate reader (SpectraMax M2, Molecular Devices, Sunnyvale, CA). The absorbance is proportional to the amount of live cells in the well, with larger amount of cells resulting in higher absorbance.

2.6.3 Direct contact test

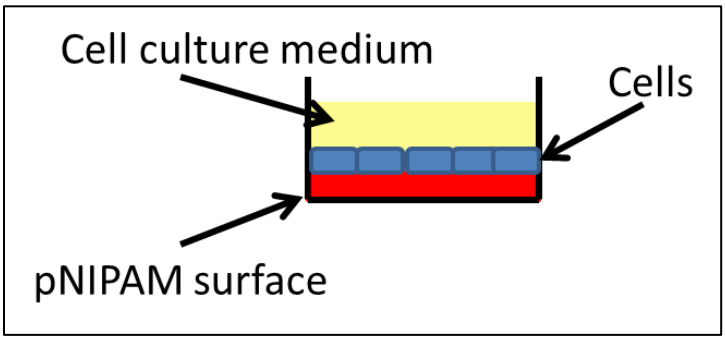

Figure 2.17 Schematic of the direct contact test experiment. Red – pNIPAM-coated surface, blue – cells, yellow – media.

For the direct contact test, cells were seeded directly on spNIPAM, frpNIPAM, cpNIPAM, and ppNIPAM surfaces (as shown in Figure 2.17). This test allows seeing how pNIPAM-coated surfaces affect cellular attachment, growth, proliferation, and survival.

The pNIPAM-coated surfaces were placed in a 24-well plate. Twenty thousand cells were seeded in each well. The cells were allowed to attach and grow on the pNIPAM-coated surfaces for up to 96 hours in a regular cell culture media.

Morphological observations, MTS assay, and LIVE/DEAD assay were performed after 48 and 96 hours of cell culture.

2.6.4 Preparation of extracts

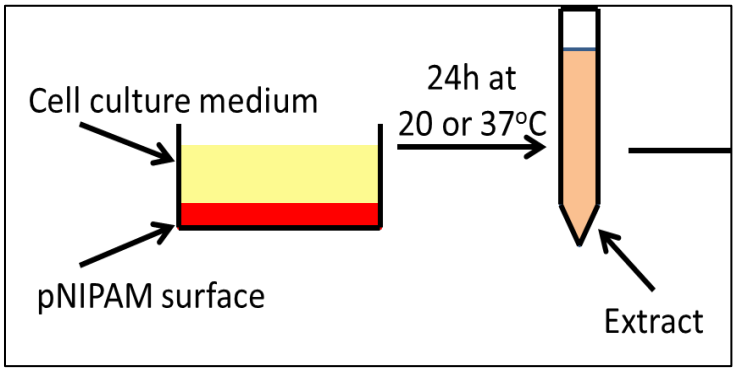

Figure 2.18 Schematic of the preparation of extracts.

Extracts from ppNIPAM, spNIPAM, cpNIPAM, and frpNIPAM were obtained at room (20°C) and body (37°C) temperature. Figure 2.18 shows a schematic of how the extracts were prepared. The protocol for generating extracts was developed based on ISO standards.[61] To make extracts, a pNIPAM surface was incubated in regular cell culture media (surface to liquid volume ratio of 1.5 cm^2/mL) for 24 hours at room and body temperature. After 24 hours, the resulting extracts were transferred to a centrifuge tube and kept in a refrigerator at 4°C for experiments with cells.

2.6.5 Plating efficiency

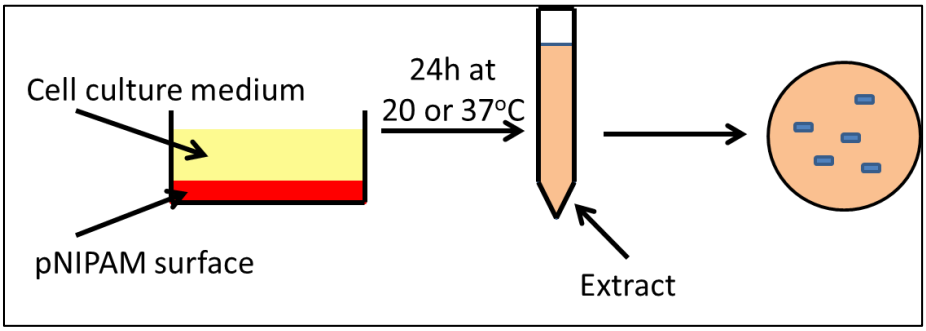

Figure 2.19 Schematic of the plating efficiency experiment.

The above mentioned extracts were used for a plating efficiency assay. Plating efficiency is a very sensitive assay. A small amount of isolated cells is "plated" in Petri dishes and allowed to form colonies. Since cells are seeded at very low densities, they are at their most sensitive, as they do not have their neighbors to protect them from harmful environment. The test determines the number of cells that can survive and reproduce under given conditions. If the media contain harmful substances, plating efficiency (i.e. number of colonies) will decrease when compared to controls.

The assay was performed according to the method developed by Ham and Puck.[91] Two hundred cells were seeded in a round Petri dish containing 5 mL of the extracts or 5 mL of regular cell culture media (control). Cells were left in an incubator for an amount of time that allowed them to double ten times (that time was determined based on the doubling time of the specific cell line). Doubling times were determined experimentally for BAECs (20 hours), 3T3s (18 hours), and SMCs (34 hours). Doubling time for Veros (24 hours) was obtained from the literature.[92] After the required amount of time, cells were fixed and stained using Carnoy's fixative (3:1 methanol : acetic acid by volume, 0.5% crystal violet by weight). The colonies formed on the dish were counted and compared to the colonies formed on the control. The plating efficiency was calculated using the following equation:

$$Plating\ efficiency\ (\%) = \frac{\#\ of\ colonies\ formed}{\#\ of\ cells\ seeded} * 100$$

Eqn. 2.1 Equation for calculating plating efficiency.

2.6.6 Extracts study

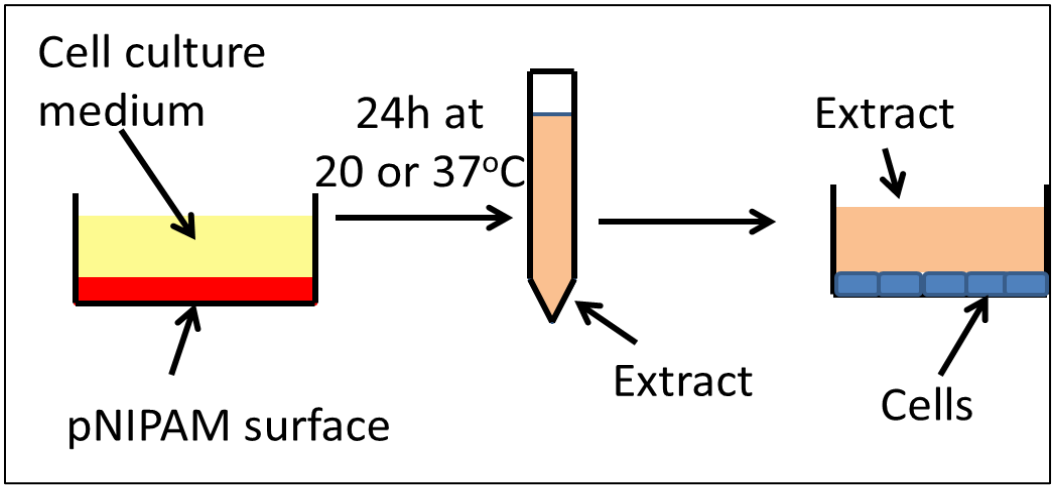

Figure 2.20 Schematic of the extract experiment.

For further experiments, extracts were tested in conditions that are closer to the regular cell culture conditions than plating efficiency. Here, cells were not isolated. They were exposed to extracts after they grew and proliferated in regular cell culture medium in the absence of pNIPAM. It is only after they reach ~60/70% confluency, that the media is replaced with different concentrations of extracts.

To perform experiments with extracts, 8000 cells were seeded per well in a 96-well plate. After 24 hours in regular cell culture media, the media were replaced with extracts in 3 concentrations (1%, 10%, and 100% extracts). MTS assay was performed after 24 and 48 hours.

2.6.7 Concentration gradient

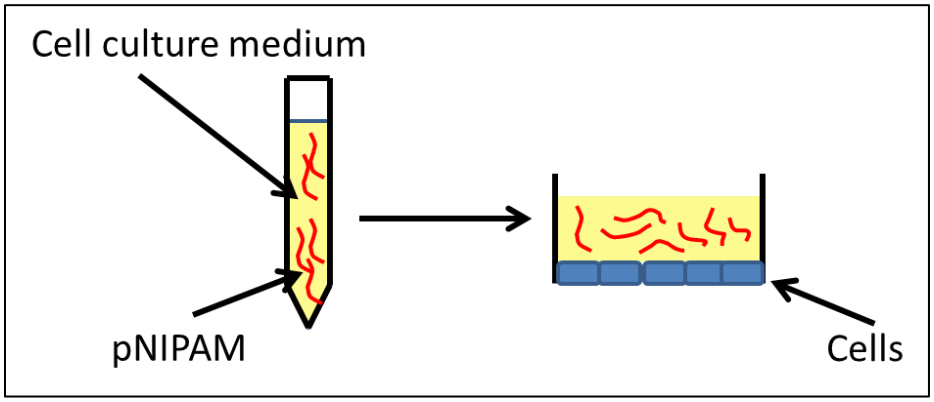

Figure 2.21 Schematic of the concentration gradient experiment. Cell culture medium in yellow; pNIPAM chains in red.

For concentration gradient experiments, frpNIPAM and cpNIPAM were dissolved in tissue culture media in the concentrations of 0.1, 0.5, 1, 2, 3, 4, 5, 6, 7, 8, 9, and 10 mg/mL. Cells were seeded in 96-well tissue culture polystyrene (TCPS) plates at the concentration of 8000 cells/well. Cells were cultured in the presence of the regular cell culture media for 24 hours. After 24 hours, the culture media was replaced with the test solution (pNIPAM dissolved in media). Morphology observations and MTS assay were performed after 24 and 48 hours of exposure to the test solutions.

CHAPTER 3: BIOLOGICAL CELL DETACHMENT FROM POLY(*N*-ISOPROPYL ACRYLAMIDE) AND ITS APPLICATIONS

This chapter has been revised and updated from a previous publication by M.A. Cooperstein and H.E. Canavan in *Langmuir*.[17]

3.1 Introduction

A number of reviews already exist on this remarkable polymer, including a review on the synthesis, characterization, and known applications of pNIPAM from 1956 to 1991,[19] synthesis, structure, properties and application areas in bioengineering of copolymers of *N*-isopropyl acrylamide,[93] and methods of producing thermoresponsive substrates coated with pNIPAM for cell sheet engineering.[13] There are reviews available on the synthesis and classification of thermoresponsive polymers,[11, 12] the use of stimuli-responsive polymers in chronotherapy,[30] and on the developments in the area of thermoresponsive aqueous microgels.[94] A recent publication evaluated the most common switchable materials and methods applied to protein- and cell-surface interactions, with a special focus on molecular and physico-chemical aspects.[16] However, to date, no one has reviewed the different methods and purposes for which pNIPAM has been used to manipulate biological cells; therefore, this work focuses on that aspect of pNIPAM research.

PNIPAM has been used for research with many organisms (with the focus on studying the properties of the polymer), and it has been used for research on numerous organisms (with the focus on the organisms). Among these organisms are various mammalian cells (e.g., red blood cells, endothelial cells, chondroblasts, and

macrophages), different strains of bacteria, and yeast. This chapter reviews different ways in which pNIPAM has been used for cell-based research. In the subsequent sections, we discuss how pNIPAM has been used for the investigation of the extracellular matrix underlying cells. We survey the different ways cell attachment and detachment from pNIPAM surfaces can be enhanced. In addition, we review how pNIPAM has been used to make hydrogels, spheroids, and patterned or shaped tissue constructs. Finally, we investigate such applications as tissue transplantation, cell deformation and manipulation, bioadhesion and bioadsorption, and manipulation of microorganisms. All articles discussed in this chapter are listed and briefly summarized in Table 1 in the Appendix.

3.2 Extracellular matrix

The behavior of the extracellular matrix (ECM) deposited by the cultured cells is a subject of investigation of many research groups. As one of the functions of the ECM is anchoring and providing support for the cells, a method that detaches cells from their culture surfaces with intact ECM is desirable.

Kushida et al. in their 1999 study investigated the amounts of fibronectin present in the ECM of cultured cells before and after low-temperature detachment.[36] Immunofluorescence study of BAECs growing on pNIPAM-grafted surfaces revealed that the cells adhered, spread and deposited fibronectin on the surfaces over the time of the culture. Upon lowering the temperature, intact cell sheets detached from the grafted surfaces. Immunostaining of the detached sheets showed that a majority of fibronectin detached with the cell sheets. The area from which the cells detached did not show the presence of fibronectin. In comparison, after treatment with trypsin, fibronectin was only faintly detected. Physical scraping recovered comparable amounts of fibronectin to low-

temperature treatment. Kushida et al. obtained similar results in their study of MDCK cell detachment from pNIPAM grafted surfaces.[40]

Canavan et al. examined the location of laminin, fibronectin, and type I and type IV collagen after cell detachment from plasma polymerized pNIPAM. [39]

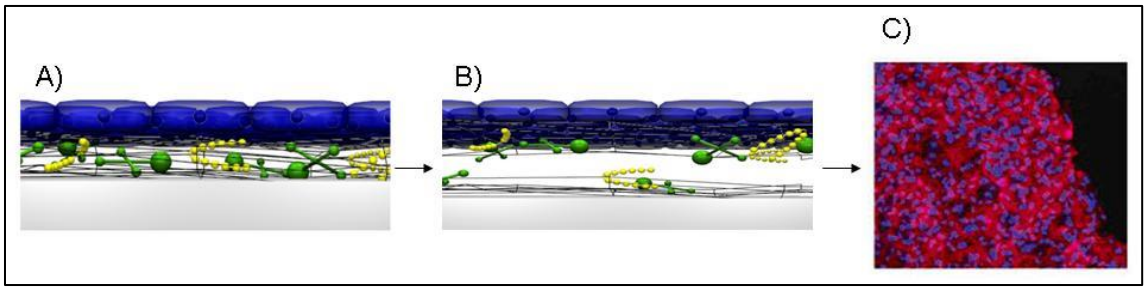

Figure 3.1 Detachment of intact cell sheets from a pNIPAM-grafted surface: A) attached cell sheet; B) detachment of the cell sheet; C) doubly stained detached cell sheet: LN stained with Texas Red (appears red), the cell nuclei stained with Hoechst 33342 dye (appears blue). Image adapted from Ref. [35] (image A and B), Ref. [39] (image C).

Immunoassays revealed that, after detachment with low-temperature treatment, fibronectin and laminin remain for the most part with the detached cell sheet. Figure 3.1 shows a schematic representation of cell sheet detachment from pNIPAM-grafted surfaces. Panel A shows cells (in blue) attached to the grafted surface. The green and yellow structures represent the ECM proteins. Panel B shows the cell sheet detaching from the surface, with some of the proteins remaining on the surface. Panel C shows the results of immunostaining of the detached cell sheet. Laminin, which was stained with Texas Red and appears red, is co-localized with cells nuclei, which are blue in the image. The underlying surface does not fluoresce, indicating that most of laminin detached with the cell sheet. Collagen results were less conclusive. According to time-of-flight secondary ion mass spectroscopy (ToF-SIMS), low-temperature liftoff leaves the surfaces

rich in glycine and proline. Since collagen is rich in these amino acids, it was concluded that some collagen remains at the surface after the detachment.

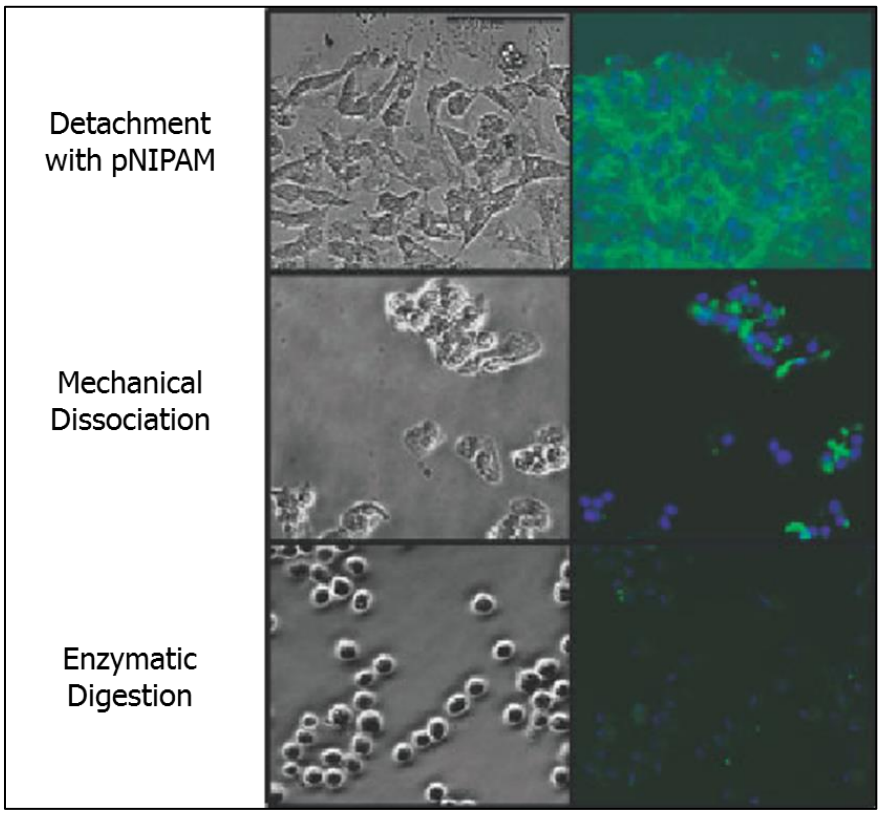

Figure 3.2 Bright-field (left column) and immunostained (right column) images of cell sheets detached using pNIPAM, mechanical dissociation, and enzymatic digestion. Fibronectin in cells was stained green with FITC-labeled secondary antibody; cell nuclei were stained blue with Hoechst 33342 dye. Bar is 100 μm. Image adapted from Ref. [34]

In two other studies, Canavan et al. compared how low-temperature treatment, mechanical scraping and enzymatic digestion affect the ECM.[34, 37] Here they reached the same conclusion about fibronectin, laminin and collagen as in their previous study. As can be seen in Figure 3.2, mechanical scraping left the ECM mostly intact; however, the cells were to some extent rounded, and the cell layer was broken into pieces. Enzymatic treatment resulted in single, round cells and the ECM proteins only weakly

fluorescing. Based on the X-ray photoelectron spectroscopy results, the authors concluded that low-temperature treatment resulted in the most reproducible ECM. ToF-SIMS revealed that mechanical scraping left the surfaces rich in hydrocarbons and lipids but not amino acids, which implies that this method breaks cell walls while scraping, and releases lipids ("blebbing").[34] There were some lipids detected on surfaces after low-temperature detachment, however in smaller amounts than after mechanical scraping. It was concluded that rupture of cell/ECM junctions and protein/protein or protein/surface interfaces can occur during low-temperature detachment.[37]

In a later study of the ECM, Canavan et al. compared the ECM obtained from the low-temperature detachment to the ECM obtained from proteins adsorbed onto plasma polymerized pNIPAM surface from single protein solutions.[35] They discovered that the surfaces remaining after the low-temperature detachment are similar to surfaces treated with bovine serum albumin and laminin, but are distinct from surfaces treated with fibronectin. This implies that most of fibronectin detaches with the cell sheets, whereas some amounts of the other proteins remain on the surface. Ide et al. performed a study of the ECM after cell detachment from pNIPAM using human corneal endothelial cells and surfaces grafted with pNIPAM by electron beam irradiation, and came to similar conclusions.[38]

There is a consensus among the researchers that low-temperature cell sheet detachment using pNIPAM-grafted surfaces is less invasive than detachment using mechanical scraping or enzymatic digestion. This method causes the least amount of damage to the cells and it is therefore the best method of detaching intact cell sheets for use in tissue engineering. It is now known that most of the ECM proteins detach together

with the cells during low-temperature cell release from pNIPAM-grafted surfaces. However, some of the ECM proteins remain on the surface. It is still not completely clear which proteins and how much of them detach with the cell sheet and how much stays on the surface. More research should be conducted to resolve this matter.

3.3 Controlling cell attachment and detachment

Many different approaches have been undertaken to find pNIPAM surfaces that enhance cell adhesion, decrease the detachment time, or do both simultaneously. Researchers experimented with different parameters, such as additives, media type, or temperature. This section reviews some ways scientists have approached this issue.

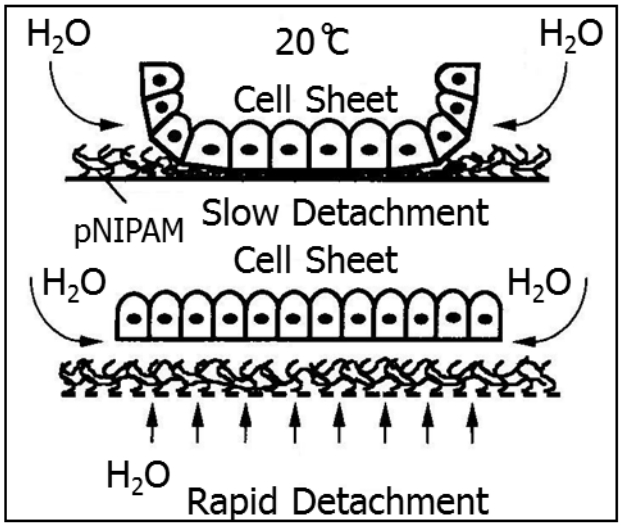

Figure 3.3 Controlling cell attachment and detachment with pNIPAM using water-permeable membranes. Image adapted from Ref. [95].

To enhance cell sheet detachment, Kwon et al. used porous membranes.[95] Figure 3.3 shows how cell sheets detach from a porous pNIPAM-grafted membrane and from a pNIPAM-grafted TCPS. With a membrane, water reaches the sheet from the sides (such as happens with TCPS), as well as from the bottom. Over 90% of BAECs detached

from the membrane within 50 min., while only ~75% of cells detached from grafted TCPS in the same amount of time (as single cells). In a cell sheet detachment experiment, it took 30 min. for cell sheet to detach from the porous membrane, and 75 min. for cell sheets to detach from a TCPS dish.

A different approach to controlling of cell attachment and detachment was undertaken by Reed et al.[96] Highly porous, thermoresponsive pNIPAM mats were synthesized utilizing electrospinning. The resulting mats were composed purely of pNIPAM, and were shown to promote cell attachment and detachment. The mats were tested with 3T3 and EMT6 cell lines. As reported, 80% of the cells detached within 5 minutes from the pNIPAM mats, when the temperature was lowered to below the LCST.

Figure 3.4 shows a way of controlling cell detachment from pNIPAM-grafted surfaces by manipulating the composition of the grafted polymer.

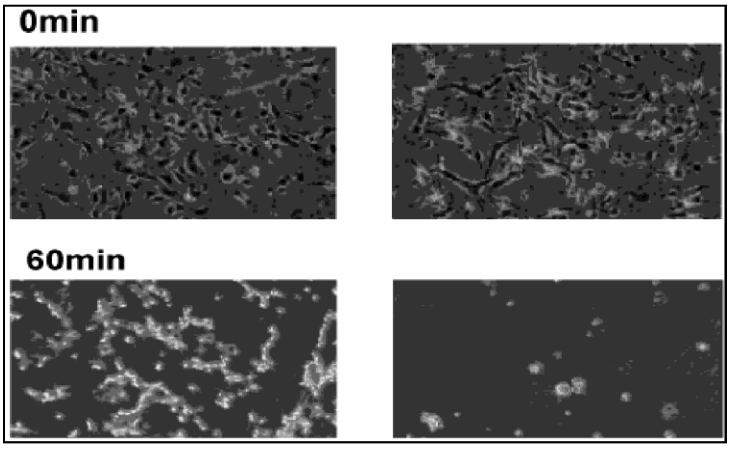

Figure 3.4 Controlling cell attachment and detachment with pNIPAM by changing composition of the substrate. Image adapted from Ref. [97].

BAECs detaching from pNIPAM-grafted TCPS are shown in the left column, and from TCPS dishes grafted with pNIPAM copolymerized with 2-carboxyisopropyl

acrylamide, p(NIPAM-co-CIPAAM), in the right column. Initially, the same amount of cells is attached to both types of surfaces. After 60 minutes at 20^{o}C, almost all cells detached from the pNIPAM-co-CIPAAM, while cells only started detaching from pNIPAM. The authors attributed the accelerated cell detachment from p(NIPAM-co-CIPAAM) surfaces to the presence of hydrophilic carboxyl groups. The amount of charged carboxyl groups on the polymer increases with decreasing temperature. The interactions of the polar groups with water are proposed to accelerate surface hydration, and decrease the amount of time required for complete cell and cell sheet detachment. The mechanism of accelerating cell detachment proposed by the authors of this article is an area for future study and should be further investigated.[97]

A different approach to cell release was taken by Reed et al.[27] They investigated the type of medium used for the detachment of BAECs (serum free medium, medium with serum, Dulbecco's phosphate-buffered saline (DPBS) and serum free medium with a DPBS wash) and the temperature at which the detachment occurred (37^{o}C, 25^{o}C and 4^{o}C) for most rapid cell detachment. They found that using serum-free medium at 4^{o}C yielded the fastest cell release.

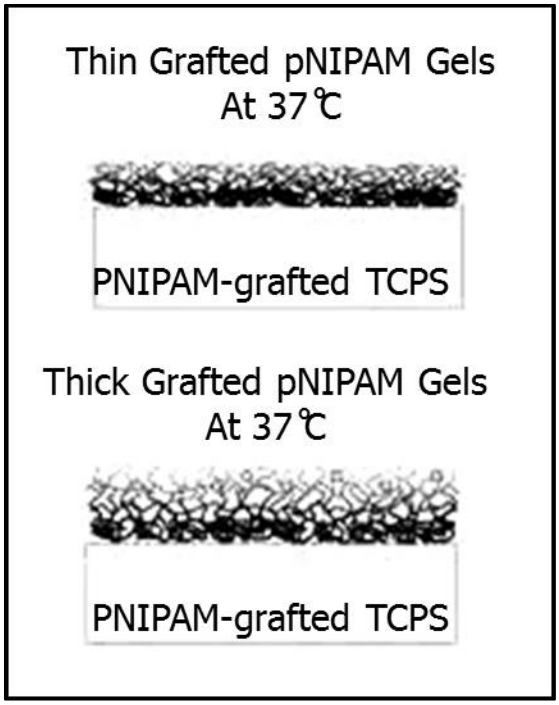

Figure 3.5 Controlling cell attachment and detachment with pNIPAM by adjusting the thickness of the substrate. Image adapted from Ref. [82].

Figure 3.5 shows an approach to enhancing cells attachment to pNIPAM-grafted surfaces by controlling the thickness of the grafted polymer. Akiyama et al. found that endothelial cells adhered and spread to surfaces with a thinner layer of pNIPAM (~15.5 nm) and did not adhere to surfaces with a thicker film (~29.3 nm). Cell detachment was achieved from the thinner surfaces. A thicker film layer resulted in more hydration, even at 37^{o}C, preventing cell adhesion. Fibronectin adsorbed on the thin surfaces, but the adsorption on the thicker surfaces was negligible. The authors concluded that the hydrophobic and hydrophilic properties are influenced by the thickness and the amount of the polymer.[82] However, Cole et al. pointed out that cells have been cultured and detached from thicker surfaces, and that different pNIPAM coatings may show different behavior due to varying brush density and thickness. Therefore, a more thorough

investigation of substrate properties (such as thickness, swelling, brush density, chemical composition, etc.) is needed before a conclusion on the optimal design of pNIPAM film can be made.[16]

The correlation between molecular weight of the polymer and cell attachment, was studied by Zhao et al. [98] The authors grafted polyurethane surfaces with pNIPAM of varying molecular weights. Experiments with L929 fibroblasts showed that surfaces with higher molecular weight pNIPAM were resistant to cell attachment. The density of cells and the percentage of spread cells decreased with increasing molecular weight. No detachment experiments were performed; therefore, no conclusions could be drawn to the effect of molecular weight on cell detachment dynamics.

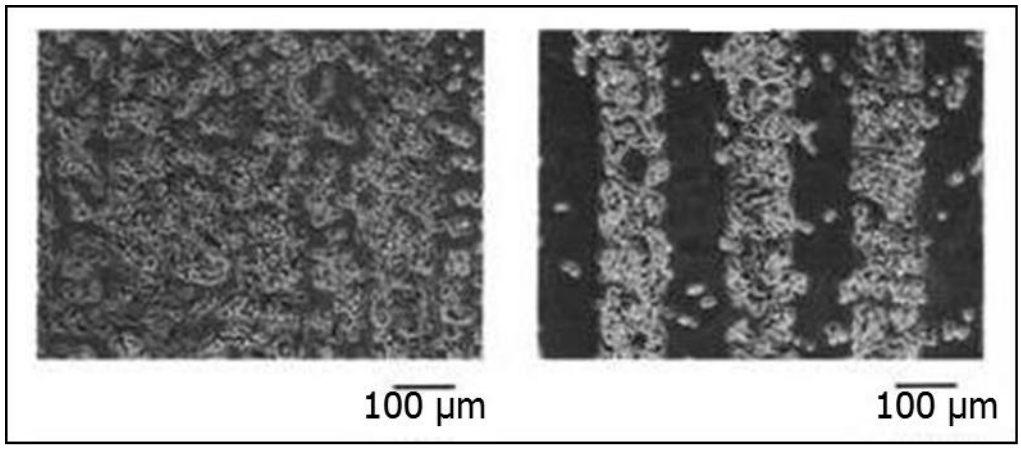

Figure 3.6 Controlling cell attachment and detachment with pNIPAM by using patterns. Image adapted from Ref. [99].

Several different studies investigated the effects of grafting gelatin with pNIPAM on cell attachment, and used thermoresponsive gelatin for cell sheet engineering.[99-104] Liu and Ito experimented with poly(*N*-isopropyl acrylamide-co-acrylic acid) coupled with azidophenyl groups (PIA-Az) and gelatin.[99] A micropattern of regions coated with

the copolymer without gelatin, and regions coated with copolymer with gelatin was obtained using a photomask and UV irradiation (see Fig. 3.6). Cells did not detach from PIA-Az-gelatin regions. The authors suggested that gelatin enhanced cell attachment so strongly that detachment did not occur. In the study of Morikawa and Matsuda, no BAECs adhered to pure pNIPAM or a mixed coating of pNIPAM and gelatin. Complete cell adhesion and spreading were found on a surface coated with a mixture of pNIPAM-gelatin (20.8 $\mu g/cm^2$) and pNIPAM (416 $\mu g/cm^2$), which was found to be an optimal ratio for cell attachment.[104] Ohya and Matsuda found that regardless of the concentration of pNIPAM-gelatin, smooth muscle cells attached to and proliferated on surfaces with pNIPAM to gelatin ratio higher than 12:1, which results in mechanically strong, stiff gels. The authors concluded that for best cell attachment and proliferation, a ratio of at least 12:1 and low concentration of pNIPAM-gelatin (which means larger pores and more void volume) should be used.[100]

PNIPAM copolymers grafted with RGD peptides (peptides containing arginine, glycine and aspartic acid) and insulin were also investigated. It was found that RGD enhanced cell attachment, while insulin enhanced cell growth.[105] Other approaches to controlling cell release from and attachment to pNIPAM-grafted surfaces include grafting pNIPAM with epidermal growth factor and ECM molecules, copolymerizing it with n-butyl methacrylate, or adding potassium ions to shift the LCST.[16, 106]

There are different hypotheses of how to improve cell adhesion, growth, as well as release. The various ways of enhancing cell attachment and detachment from pNIPAM grafted surfaces include using a porous membrane,[95] manipulating the composition of the grafted polymer,[16, 97] using different media for cell detachment than for cell

attachment,[27] controlling the thickness of the grafted polymer,[82] using various additives, such as gelatin, epidermal growth factor, RGD peptides, insulin, or ECM molecules,[16, 99-105] or adding ions to shift the conformation change to a different temperature.[106] Most methods for enhancing cell attachment and detachment relate to physical (rather than chemical) properties. A study on chemical properties of the surfaces would be desirable. In addition, although researchers developed hypotheses as to why some approaches are better than others, no one has compared all of the parameters (additives, media, substrate, temperature, etc.). A study finding the best set of parameters for cell attachment and release from pNIPAM-based thermoresponsive surfaces would be desirable to completely prove or disprove those mechanisms.

3.4 Hydrogels

Regenerative medicine is in need for injectable scaffolds from which cells or cell sheets can easily detach without undergoing any damage. Scaffolds provide a support for cells while they grow, develop ECM, and form a tissue. Thermoresponsive hydrogels composed of pure pNIPAM or pNIPAM copolymers are great candidates for such applications. Such hydrogels have several advantages: they allow cellular matrix reorganization, cell anchorage to the surface, permit diffusion and delivery of nutrients and growth factors, and their transition point can be changed by modifying their composition.[107] PNIPAM hydrogels respond to changes in temperature similarly as does pure pNIPAM: they become hydrated and swell when the temperature is below the LCST, and expel water, collapse, and become stiffer when the temperature is above the LCST.[108]

A study by von Recum et al. investigated poly(*N*-isopropyl acrylamide-co-4-(N-cinnamoylcarbamide) methylstyrene, which was UV crosslinked to form a hydrogel surface. Successful cell detachment using BAECs and adult human retinal pigmented epithelium was achieved. Due to the nature of the polymer (particularly the existence of functional amine groups), signaling and attachment molecules can be covalently attached to the polymer surface.[109] Another group developed peptide modified pNIPAM-co-acrylic acid hydrogels.[108] The hydrogels were modified with peptide chains to induce interaction of the hydrogels with cells on the molecular level. Rat calvarial osteoblasts, which were injected into the hydrogels, attached and proliferated. However, these hydrogels swell considerably due to presence of peptide chains, and may not have adequate mechanical integrity for extensive cell spreading and proliferation.

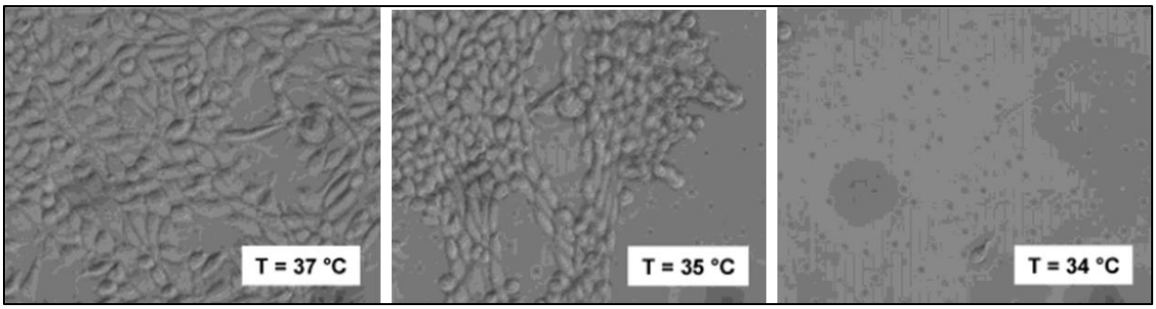

Figure 3.7 Mouse fibroblasts attached to pNIPAM hydrogels at 37^{o}C and detached at 34^{o}C. Image adapted from Ref. [107].

Schmaljohann et al. investigated graft copolymers of pNIPAM and poly(ethyleneglycol) (PEG) hydrogels.[107] As shown in Figure 3.7, mouse fibroblasts proliferated on the pNIPAM-PEG hydrogels and detached rapidly. The fast detachment was attributed to the presence of the hydrophilic PEG, as cells do not adhere readily to this hydrophilic surface. The researchers found that adding PEG to pNIPAM increased

the LCST of the copolymer. Other studies also found that adding a hydrophilic monomer to pNIPAM raises the LCST, while adding a hydrophobic monomer decreases it.[106] Based on experiments with pNIPAM in the phosphate-buffered saline solution, the researchers concluded that the addition of electrolytes decreases the LCST, which would allow higher PEG content without raising the LCST.[107] However, yet other researchers found that potassium ions increase the LCST.[106] These contradictory results can be attributed to using different copolymers of pNIPAM, which could respond differently to addition of electrolytes. The method of polymerization may affect whether the LCST changes as well, and should be considered when trying to determine the origins of the shift in the LCST.

PNIPAM-gelatin hydrogels were prepared with different graft chain densities to determine the optimal pNIPAM to gelatin ratio (P/G). Human umbilical vein endothelial cells adhered and spread on hydrogels with high P/G (12:1 and 18:1). The hydrogels with higher P/G had rougher surface topography than hydrogels with lower P/G. The researchers suggested that the hydrogels contain interconnected micropores or voids which allow diffusion of nutrients and oxygen. Better cell spreading on the hydrogels with higher P/G could be attributed to aggregation among pNIPAM chains, which gives the hydrogels greater strength and, in turn, greater capability of withstanding cell traction force.[101]

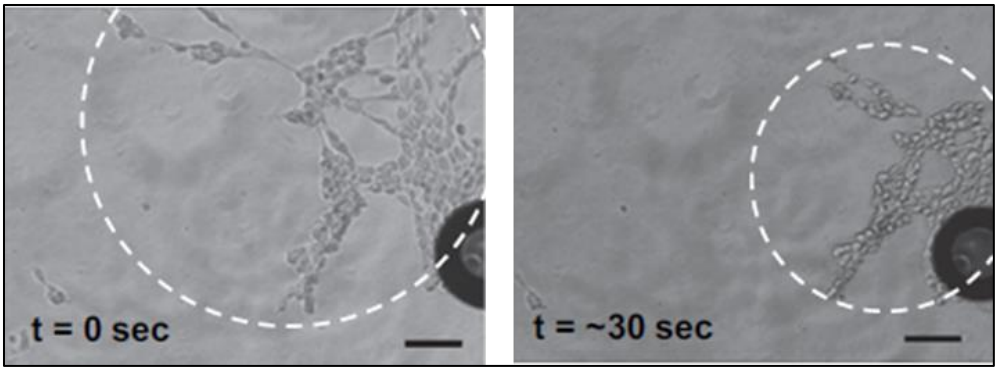

Figure 3.8 Smooth muscle precursor cells attached to pNIPAM hydrogels containing 2% nanoparticles and detached after 30 seconds at 25^{o}C. Image adapted from Ref. [110].

Nanocomposite hydrogels were developed to improve poor mechanical properties of chemically cross-linked pure pNIPAM hydrogels.[110, 111] Hou et al. made hydrogels consisting of a pNIPAM and polysiloxane nanoparticles. The LCST of the hydrogels remained unchanged. The researchers found that higher nanoparticle content improved the mechanical properties of the hydrogels, such as stiffness and resistance to deformation. Mouse smooth muscle precursor cells readily attached and detached from the hydrogels, which can be seen in Figure 3.8.[110] Haraguchi et al. studied hydrogels composed of pNIPAM and clay.[111] These nanocomposite hydrogels had high extensibility, as well as high modulus and strength, which can be controlled over a wide range without losing the extensibility. Human hepatoma cells, human dermal fibroblasts and human umbilical vein endothelial cells adhered and proliferated on the nanocomposite hydrogels regardless of the thickness of the gel, while little adhesion and no proliferation were observed on pure pNIPAM hydrogels. Complete cell sheet detachment was achieved. The authors attributed improved cell attachment and proliferation on polymer/clay hydrogels to increased protein absorption, surface flatness,

the balance of hydrophobicity (due to pNIPAM chains) and hydrophilicity (due to hydrophilic clay), and the surface ionic charges contributed by the exfoliated clay.

Hydrogels are a promising source for injectable scaffolds. They can adjust to the shape of the environment they are in, they allow diffusion of important nutrients, promote cell attachment and proliferation, and allow intact cell sheet detachment. PNIPAM hydrogels of various compositions have been investigated. Among them are hydrogels composed of poly(*N*-isopropyl acrylamide-co-4-(N-cinnamoylcarbamide)methylstyrene,[109] pNIPAM-co-acrylic acid,[108] pNIPAM-PEG,[107] pNIPAM-gelatin,[101] as well as nanocomposite hydrogels.[110, 111] It was found that nanocomposite hydrogels are an improvement over pure pNIPAM hydrogels, with better mechanical properties and improved cell adhesion.

3.5 Spheroids

Spheroid formation is another application of pNIPAM-modified surfaces. It is desirable to make multicellular spheroids because their morphology and functionality are similar to the morphology and functionality of tissues and organs.[112, 113] Spheroids can be used for toxicology tests, for developing hybrid artificial organs[112], for the study of tumor environments, or for evaluation of the effects of chemotherapy or radiation therapy on tumors.[113]

Spheroids made using pNIPAM-modified surfaces were first mentioned in a 1990 study by Takezawa et al.[114] PNIPAM conjugated with collagen was used as a substratum for the cell culture of human dermal fibroblasts. Once the cells grew to confluency, the resulting cell sheet was detached. The detached cell sheet was transferred to a hydrophobic dish in which the sheet gradually aggregated and formed a multicellular

spheroid. Because the spheroids adhered to tissue culture dishes, the authors of the study concluded that at least the surface cells of the spheroids were viable.

One drawback to this method of spheroid formation is that it does not allow control of the size and number of spheroids formed. In a later study, researchers tried to control the size and cell population ratio of the formed spheroids by changing the seeding area and the seeding cell density.[115] Using collagen-conjugated pNIPAM, the researchers obtained heterospheroids composed of human dermal fibroblasts and rat hepatocytes, and successfully controlled the diameter and population ratio of the spheroids. Spheroids formed in this manner were covered with a few layers of squamous fibroblasts. These fibroblasts resembled epithelial cells and differed morphologically from the fibroblasts in the inside of the spheroids. The researchers concluded this to be a useful model of the tissue architecture of the liver.

For better size regulation, cell adhesive and non-adhesive regions were created using ultraviolet (UV) irradiation and photomasks.[112, 116] A schematic of spheroids formation using this method is shown in Figure 3.9. Photomasks were used to direct UV irradiation over the surfaces coated with collagen-conjugated pNIPAM. The irradiated areas promoted cell adhesion, and the non-irradiated areas were non-adhesive. Seeded cells adhered and grew only on the irradiated areas. Confluent cell sheets were detached from the surface and transferred to a non-adhesive dish. There they formed spheroids.

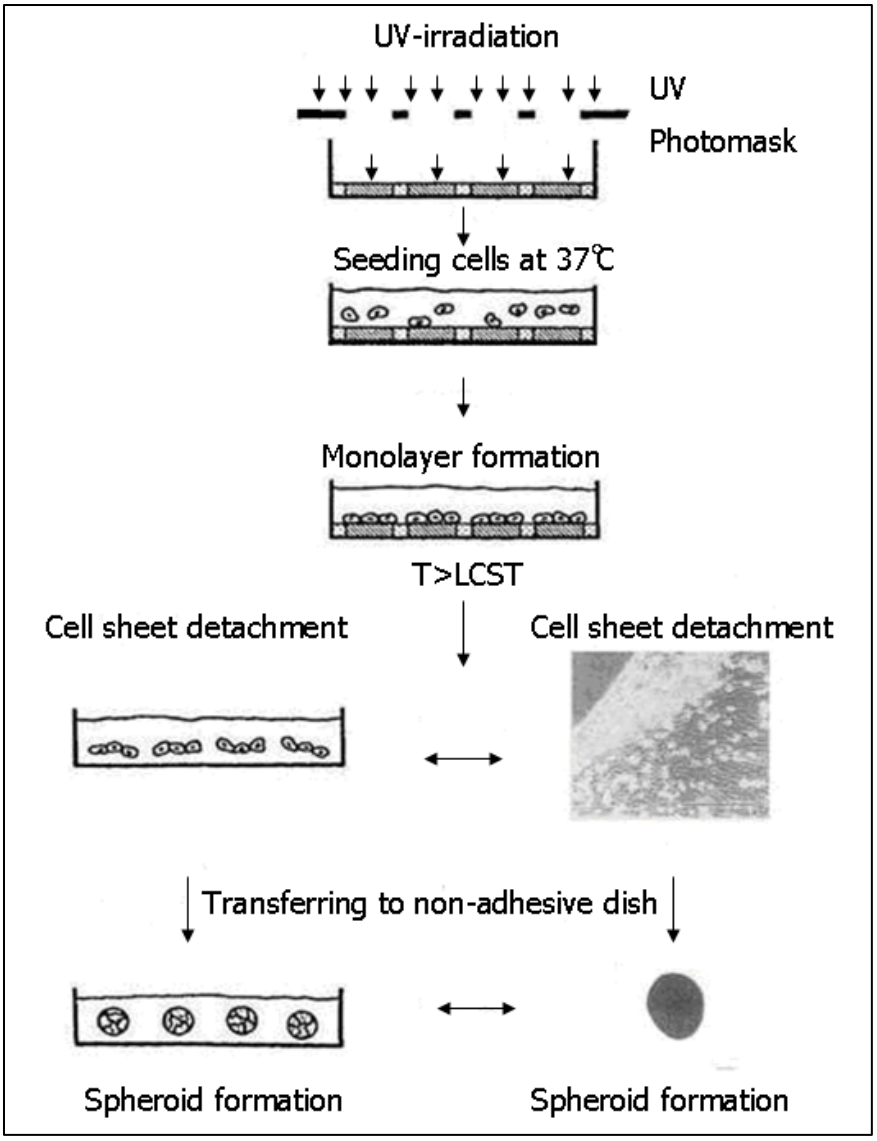

Figure 3.9 Schematic of formation of multicellular spheroids and micrographs illustrating resultant spheroids from human dermal fibroblasts and rat hepatocytes. Bars are 300 μm. Image adapted from Ref. [115] (pictures) and Ref. [112] (schematic).

This method makes regulation of the size and number of spheroids possible. Yamazaki et al. used this method in their study to obtain spheroids composed of human dermal fibroblasts.[112] They found that the optimal content of collagen for 100% attachability and detachability is 4-5% and the optimal UV energy level is 2000 J/m^2. The

viability of the cells in the spheroids depended on the size of the spheroids. Cells in larger spheroids lost their viability over time, while cells in smaller spheroids retained theirs.

The formation of spheroids from 23 different cell types was investigated using the above mentioned method.[116] Different types of mesenchymal and epithelial cells were used for the experiments. Out of the 23 different cell types, 19 cell types formed cell sheets, and 15 formed spheroids. Four types of cells (rabbit chondrocytes, human umbilical vein endothelial cells, MDCK epithelial cells, and human cholagioadenocarcinoma cells) did not form spheroids, but no explanation was given for this anomaly. Shima et al. investigated heterospheroids composed of esophageal squamous cell carcinoma cells and esophageal fibroblasts.[113] The spheroids were composed of an outer zone containing carcinoma cells, and an intermediate and a central necrotic zone composed of fibroblasts. The authors hypothesized that the necrotic center could be due to the tight contact of the cells in the center of the spheroid, and low permeation of medium for nutrient and waste exchange.

Endoh et al. obtained various spheroid sizes by etching the surfaces coated with collagen-conjugated pNIPAM [117]. The diameter of the spheroids could be estimated by the diameter of the cell sheet (the spheroids were 10% size of the cell sheets). After performing biochemical studies, the authors found that larger spheroids are characterized by lower DNA and lactate dehydrogenase content, and lower albumin secretion when compared to smaller spheroids. They concluded that cells making up larger spheroids show decreased viability and activity.

Recently, our group developed a promising method for generation of spheroids using pNIPAM hydrogels.[96] With the control of the area to which the cells attach,

uniform spheroids of desired size can be generated in a relatively short amount of time (4 to 28 hours, depending on cell type). A similar approach was undertaken by Wang et al.[118] In their work, Wang et al. generated p(NIPAM-co-acrylic acid) microgels that supported cell attachment and proliferation when kept at 37^{o}C. Cells attached to microgels formed multicellular spheroids. When the temperature was lowered to room temperature, the microgels liquefied, releasing the spheroids.

Spheroids were originally made by detaching confluent cell sheets and letting them aggregate.[114] Researchers developed different methods of controlling the size and number of spheroids by changing the seeding area and the seeding cell density,[115] by creating cell adhesive and non-adhesive regions using UV irradiation and photomasks,[112, 116] or by etching collagen-pNIPAM-grafted surfaces.[117] Fifteen different cell types were proven to be capable of forming spheroids.[116] Currently, spheroids are of special interest in oncology research. Other methods that are commonly used for spheroid formation for research are liquid overlay technique or hanging drop method.[53] These methods, however, do not regulate the size and number of spheroids very well. When the size is important, preparation of the spheroid using a thermoresponsive polymer is recommended.

3.6 Pattern and shape engineering

Once it was demonstrated that culturing cells on pNIPAM-grafted dishes could produce intact cell sheets that can be detached and used for other applications, researchers moved on to constructing three-dimensional cell sheets (which can mimic native tissue better than single-layered cell sheets), and to controlling the shape and size

of the cell sheets (which then can be applied to surfaces where specific shape and size of the sheet is required).

In an attempt to create micropatterned surfaces, Ito et al. and Chen et al. used pNIPAM copolymerized with acrylic acid and coupled with azidoaniline immobilized in a pattern on TCPS by photolithography. Mouse fibroblast STO cells detached only from the copolymer grafted domain (shown in Figure 3.10).[46]

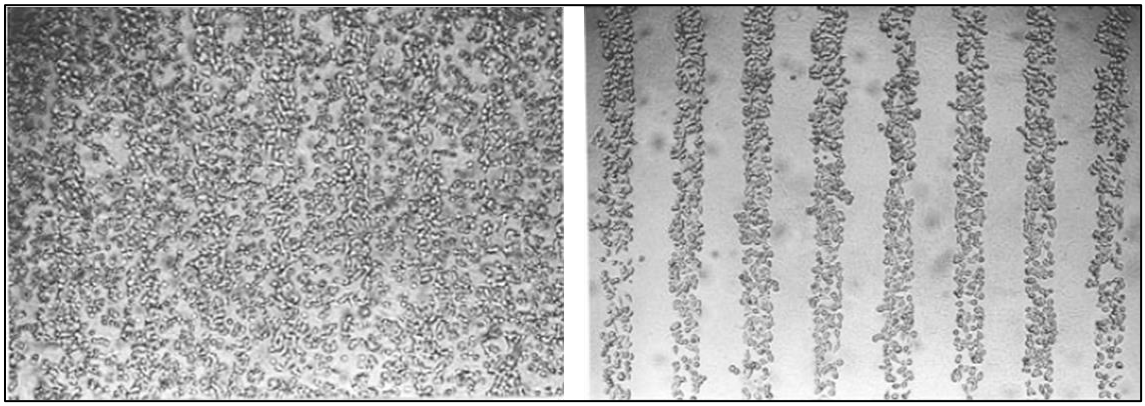

Figure 3.10 Mouse fibroblast cells attached to tissue culture polystyrene dishes patterned with NIPAM-acrylic acid copolymer at 37^{o}C (first image) and after 30 minutes at 10^{o}C. Image adapted from Ref. [46].

Chen et al. investigated the effect of fibronectin and albumin adsorption to these surfaces on cell attachment and detachment. Cell detachment was observed from grafted regions that were not adsorbed with a protein or preadsorbed with albumin.[45] Yamato et al. used laser ablation to form micropatterning on pNIPAM surfaces with high grafting density. Fibronectin was preadsorbed to the ablated regions at 20^{o}C. Hepatocytes adhered only to the ablated regions, since pNIPAM inhibits cell adhesion below its LCST. When the temperature was raised to 37^{o}C (normal cell culture temperature), cells remained on the ablated regions because they do not adhere to pNIPAM with high grafting

density.[119] Cheng et al. coated surfaces with an embedded microheater array with plasma polymerized pNIPAM. The use of the microheater/pNIPAM array allowed for localized phase transition and, therefore, localized cell adhesion. At room temperature, BAECs and bovine smooth muscle cells attached to the area heated by the heaters, but did not attach to the surrounding areas, creating in this way a pattern on the surface.[120]

There also have been studies on constructing layered sheets composed of different cell types. Hirose et al. constructed a single layer patterned cell sheet using pNIPAM and poly(*N,N'*-dimethyl acrylamide) (PDMAM). The tissue culture dishes were grafted with pNIPAM using electron beam irradiation, after which a mask in a shape of a square was used to cover a portion of the grafted surface, and PDMAM was grafted onto the uncovered surface. PDMAM does not support cell adhesion, therefore cell adhesive (pNIPAM) and non-adhesive (PDMAM) domains were created. Human aortic endothelial cells (HAECs) were seeded onto the grafted surface. Such grafting arrangements resulted in a square-shaped HAEC cell sheet.[25] Harimoto et al. constructed a three-dimensional double-layered co-culture of HAECs and rat hepatocytes using the previously described method. HAECs were cultured to confluency on dishes co-grafted with pNIPAM and PDMAM. After detachment, the HAEC cell sheet was laid over a confluent cell sheet of rat hepatocytes. Close cell-to-cell interactions were established and the differentiated cell shape and albumin expression of HAECs were maintained while in co-culture.[121]

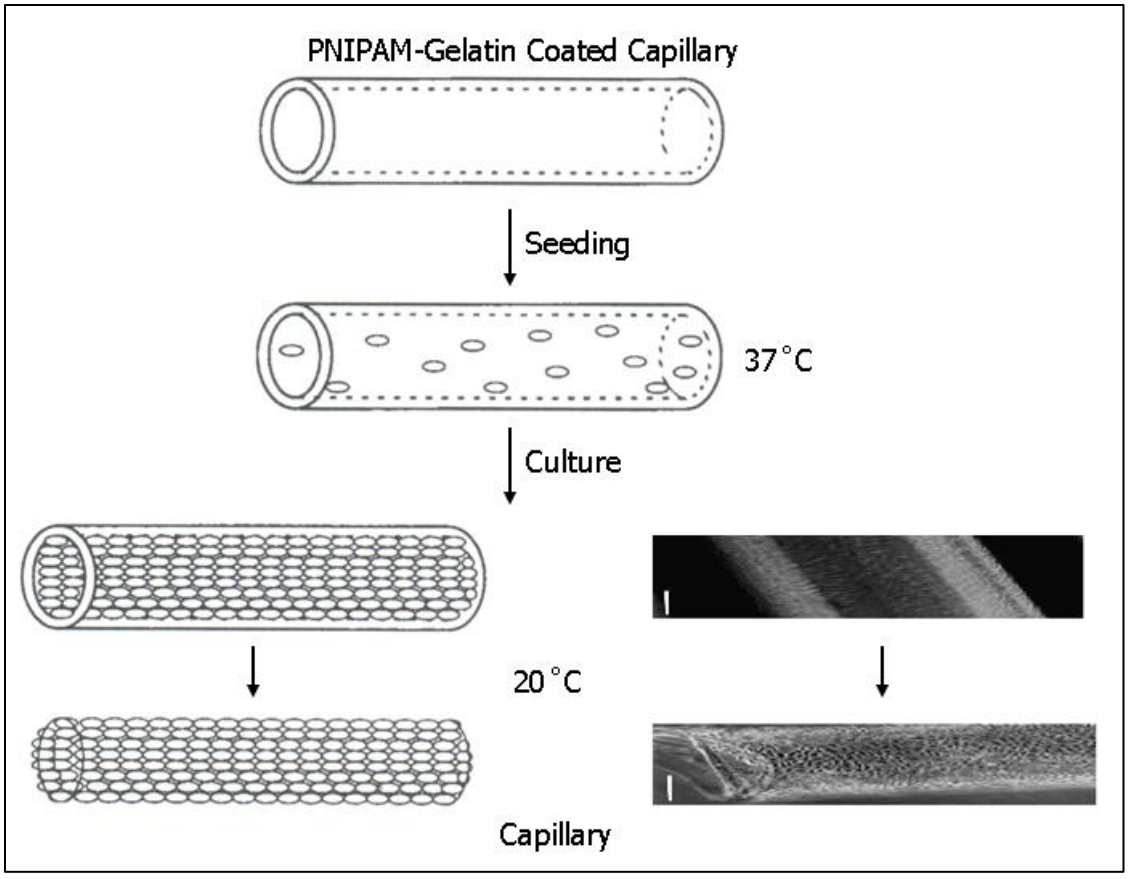

Figure 3.11 Formation of a tubular endothelial cell sheet. Image adapted from [102].

In another study, Hirose et al. used hepatocytes, BAECs and HAECs to form patterned single-cell type and patterned two-cell types cultures. PNIPAM and PDMAM were grafted onto cell culture dishes using a mask to create patterns. HAECs attached and spread only on the pNIPAM-grafted domains. This method allows the creation of cell sheets of desirable size and shape. For the patterned co-culture of hepatocytes and BAECs, a TCPS dish was grafted with pNIPAM using a mask to create a pattern. Hepatocytes were seeded on the grafted dish and detached only from the pNIPAM domain, remaining attached to the ungrafted TCPS domain. BAECs were then seeded and attached to the newly exposed pNIPAM domain. In this manner a patterned co-culture of the two different cell types was established.[122]

Matsuda attempted to construct a 3-D tubular cell construct using a pNIPAM-grafted gelatin and a glass capillary tube. Figure 3.11 shows the formation of the tubular construct. First, the capillary tube was coated with aqueous solution of pNIPAM-grafted gelatin and air dried. Endothelial cells were seeded in the tube, after which the tube was immersed in medium. After the cells reached confluence, the tubular construct detached from the capillary tube. Images next to the schematic show the capillary tube with a confluent sheet of endothelial cells growing on it, as well as the detached tubular construct.[102]

PNIPAM surfaces have been used for the formation of multi-layered sheets and 3D tissue-like constructs. Shape-engineered tissues have been created via micropatterning achieved in many different ways (photolithography,[45, 46] laser ablation,[119] microheater arrays,[120] cell adhesive and cell non-adhesive regions [25, 121, 122]). Shape-engineered tissues could be used for transplantations, modeling of organs and tissues for in vitro investigations, cell separation, or research on cellular communication. PNIPAM provides researchers with an opportunity for creating and manipulating such constructs. Using this thermoresponsive polymer made it possible to engineer single- and multi-layered cell sheets composed of one or more different cell types. The engineered cell sheets retain their morphological and physiological properties during the manipulations and therefore can be used for other applications.

3.7 Tissue transplantation

The ultimate goal of tissue engineering is to repair or even replace a damaged organ. Tissue transplantation requires the engineered tissue to have morphological and physiological properties identical to the ones of the native tissue. Such resemblance

lowers the risk of transplant rejection and helps ensure successful transplantation. In vitro formation of different tissue types has been reported. The following section gives a brief overview of advances that have been made in tissue transplantation using pNIPAM-grafted surfaces as a substrate.

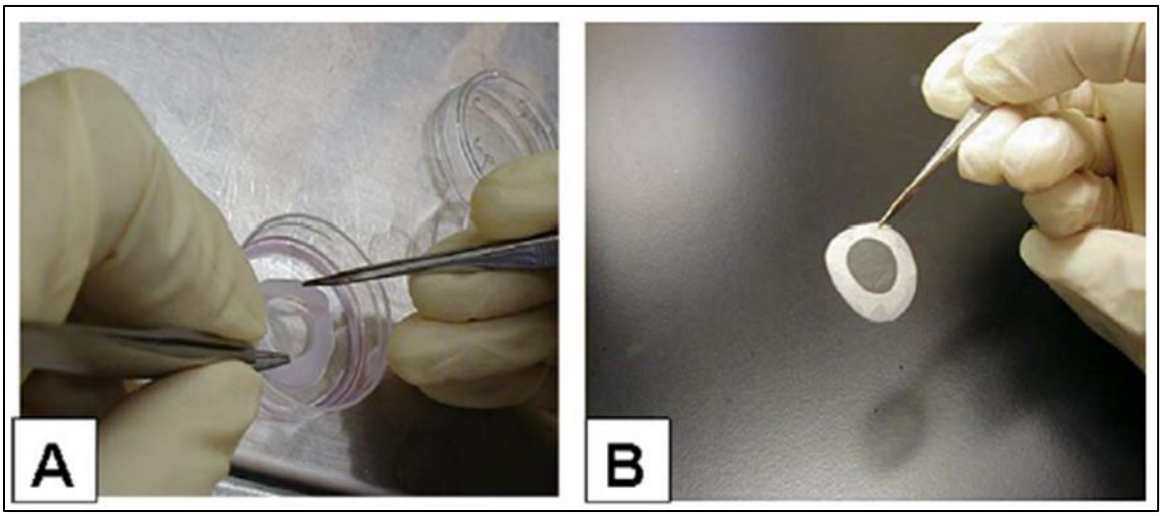

Figure 3.12 Chondrocyte sheets growing on pNIPAM substrate (A) and detached after lowering the temperature (B). Image adapted from Ref. [49].

Kaneshiro et al. transplanted chondrocyte sheets into Japanese white rabbits to examine their effectiveness in repairing defects of articular cartilage. Chondrocytes were cultured on pNIPAM-grafted dishes and then detached with a help of a PVDF membrane (see Figure 3.12). The cell sheets readily attached to the transplantation area. Rabbits with the transplants showed only slight degeneration of the cartilage compared to rabbits with untreated cartilage, which suffered progressive cartilage degeneration.[49] Ibusuki et al. used a pNIPAM-gelatin solution as a moldable scaffold for cartilage repair. Injured knees of Japanese white rabbits were repaired using 5 different transplantation methods. The researchers used combinations of pNIPAM-gelatin solution, chondrocytes and

precultured tissue with periosteum or collagen film as covering material. Using either the periosteum or collagen film together with the cell-incorporated pNIPAM-gelatin solution and the precultured tissue proved to be the best method for the application. The transplantation resulted in a smooth surface, no leakage of the transplant was observed, and the foreign-body response and the surface deformation was minimal.[103]

Several studies were performed on repairing damaged corneal tissue. Sumide et al. transplanted human corneal endothelial cell sheets obtained by detachment from pNIPAM-grafted dishes into eyes of New Zealand White rabbits. The cell sheets attached to the stroma within 5 minutes. The swelling of the eyes was significantly reduced and the corneal transparency was visibly improved.[51] Nishida et al. performed cell sheet transplantation into rabbits' eyes. The sheet covered the entire corneal surface. The corneal epithelium had normal appearance and all epithelial cell layers expressed keratin.[26] In a later study, Nishida et al. transplanted oral mucosal epithelial cell sheets into human eyes. They collected oral mucosal tissue from patients with bilateral total corneal stem cell deficiencies and cultured them on pNIPAM-grafted dishes. Figure 3.13, image A, shows how a cell sheet was detached from the dish using a PVDF membrane. The detached cell sheet (image B) had characteristics of the native cells. The sheet was then overlaid onto the corneal stroma (image C). After a few minutes the membrane was removed. The transplantation restored corneal transparency and patients' vision was markedly improved.[50]

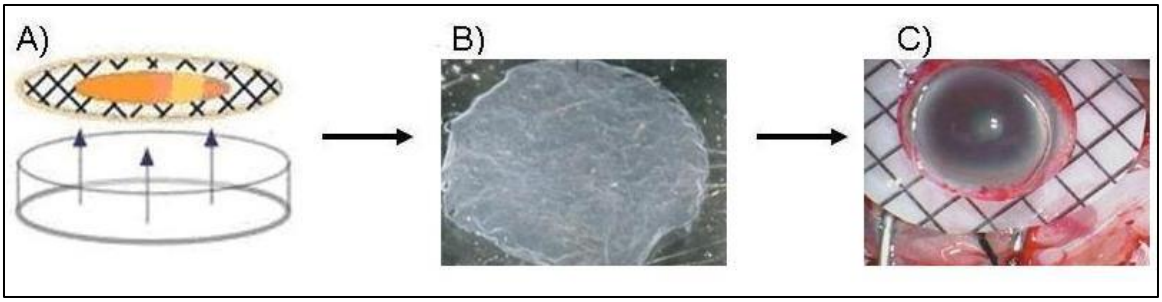

Figure 3.13 Transplantation of engineered corneal epithelial cell sheet onto the corneal stroma: A) schematic of detaching a cell sheet; B) detached cell sheet; C) transplantation of the detached cell sheet onto the eye. Image adapted from Ref. [26] (image A), Ref. [50] (image B and C).

Cardiac tissue transplantation was a subject of studies by Shimizu et al. and Memon et al.[48, 52] Shimizu et al. engineered cardiac tissue by layering cell sheets composed of neonatal rat ventricular myocytes with the use of dishes coated with pNIPAM. The engineered cell sheets pulsed simultaneously and spontaneously, indicating established connections between the layered sheets. The sheets were then transplanted into dorsal subcutaneous tissue of nude rats. The sheets continued to pulsate spontaneously. The tissue had characteristic structures of heart tissue and exhibited multiple neovascularization.[52] Memon et al. attempted to repair injured myocardium by implantation of myoblast cell sheet into Lewis rats' hearts. Single-layered cell sheets were detached from pNIPAM-grafted dishes and overlaid to make one thicker sheet. After the transplantation, evident reduction of myocardial fibrosis occurred. The scar area was replaced by the new cells. Increased number of local capillaries and uniform and a thicker anterior wall was observed.[48]

Engineering cell sheets using pNIPAM-grafted dishes produces cell sheets ready for transplantation. Cells grown on pNIPAM have been used to repair damaged cartilage, corneal and cardiac tissue. Because low-temperature liftoff is a mostly non-destructive

method of detachment, cell sheets retain their structure and functions after the detachment. They can readily attach to a new surface, often without any sutures. This method eliminates the problem of the patient's immune response, because the patient's own cells can be extracted, cultured and used for transplantation, and, therefore, it assists faster recovery. There are examples of treatment of patients (e.g., in Japan), and preliminary research has been published.[50] However, these treatments are not common worldwide as of yet. More clinical trials need to be done for this method to be widely available for use in humans and for it to replace the traditional donor organ and tissue transplantations.

3.8 Other uses of pNIPAM with cells

PNIPAM has a wide range of applications besides tissue engineering. As previously mentioned, it can be used for manipulation of microorganisms or for control of bioadhesion and bioadsorption. A different way of applying pNIPAM in research with cells is cell deformation and separation.

The characteristic phase transition of pNIPAM was used in a study of deformation of red blood cells. The extent to which red blood cells can deform influences blood flow greatly. Studying such deformation could help understand the cause of various diseases, e.g., anemia and malaria.[123] In their study, Pelah et al. used a pNIPAM gel as an actuator for inducing shape deformation in red blood cells.[124, 125] Cells were embedded either between a glass slide and a layer of pNIPAM gel, or between two layers of pNIPAM gel.

The deformation of the cells was achieved through stretching and compression of the polymer. Figure 3.14 shows such a cell manipulation through planar actuation. Panel

A shows a schematic representation of the deformation. The cells are placed between a glass slide and a layer of a pNIPAM gel. Below the LCST, the gel swells, and the cells deform (contract) under the pressure of the swollen pNIPAM. Once the LCST is raised, the gel expels the water, and it contracts. The pressure on the cells is relieved, and the cells come back to their normal shape. Panel B shows images of red blood cells undergoing such planar actuation. Panel C shows an experiment with rigid and soft red blood cells. Arrows in the picture point to the rigid red blood cells. Rigid cells form a dimple upon deformation and seem to deform less than soft cells.

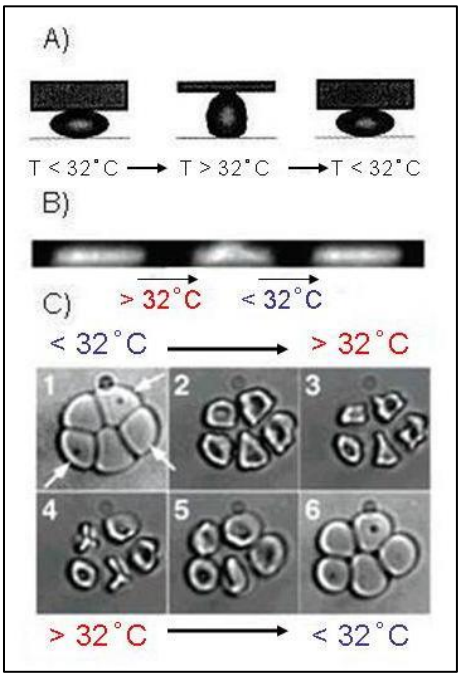

Figure 3.14 Reversible deformation of red blood cells using pNIPAM actuator: A) schematic of planar deformation (side view); B) and C) deformation of red blood cells by planar actuator. Image adapted from Ref. [124] (image A), Ref. [125] (image B and C).

The authors proposed that using this method, cells could be differentiated based on their different mechanical properties.[124] The researchers found this method of cell

manipulation advantageous in comparison to other cell techniques such as tweezers or micropipettes. Using pNIPAM as an actuator allows adjustments of the LCST and incorporation of different biomolecules. This method is simple to prepare and to apply, and it can be applied to large numbers of cells, not just a single cell. The forces applied, however, cannot be directly controlled. Creation of forces of known magnitude would be desirable.[125]

Thermoresponsive polymers have also been used for cell separation. In one study, pNIPAM has been used to investigate adherent inflammatory cells: monocytes, macrophages, and foreign body giant cells.[126] According to a study performed by Collier et al., pNIPAM-modified surfaces regulate the adherence of monocytes in a different manner than the adherence of macrophages, or the formation of foreign body giant cell. The study revealed that the adhesive nature of monocytes differs from the adhesive nature of macrophages, which in turn differs from the adhesive nature of foreign body giant cells. This implies increased specialization of these cells on material surfaces. Lowering the temperature of the surfaces caused all cell types to detach. However, monocytes and macrophages detached more easily than foreign body giant cells. The differences in the adhesiveness and the detachment of the cells allowed cell separation for study of adhesion mechanisms and phenotypic expression.

PNIPAM has also been used for separation of cells in an aqueous two-phase system (ATPS).[127] The polymer was used as a ligand carrier in ATPS. PNIPAM was copolymerized with monoclonal antibodies which recognize specific cell surface receptors. Monoclonal antibodies are more expensive than fatty acids or dye molecules commonly used as ligands for the partitioning; they are, however, more specific. This

method was used to separate human acute myeloid leukemia cells from human T lymphoma cells and colon cancer cells. With this method, cells partition to the top phase and the polymer is recycled for future cell separation. The optimal number of cells was found to be 3.5 x 10^5 cells/1.4 g of ATPS. The maximum cell partitioning was 93%, with the ligand concentration of 40 μg/mg of polymer (80 μg/1.4 g of ATPS) or above. The researchers found that although increased ligand density improved cell partitioning, separation was still less effective if more than the optimal number of cells was used.

PNIPAM-grafted surfaces can be applied not only for cell sheet engineering, but also for manipulation of single cells. They already have been used for the study of deformation of red blood cells and for cell separation.[124-127] Using pNIPAM as a tool for cell deformation and separation offers new ways of obtaining important experimental results. Cell deformation with pNIPAM as an actuator seems to be an improved way of cell manipulation when compared to the traditional methods. PNIPAM is also useful for separation and fractionation. ATPS is a traditional method for separation and fractionation. However, using monoclonal antibodies for this process is expensive. Using a thermoresponsive polymer as a ligand carrier and recycling it for another use (about 90% of the polymer-antibody conjugate can be recovered) makes the otherwise costly process more affordable.[127]

3.9 Bioadhesion and bioadsorption

Biofouling, or the adhesion of deleterious organisms, is a common problem in the medical device, food and marine industries.[128, 129] Biofilms result from the accumulation of bacteria, bacterial metabolites, and organic molecules on a surface. While biofilms are beneficial for bacteria, they can be harmful for humans. Biofilm

formation, or biofouling, is often responsible for various infections (e.g., cystic fibrosis), device failures (catheters), or corrosion (ship hulls), leading to lost revenues. Surfaces exposed to biofouling have been coated with various paints and compounds containing metal organocomplexes to prevent degeneration. However, a compound that is toxic for bacteria may also be detrimental for other organisms, which is an unwanted side effect[130]. The ability of pNIPAM to resist cell adhesion (and its apparent non-toxicity) caught the attention of those interested in limiting biofouling of materials.

Callewaert et al. investigated modifying stainless steel surfaces with thermoresponsive polymers.[128] In this case, cell adhesion experiments were performed using *Saccharomyces cerevisiae. S. cerevisiae* is used in wine fermentation and ethanol production. The study reported ~2 x 10^4 cells/cm^2 adhering to stainless steel surfaces coated with pNIPAM at room temperature, while as much as 55 to 75 x 10^4 cells/cm^2 adhered to untreated stainless steel surface exposed to an identical cell population. The authors suggested that using a pNIPAM coating could be an effective way of preventing cell adhesion to surfaces and, therefore, preventing biofouling.

The topic of biofouling also interested Ista et al.[130] They performed multiple experiments using two different strains of bacteria (*Staphylococcus epidermidis* and *Halomonas marina,* now referred to as *Cobetia marina)* to determine the effectiveness of pNIPAM as a biofouling release agent. *H. marina* (*Cobetia)* is a Gram-negative bacterium that is often used as a marine biofouling model organism, whereas *S. epidermidis* is Gram-positive bacterium which is important for medical biofouling applications.

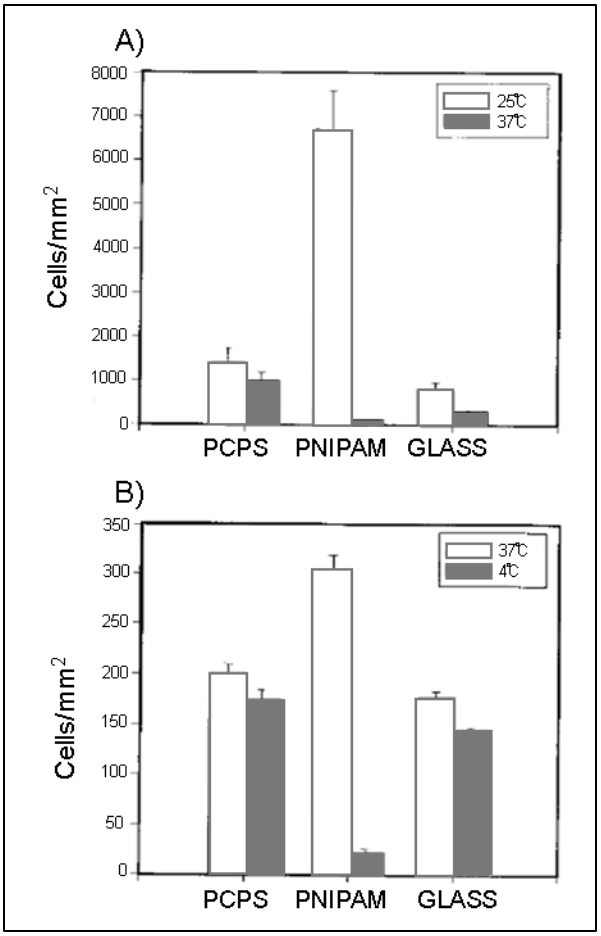

Figure 3.15 Long-term incubation and detachment of A) *S. epidermidis* and B) *H. marina* from plasma-cleaned polystyrene (PCPS) dishes, pNIPAM-grafted surfaces, and glass. Image adapted from Ref. [130].

Figure 3.15 shows the results of one such experiment. The authors carried out a series of long-term incubation experiments. The incubation was performed at 25°C with *S. epidermidis* (A), and at 37°C with *H. marina* (B), at which temperatures the growth and attachment of the bacteria is enhanced. PNIPAM-grafted surfaces promoted bacterial attachment at these temperatures to a much larger extent than plasma-cleaned polystyrene (PCPS) dishes and glass (white bars). After 72 hours of incubation, the *S. epidermidis* surfaces were washed with phosphate-buffered saline at 37°C, and the *H. marina* surfaces were washed with artificial seawater at 4°C. In both cases only small detachment was

observed from PCPS and glass surfaces, while 98% of *S. epidermidis* and 93% of *H. marina* detached from pNIPAM-grafted surfaces (gray bars).

Bacterial adsorption to surfaces coated with thermoresponsive pNIPAM films was also investigated by other groups.[129, 131] Studies were performed with *Salmonella typhimurium, Bacillus cereus,*[131] and *Listeria monocytogenes.[129] L. monocytogenes* is a motile, Gram-positive bacterium. It is a foodborne pathogen causing the disease listeriosis. *S. typhimurium* is a Gram-negative, motile bacterium responsible for gastroenteritis in humans. *B. cereus* is a Gram-positive, non-motile bacterium and is a foodborne pathogen as well. In all three cases, the researchers concluded that thermoresponsive polymers can be used for controlling bacterial adsorption to surfaces. Below the LCST of the polymers, there is a decreased adsorption of bacteria to the surfaces. The adsorption increases above the LCST. All three studies suggested that bacteria adhere less to hydrophobic surfaces than to hydrophilic surfaces.

PNIPAM-grafted surfaces have been used for studies of adhesion and detachment from thermoresponsive surfaces of various microorganisms, such as yeast (*S. cerevisiae*) ([128]) and bacteria (*S. epidermidis, H. marina, S. typhimurium*, *B. cereus,* and *L. monocytogenes,* [129-131]). Studies performed on pNIPAM as an anti-fouling coating have shown that pNIPAM coatings are not toxic to microorganisms, but can reduce bioadhesion and biofouling. The toxicity of pNIPAM and pNIPAM-coated surfaces to mammalian cells is evaluated in detail in Chapter 4. PNIPAM coatings could be used as an alternative to standard coatings (e.g., paints containing metal organocomplexes). However, a study comparing effectiveness for pNIPAM-coating versus a standard non-fouling coating would be recommended to examine how effective pNIPAM is versus

commercially available coatings. Furthermore, the pNIPAM coatings were exposed to highly controlled environments (i.e., single strains of bacteria in solution, rather than the highly complex milieu they would be exposed to in aquatic environments). Therefore, expanded studies of the utility of pNIPAM coatings to resist biofouling from a mixture of many bacterial strains would also be advisable before their adoption.

3.10 Manipulation of microorganisms

The conformation change of pNIPAM due to change in temperature can also be useful for work with organisms like yeast or bacteria. In order to examine such organisms more closely, techniques of manipulating the cells need to be developed. Researchers have been using pNIPAM for bioseparation of bacteria,[132] laser manipulation of yeast cells,[133] magnetic manipulation of yeast cells,[134] and manipulation using elastic deformation.[135] In some cases, using pNIPAM to manipulate microorganisms is more advantageous than using methods like laser tweezers or phage-display systems.[133, 134] The rationale for these advantages is given below.

PNIPAM can be used to concentrate dilute dispersions of bacteria.[132] Researchers achieved bioseparation of *Staphylococcus epidermidis* bacteria by means of pNIPAM-co-acrylic acid hydrogels. When added to the aqueous dispersion of the bacteria, hydrogels swell upon lowering temperature. While swelling, the hydrogels absorb water from the dispersion, and therefore, increase the concentration of the bacterial suspension. This method was successful in concentrating the suspension; however, agitation of the mixture was required to prevent bacterial absorption to the surface of hydrogels.

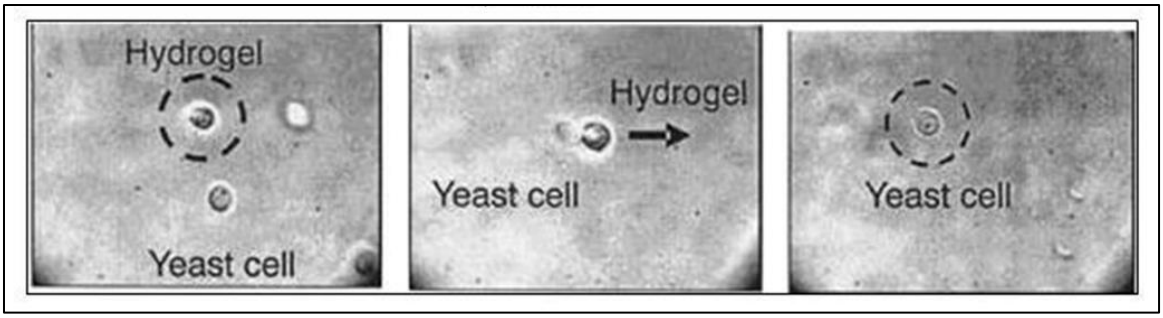

Figure 3.16 Manipulating microorganisms using pNIPAM by laser manipulation. Image adapted from Ref. [133].

Figure 3.16 shows how a yeast cell can be manipulated using a pNIPAM-gel microbead and a laser.[133] The goal of this process is to remove one yeast cell from the population, without destroying or injuring the cell. The first picture shows formation of the pNIPAM-gel at the point of the laser beam. Once formed, the gel is moved towards the target cell using the laser. The yeast cell adheres to the gel and is moved together with the gel in the desired direction (second picture). Finally, when the gel-yeast cell complex arrives at the desired destination, the laser is turned off. The gel dissolves, and the yeast cell is released (last picture). According to the authors, such laser manipulation is superior to using laser tweezers (without pNIPAM). The previous method caused damage to the cells due to irradiation. This damage is avoided using the new method, where laser manipulates the hydrogel, not the cell.

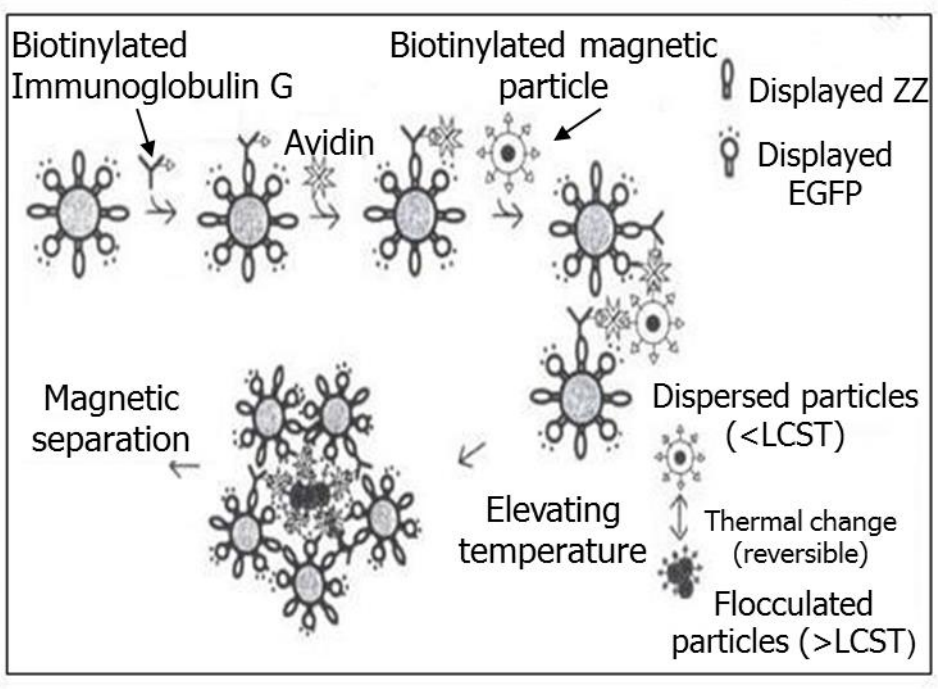

Figure 3.17 Manipulating microorganisms using pNIPAM by magnetic separation. (ZZ – protein binding immunoglobulin G; EGFP – enhanced green fluorescent protein). Image adapted from Ref. [134].

Figure 3.17 shows a novel method of affinity selection of cells from a yeast-cell surface display library.[134] Thermoresponsive pNIPAM magnetic nanoparticles were used for the selection. Yeast cells displaying an immunoglobulin G binding protein specifically bind biotinylated immunoglobulin G, which in turn binds avidin. Dispersed magnetic nanoparticles bind to avidin, therefore indirectly binding to the yeast cells. The temperature is then elevated, causing the nanoparticles to flocculate. A magnet is used to capture the particles together with captured yeast cells. This method was found to be fast and effective. The enrichment ratio of target cells was high (up to 70-fold per cycle) and the target cells could be subsequently amplified by cultivation. Furthermore, this method is faster than using phage display system, because it reduces the amount of steps required for the affinity selection.

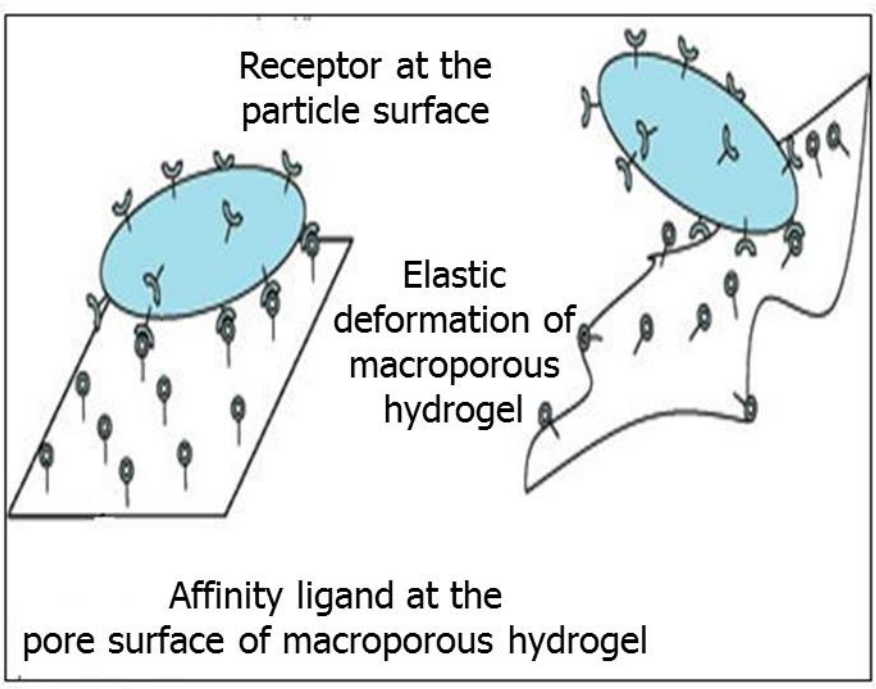

Figure 3.18 Manipulating microorganisms using pNIPAM by elastic deformation. Image adapted from Ref. [135].

Figure 3.18 is an example of manipulation using elastic deformation. A particle or cell bound to an affinity ligand at the surface of a macroporous pNIPAM hydrogel can be detached from the hydrogel by means of increasing the temperature.[135] The change in temperature causes the hydrogel to shrink, resulting in the detachment of particles from the hydrogel. The authors of the study concluded that the detachment was induced by the deformation of the surface to which the particles were bound. The authors used yeast cells bound to Concanavalin A. Hydrogels with different cross-linking densities and monomer concentrations were investigated. The highest cell release (37%) occurred from hydrogels with lowest cross-linking density and monomer concentration. The authors attributed this result to higher elastic deformation of those hydrogels. According to the authors, this method could be used for affinity selection of cells, which would serve as a model to mimic interactions of bacteria in biological systems. However, it should be

noted that the highest % cell release was 37%, which is low when compared to 80% to 100% recovery of yeast cells when applying external compression force to Concanavalin A bound monolithic polyacrylamide macroporous hydrogels.

The manipulation of microorganisms using pNIPAM appears to be an attractive alternative to traditional methods such as laser tweezers and phage-display systems. Using pNIPAM often proves to be a more effective and safer method than previous methods.[133] PNIPAM has been used for concentrating dilute dispersions of bacteria,[132] and manipulating yeast cells using laser, [133] elastic deformation,[135] and magnetic manipulation.[134] However, some obstacles need to be overcome. Successful bioseparation using pNIPAM is hindered by bacterial adsorption to the hydrogels.[132] Also, a higher degree of detachment needs to be achieved for elastic deformation to be an effective tool for binding and releasing particles.

3.11 Conclusions

Over the past two decades, poly(*N*-isopropyl acrylamide) (pNIPAM) has become widely used for bioengineering applications. In particular, pNIPAM substrates have been used for the non-destructive release of biological cells and proteins. In this chapter, we review the applications for which pNIPAM substrates have been used to release biological cells, including for the study of the extracellular matrix (ECM), for cell sheet engineering and tissue transplantation, the formation of tumor-like spheroids, the study of bioadhesion and bioadsorption, and the manipulation or deformation of individual cells.

The literature surveyed in this chapter includes research performed on mammalian cell release, cell sheet engineering, tissue transplantation, study of the extracellular matrix underlying cells, and the formation of shapes or spheroids. In addition, this chapter

reviews research performed to manipulate the adhesion and detachment of individual cells (versus cell sheets), including prokaryotic and eukaryotic cells. Finally, the efforts researchers have made to optimize pNIPAM films for attachment and detachment are presented.

CHAPTER 4: ASSESSMENT OF CYTOTOXICITY OF *N*-ISOPROPYL ACRYLAMIDE AND POLY(*N*-ISOPROPYL ACRYLAMIDE)-COATED SURFACES

Initially published by M.A. Cooperstein and H.E. Canavan in *Biointerphases*.[81]

4.1 Introduction

As described in Chapter 1, pNIPAM is one of the most commonly used stimulus-responsive polymers for research [11, 12], especially in the field of tissue engineering. [24, 48, 50, 51] The ultimate goal of that research is generation of pNIPAM- based devices that will be used for synthesis of tissue for implantation in humans. While it is known that the NIPAM monomer is toxic [62], there has been relatively little conclusive research regarding the extent of cytotoxicity or biocompatibility of the polymerized form of NIPAM.[54-60]

There are conflicting opinions whether pNIPAM is toxic to cells, with very few publications (fewer than 15 studies) [54-60, 63-68] that explore the cytotoxicity of this polymer, as compared to hundreds of publications on applications of pNIPAM. As previously described, none of the currently available studies on pNIPAM's cytotoxicity are comprehensive. They focus on isolated cell lines, employ different methods of cytotoxicity testing, and test copolymers of pNIPAM instead of the pure pNIPAM. They also concentrate on only one polymerization technique, although various polymerization and deposition techniques are used to generate pNIPAM surfaces and examine different forms of pNIPAM (e.g. hydrogels or nanoparticles). While pNIPAM is used for cell culture below and above its LCST, only one study investigated its cytotoxicity below the

LCST. None of the studies tested the effects of growing cells directly on pNIPAM-coated surfaces, or the effect of pNIPAM extracts. The contradictory results of these studies and the lack of consistency in testing of pNIPAM's cytotoxicity, warrant a new, comprehensive cytotoxicity study of pNIPAM.

In this chapter, we examine the cytotoxicity of the NIPAM monomer, pNIPAM, and pNIPAM films. PNIPAM was synthesized using free radical polymerization (frpNIPAM), as this is one of the most commonly used methods for the synthesis of pNIPAM for cytotoxicity studies.[54-57, 59] Commercially available pNIPAM was also used for the experiments (cpNIPAM). PNIPAM films were generated using vapor-phase plasma polymerization of NIPAM (ppNIPAM), spin-coating of cpNIPAM/tetraethyl orthosilicate sol gel (spNIPAM), spin-coating of cpNIPAM dissolved in isopropanol (cpNIPAM/IPA), and spin-coating of frpNIPAM, also dissolved in isopropanol (frpNIPAM/IPA). These techniques alone account for the majority of the ongoing research in this area (~90%). The cytotoxicity of NIPAM and pNIPAM was assessed using four different cell lines: endothelial cells, epithelial cells, smooth muscle cells, and fibroblasts. PNIPAM's toxicity was assessed in two ways: by direct contact with the cells and by testing pNIPAM extracts.

4.2 Methods

The experiments performed in this chapter follow the procedures outlined in Chapter 2, including free radical polymerization of NIPAM, plasma polymerization, spNIPAM deposition, deposition of cpNIPAM and frpNIPAM, XPS, goniometry, and cell culture. For cytotoxicity testing, endothelial cells (BAECs), epithelial cells (Veros), smooth muscle cells (SMCs), and fibroblasts (3T3s) were used. Direct contact test,

plating efficiency, extracts study, and concentration gradient experiments were performed to test the cytotoxicity of pNIPAM and pNIPAM-coated surfaces.

Statistically relevant data were obtained by replicating all procedures three times. Each replication of the experiment utilized three surfaces, with each surface analyzed in three different sites across the surface. This method was used for both surface analysis and cell behavior studies. The results are expressed as average values ± STDEV. Excel's ANOVA function and a student t-test were used to verify statistical relevance, with significance established at $p<0.05$.

4.3 Results and discussion

4.3.1 Polymerization and surface preparation

Free radical polymerization is one of the most commonly used methods for the synthesis of pNIPAM for cytotoxicity studies.[54-57, 59] Therefore, in addition to performing cytotoxicity experiments with NIPAM monomer and commercially available pNIPAM (cpNIPAM), pNIPAM was synthesized by free radical polymerization using AIBN. The resulting polymer (frpNIPAM) was examined using nuclear magnetic resonance (NMR) spectroscopy to confirm successful polymerization.

Figure 4.1 shows two NMR spectra: the frpNIPAM polymer (top, in black), and the NIPAM monomer (bottom, red). Highlighted in the box is the region between 5.5 and 6.5 ppm, in which peaks for hydrogens adjacent to double bonded carbons usually appear. These 3 peaks, labeled a, b, and c, are clearly visible in the spectrum of the monomer, as NIPAM has 3 hydrogens adjacent to two carbons joined with a double bond (see them labeled with a, b, and c on the inset in Figure 4.1 of the chemical structure of NIPAM and on the NMR spectra). These peaks are, however, missing from the NMR

spectrum of the frpNIPAM. The disappearance of these peaks indicates successful formulation of the polymer.

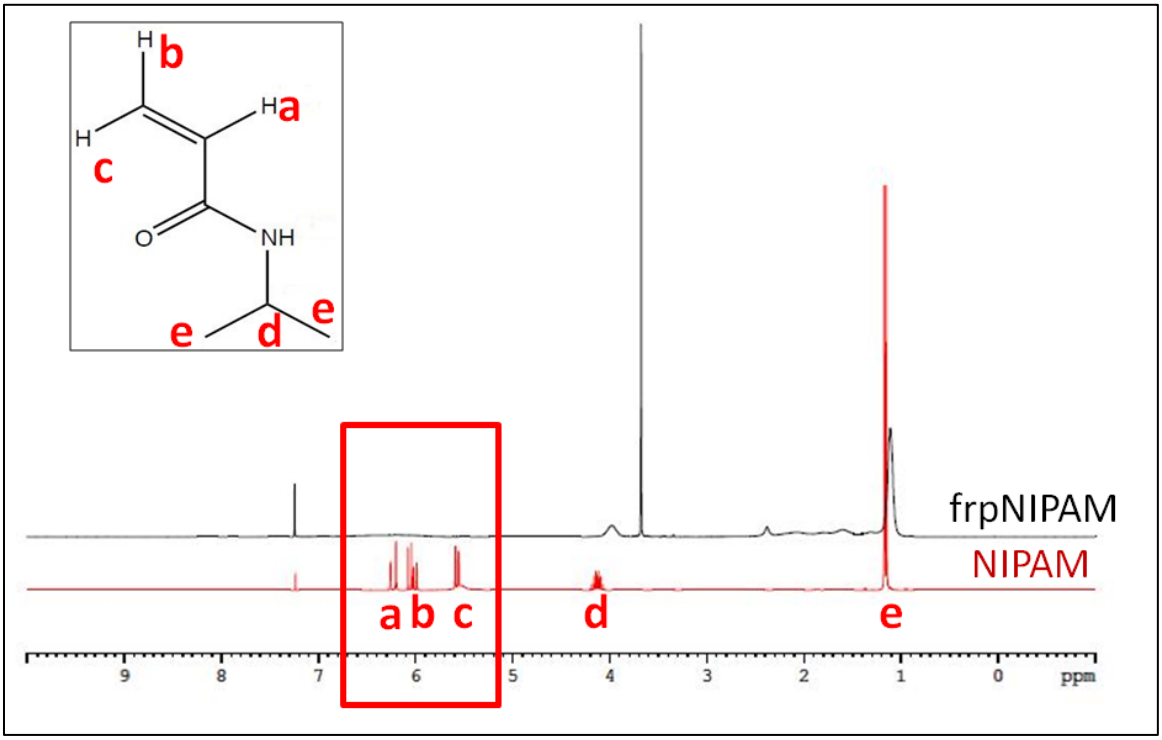

Figure 4.1 NMR spectrum for frpNIPAM and NIPAM. Inset shows chemical structure of the NIPAM monomer. Hydrogens bound to alkenes are indicated as “a”, “b”, and “c” in the inset and spectrum.

To confirm polymerization of frpNIPAM, the polymer was further tested using size exclusion chromatography. The weight-average molecular weight of frpNIPAM was found to be 104,000 Daltons, with a polydispersity index of 1.89 (data not shown). FrpNIPAM has a higher molecular weight than cpNIPAM, the other pNIPAM polymer used for testing in this study, which is reported to have a molecular weight of approximately 40,000 Daltons.

PNIPAM films were generated using vapor-phase plasma polymerization of NIPAM (ppNIPAM),[83] and spin -coating of cpNIPAM/tetraethyl orthosilicate sol gel (spNIPAM)[27]. Due to frequency of the use of isopropanol (IPA) solvent with pNIPAM, a protocol was developed for deposition of cpNIPAM and frpNIPAM dissolved in IPA. The amount of pNIPAM was optimized to 1wt% (1 wt% cpNIPAM/IPA and 1 wt% frpNIPAM/IPA) and the solutions were deposited on glass slides by spin-coating. These techniques account for the majority of the ongoing research in this area (estimated ~90% of number of publications). Figure 4.2 shows schematically how the surfaces were generated.

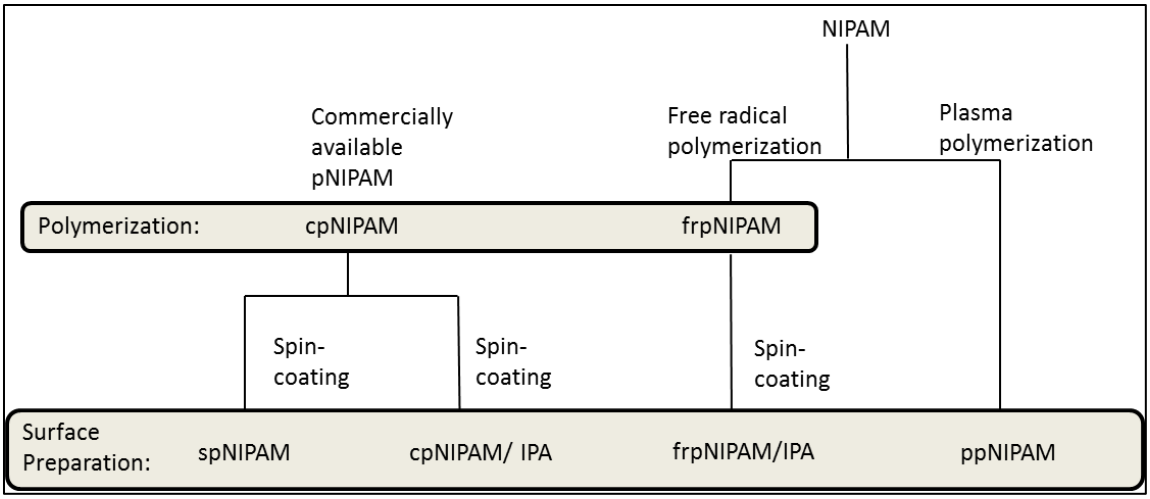

Figure 4.2 Overview of polymerization and surface preparation techniques used in this chapter.

Commercially available pNIPAM was used to make spNIPAM and cpNIPAM/IPA surfaces. The NIPAM monomer was used to directly generate plasma polymerized surfaces (ppNIPAM) as well as frpNIPAM, which was in turn used for generation of frpNIPAM surfaces. Overall, four different types of pNIPAM-coated surfaces were used for the testing of pNIPAM's cytotoxicity (ppNIPAM, spNIPAM,

cpNIPAM/IPA, and frpNIPAM/IPA), and two pNIPAM formulations were used for concentration gradient experiments (frpNIPAM and cpNIPAM). More detail about ppNIPAM and spNIPAM surfaces is provided in our earlier publications.[27, 83, 84]

4.3.2 Surface chemistry

The surface chemistry of these pNIPAM-coated surfaces was assessed by X-ray photoelectron spectroscopy (XPS). Table 4.1 shows the results of survey and high resolution C1s spectra for all four types of surfaces.

Table 4.1 Elemental composition and molecular bonding environment of pNIPAM-coated surfaces from XPS data analysis. N=9 with a standard deviation of ±1, except for spNIPAM with standard deviation of ±7.

SURFACE TYPE	RELATIVE ATOMIC %						
	SURVEY SPECTRA				HIGH RESOLUTION C1S SPECTRA		
	C	N	O	Si	C-H	C-OH/C-N	N-C=O
Theoretical	75	12.5	12.5	0	67	17	17
ppNIPAM	79.7	9.7	10.6	0	68	21	11
spNIPAM	45.7	2.0	36.8	15.5	56	37	7
cpNIPAM	76.6	11.7	11.7	0	66	19	16
frpNIPAM	76.9	11.4	11.5	0.2	68	17	15

The first row of data shows the expected values (“Theoretical”) as calculated from the stoichiometry of the monomer. An additional column for silicon (Si) was added to the table, as spNIPAM contains Si due to the TEOS solution. In addition, since the pNIPAM was coated on Si wafers, the presence of Si could indicate that pNIPAM films showing Si peaks are ≤50 nm thick. PpNIPAM, cpNIPAM, and frpNIPAM surfaces have elemental composition consistent with that predicted from the monomer structure (~75% C, 12.5% O, and 12.5% N). However, spNIPAM surfaces’ composition differs significantly from the theoretical composition (45.7% C, 36.8% O, 2% N, and 15.5% Si). The high standard

deviation of the XPS data indicates that the spNIPAM surfaces did not have an even surface coverage. The XPS analysis revealed a large percentage of either TEOS or underlying surface exposed (Si accounting for 15.5% of elemental composition), which most likely resulted from pNIPAM precipitating out of the sol gel during the deposition.[87] FrpNIPAM surfaces also show a small percentage of surface exposed (0.2% of Si present in the survey spectrum). Examination of the data showed that this variation occurs from spot to spot, not from sample to sample, and most of the surface was still covered with pNIPAM coating. Figure 4.3 shows high resolution C1s spectra for ppNIPAM (a), spNIPAM (b), frpNIPAM (c), and cpNIPAM (d).

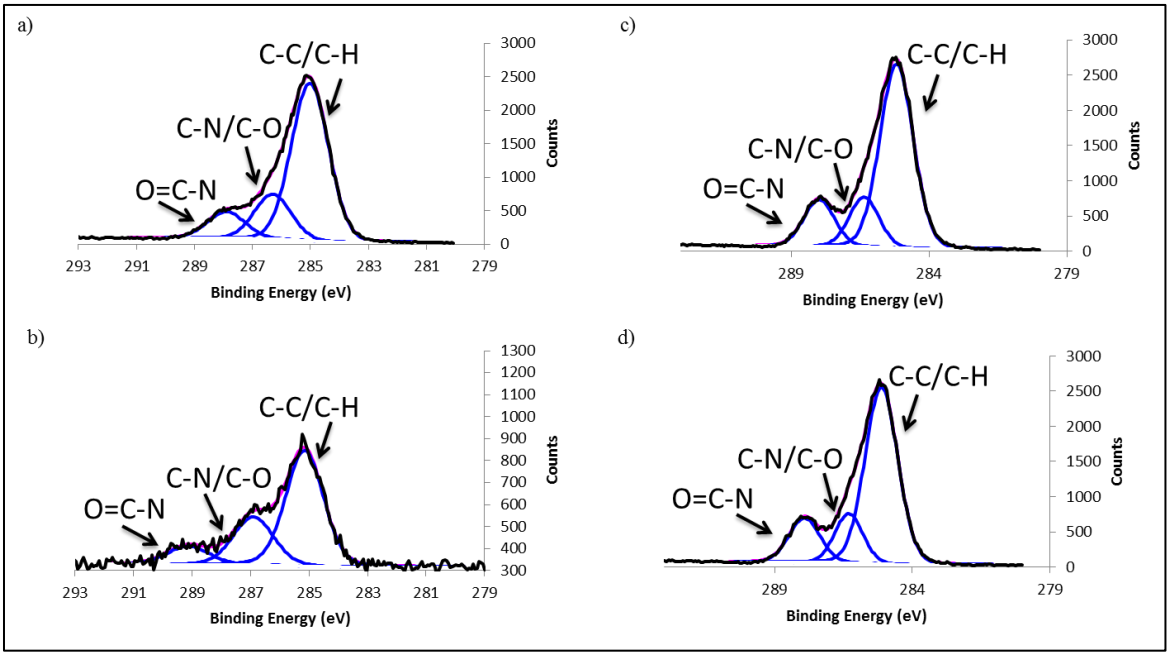

Figure 4.3 High resolution C1s spectra for (a) ppNIPAM, (b) spNIPAM, (c) frpNIPAM, and (d) cpNIPAM surfaces.

4.3.3 Polymer thermoresponse

The thermoresponse of the pNIPAM-coated surfaces was examined by goniometry. Inverted bubble contact angles were taken at room temperature (20°C) and at body temperature (37°C). Figure 4.4 shows the results of these measurements.

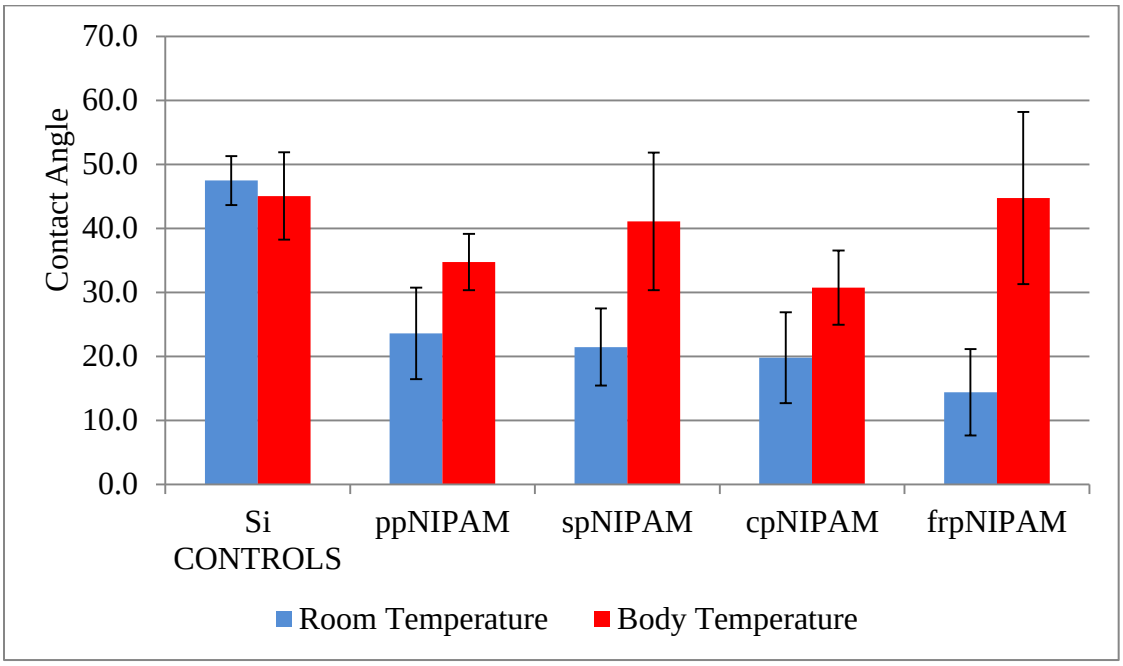

Figure 4.4 Inverted bubble contact angles of pNIPAM-coated surfaces measured at room and body temperature in ultrapure water.

The controls (Si chips) did not show any thermoresponse, with both average values at room temperature (blue) and body temperature (red) at ~45°C. In comparison, pNIPAM-coated surfaces showed thermoresponse. Although the values differ for different preparation techniques, all surfaces displayed thermoresponse with contact angles at body temperature larger than those at room temperature. It has previously been shown that the relative change in contact angles across the LCST is the desired result for surfaces coated with pNIPAM, while the specific values at each temperature are not critical. [16] The large standard deviations for spNIPAM and frpNIPAM are much larger (26 and 30% for spNIPAM and frpNIPAM respectively at body temperature) than those

of ppNIPAM and cpNIPAM (13 and 19%), indicating that spNIPAM and frpNIPAM yield substrates with more spot-to-spot variability, confirming our XPS observations.

4.3.4 Cytotoxicity experiments

All four types of pNIPAM-coated surfaces were used for cytotoxicity studies with four different cell types: bovine aortic endothelial cells (BAECs), monkey kidney epithelial cells (Veros), rat aorta smooth muscle cells (SMCs), and fibroblasts (3T3s). These four cell types were chosen because they are likely to be used for tissue engineering. In addition, it was shown that endothelial and epithelial cells can react differently to the same polymer, [136-138] and therefore, it is possible that pNIPAM may have different cytotoxic effects on different cell lines. In addition to pNIPAM-coated surfaces, we also tested the NIPAM and pNIPAM powders, without tethering them to a surface.

4.3.4.1 Cytotoxicity of the NIPAM monomer

Cytotoxicity of the monomer was evaluated using an MTS assay, which tests mitochondrial activity in live cells.[89] Table 4.2 shows the results of cytotoxicity experiments with the monomer. It was previously reported that the NIPAM monomer shows cytotoxicity effects at concentrations above 0.5 mg/mL, with cellular viability decreasing with increasing concentration of the monomer.[54] For this study, NIPAM was dissolved in cell culture media at a concentration of 5 mg/mL, and tested with the above mentioned four cell types. A compound is considered cytotoxic if cellular viability after exposure to the compound is below 70%.[61]

Table 4.2 MTS assay results of the cytotoxicity experiments for all four cell types after 24 and 48 hours of exposure to the NIPAM monomer. Bold indicates viability above 70%.

	% Viability			
	24 hours of exposure		48 hours of exposure	
	Average	Standard Deviation	Average	Standard Deviation
BAECs	38	3	18	2
Veros	32	3	16	9
SMCs	59	16	36	13
3T3s	**82**	6	48	4

All cell types showed reduced viability after 24 and 48 hours of cell culture in the presence of the monomer solution. 3T3s showed the most resistance to the toxic effects of NIPAM, with cell viability of slightly above 80% after 24 hours of exposure (at the concentration of 5 mg/mL, bold in Table 4.2). After 48 hours however, the viability of 3T3s decreased to below 70% (to 48%). The remaining cell types had significantly lowered viability after 24 hours, and this viability decreased even more after 48 hours of exposure. Therefore, although the monomer proved to be cytotoxic to all tested cell types, the extent to which it is toxic to cells at the concentration tested in this study depended on the cell type: the endothelial (BAECs) and epithelial (Vero) cells were the most sensitive to the monomer, whereas the fibroblasts (3T3s) were the most resistant.

4.3.4.2 Cytotoxicity of pNIPAM-coated substrates

The cytotoxicity of pNIPAM-coated surfaces was evaluated in three different ways: by direct contact test, plating efficiency, and by an MTS assay evaluating cellular viability after cell culture in the presence of pNIPAM extracts.[61, 91] Direct contact tests indicate how cells respond to being cultured directly on pNIPAM-coated surfaces, as opposed to plating efficiency and extracts, which test cellular response to pNIPAM in a more indirect manner.

Direct contact testing consists of cells being cultured directly on the pNIPAM-coated surfaces.[61] Briefly, cells were cultured on the surfaces for up to 96 hours. Figure 4.5 shows the MTS assay results for all four cell types after 48 and 96 hours of cell culture, after these cells were cultured on ppNIPAM (a), spNIPAM (b), frpNIPAM (c), and cpNIPAM (d). For ppNIPAM (a), frpNIPAM (c), and cpNIPAM (d) surfaces, all cell types showed viability of ≥70% for both time points. SMCs and 3T3s showed significantly lower viability (below 70%) after 48 hours of culture on spNIPAM surfaces when compared to BAECs and Veros. However, after 96 hours, cellular viability is comparable to the other surfaces (at ~90%). It appears that initial attachment and proliferation of 3T3s and SMCs is hindered on spNIPAM surfaces, indicating these cells may be more sensitive to the surface chemistry and topography differences found using XPS and goniometry.

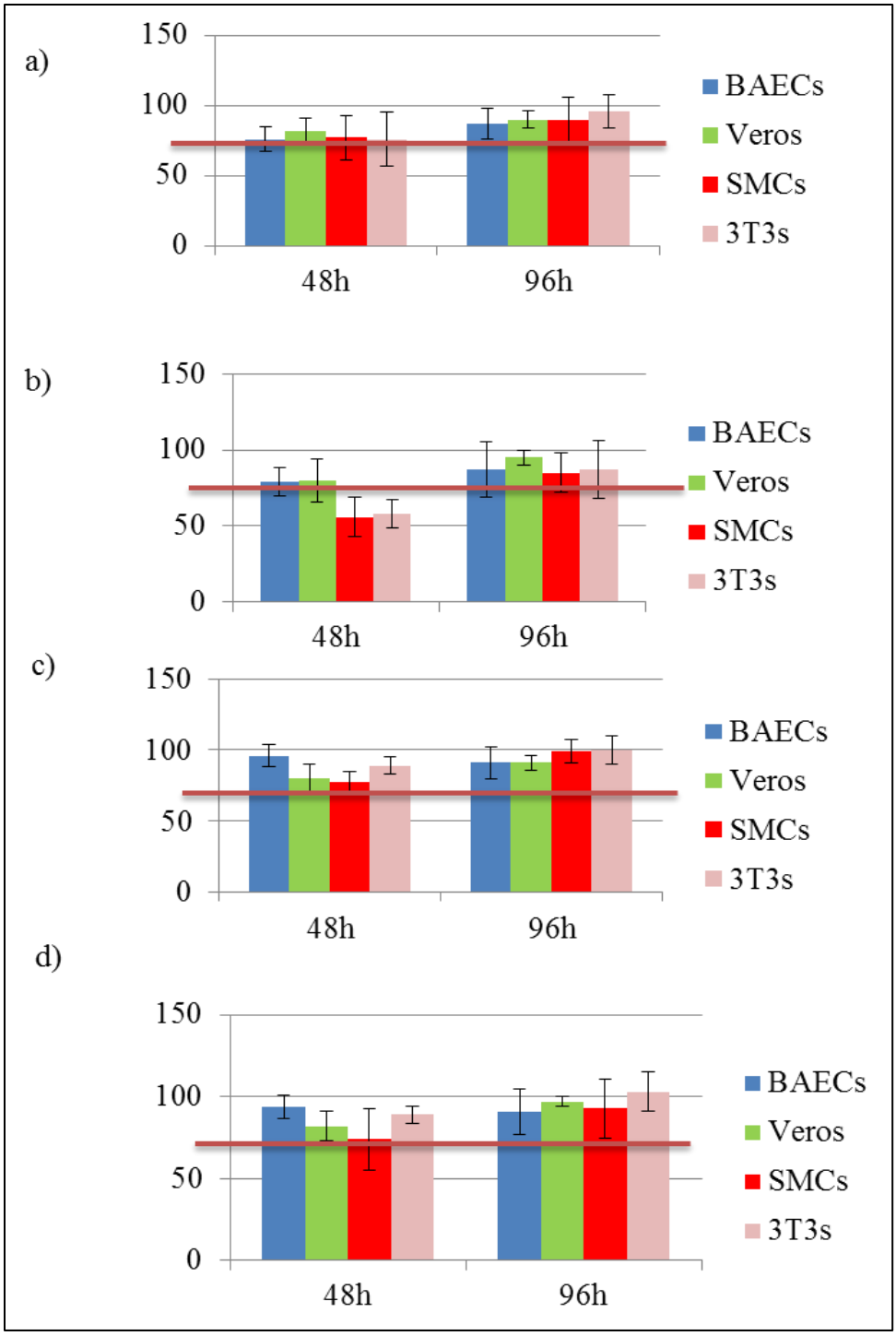

Figure 4.5 Direct contact test results: MTS assay results for all four cell types after cell culture for 48 and 96 hours on (a) ppNIPAM surfaces, (b) spNIPAM surfaces, (c) frpNIPAM surfaces, and (d) cpNIPAM surfaces. Red line indicates the viability of 70%, below which a compound is considered to be cytotoxic.

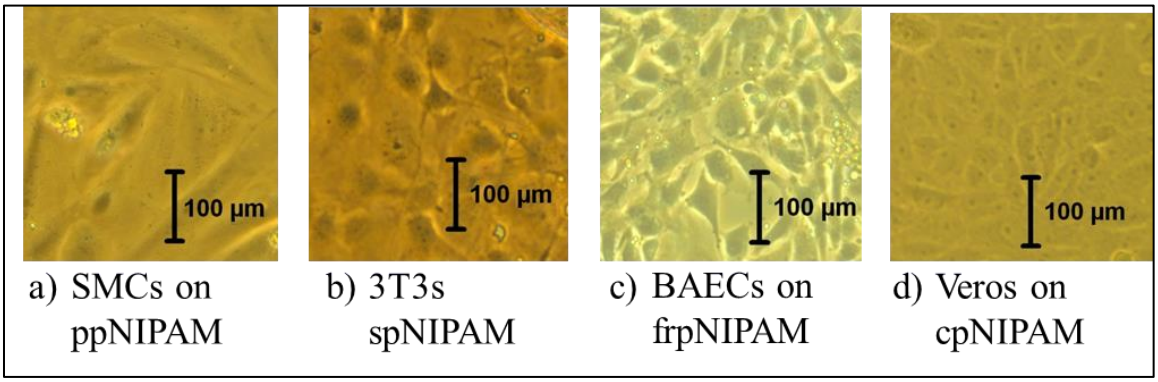

Figure 4.6 Light microscopy results for (a) SMCs after 96 hours of culture on ppNIPAM surfaces, (b) 3T3s after 96 hours of culture on spNIPAM surfaces, (c) BAECs after 96 hours of culture on frpNIPAM surfaces, and (d) Veros after 96 hours of culture on cpNIPAM surfaces.

Morphological observations (Figure 4.6, cells shown after 96 hours) revealed cells with normal morphology, spreading and growing to confluency on all four types of surfaces. However, when seeded on spNIPAM surfaces, cells first appeared to attach to the exposed glass surface, not to the pNIPAM coating. The uneven coverage on the surfaces, precipitation of pNIPAM from the sol gel solution observed at some spots on the surfaces, and the possibility of the presence of traces of other materials on the surface (such as ethanol used for sol gel process) are likely to result in surfaces that do not promote cell adhesion. Overall, there were fewer cells attached to spNIPAM surfaces after 24 hours than to the other three types of surfaces. This could explain lower values of viability after 48 hours. After 96 hours, cells that did attach to the surface had enough time to divide, resulting in higher viability values.

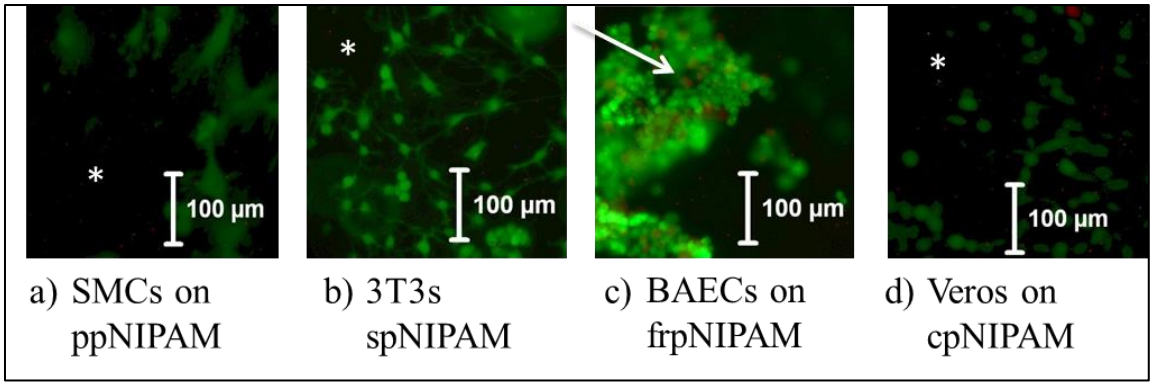

Figure 4.7 LIVE/DEAD assay results for (a) SMCs after 96 hours of culture on ppNIPAM surfaces, (b) 3T3s after 96 hours of culture on spNIPAM surfaces, (c) BAECs after 96 hours of culture on frpNIPAM surfaces, and (d) Veros after 96 hours of culture on cpNIPAM surfaces. Asterisks point to the exposed surfaces from which cells have detached (in black). The arrow points to a sheet of detached, live cells.

Figure 4.7 shows the results of a LIVE/DEAD assay on the four types of surfaces. Cells attached to the surfaces stained green, indicating alive cells. As the LIVE/DEAD assay requires incubation at room temperature, most of the cells detached from the surfaces, leaving exposed black pNIPAM surfaces (indicated by the asterisks in Figure 4.8). This detachment was expected and desired, as it proves that these surfaces are thermoresponsive. A detached, wrinkled sheet of BAECs can be seen in Figure 4.7 (c) (indicated with an arrow). There were a few red stained (dead) cells visible on some of the images taken during the test. However, controls (uncoated glass slides) also showed a small percentage of dead cells after staining (see Figure 4.8).

There was no difference in the ratio of dead cells to live cells between the controls and test surfaces. Therefore, it can be concluded that there were no cytotoxic effects found for the surfaces and cell types evaluated in this experiment.

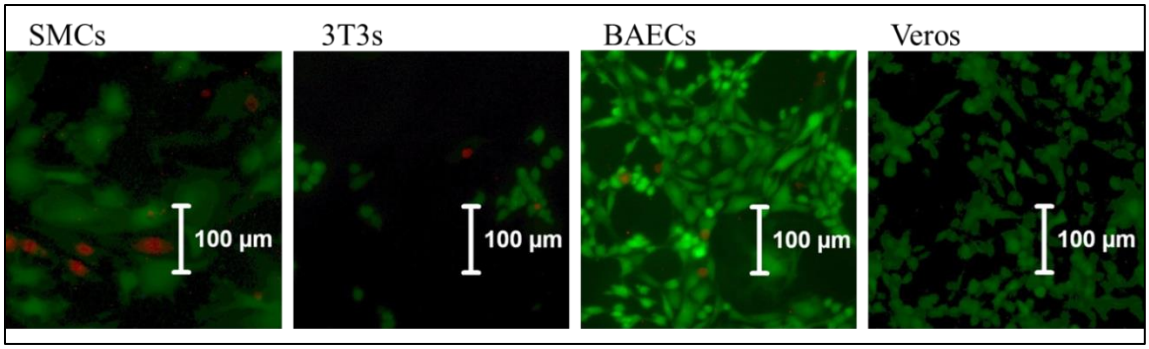

Figure 4.8 LIVE/DEAD assay results for SMC, 3T3, BAEC, and Vero cells cultured on uncoated glass slides (controls).

4.3.4.3 Extracts

The pNIPAM-coated surfaces were used to generate pNIPAM extracts, which were then used for cytotoxicity testing. One of the cytotoxicity tests performed was plating efficiency. This is a very sensitive test, as isolated cells do not have their neighbors to shield them from potentially harmful compounds present in the cell culture media.[91] The controls, cells cultured in regular cell culture without pNIPAM extracts, are under optimal conditions. If there is anything in the pNIPAM extracts that prevents the cells from proliferating, the percent plating efficiency would be decreased when compared to controls.

Table 4.3 shows the results of this test for all four cell types and for all four types of surfaces. The extracts were made at two different temperatures, 37 and 20^{o}C, to test if the temperature has any influence on what (if anything) leaches off the surface into the surrounding media. It is important to note that larger amounts of polymer are expected to be found in the extracts generated at room temperature, since the polymer films are not covalently bound to the surfaces. As expected, no colonies were formed in the presence of 5 mg/mL of NIPAM in the media, verifying that the NIPAM monomer is cytotoxic.

The remaining extracts did not result in significant decrease of plating efficiency for BAECs, Veros, or SMCs.

Table 4.3 Plating efficiency results for BAEC, Vero, SMC, and 3T3 cells exposed to the NIPAM monomer and extracts from ppNIPAM, spNIPAM, cpNIPAM, and frpNIPAM. Bold indicates extracts with decreased viability at 37°C

TYPE OF EXTRACTS	PLATING EFFICIENCY (%)			
	BAECs	Veros	SMCs	3T3s
NIPAM	0	0	0	0
ppNIPAM (20°C)	98	94	95	96
ppNIPAM (37°C)	103	93	89	91
spNIPAM (20°C)	100	96	100	101
spNIPAM (37°C)	105	91	93	**82**
cpNIPAM (20°C)	102	94	88	97
cpNIPAM (37°C)	102	90	91	**78**
frpNIPAM (20°C)	97	91	93	91
frpNIPAM (37°C)	108	90	98	**88**

3T3s showed a slightly decreased plating efficiency for cells exposed to spNIPAM, frpNIPAM, and cpNIPAM extracts generated at 37°C when compared to the same extracts generated at room temperature. This effect is not observed for ppNIPAM surfaces. This is most likely because ppNIPAM surfaces are the only physically grafted surfaces tested in this study, and consequently, are likely to be the most stable surfaces. Statistical analysis revealed that there is a significant difference in plating efficiencies for cpNIPAM surfaces between 20 and 37°C, and for spNIPAM surfaces between these two temperatures, with lower plating efficiencies values for extracts obtained at 37°C. SpNIPAM surfaces showed lower initial attachment for 3T3s during the direct contact

test, therefore, it is possible that it is the inhospitable surface chemistry of these surfaces that obstructs initial cell attachment and growth. It is important to mention that these values are still above the 70% cytotoxicity cut off; thus, the lowered values do not render these surfaces cytotoxic.

The extracts from the pNIPAM coated surfaces were further evaluated by first growing cells on uncoated TCPS for 24 hours with regular media, and then changing the media for extracts. Three extracts concentrations were used: 100%, 10% (10% extracts, 90% regular media), and 1%. Experiments on epithelial cells, smooth muscle cells, and fibroblasts did not show any drop in cellular viability for any of the extracts concentrations or time points. Figure 4.9 shows results for extracts study for SMCs.

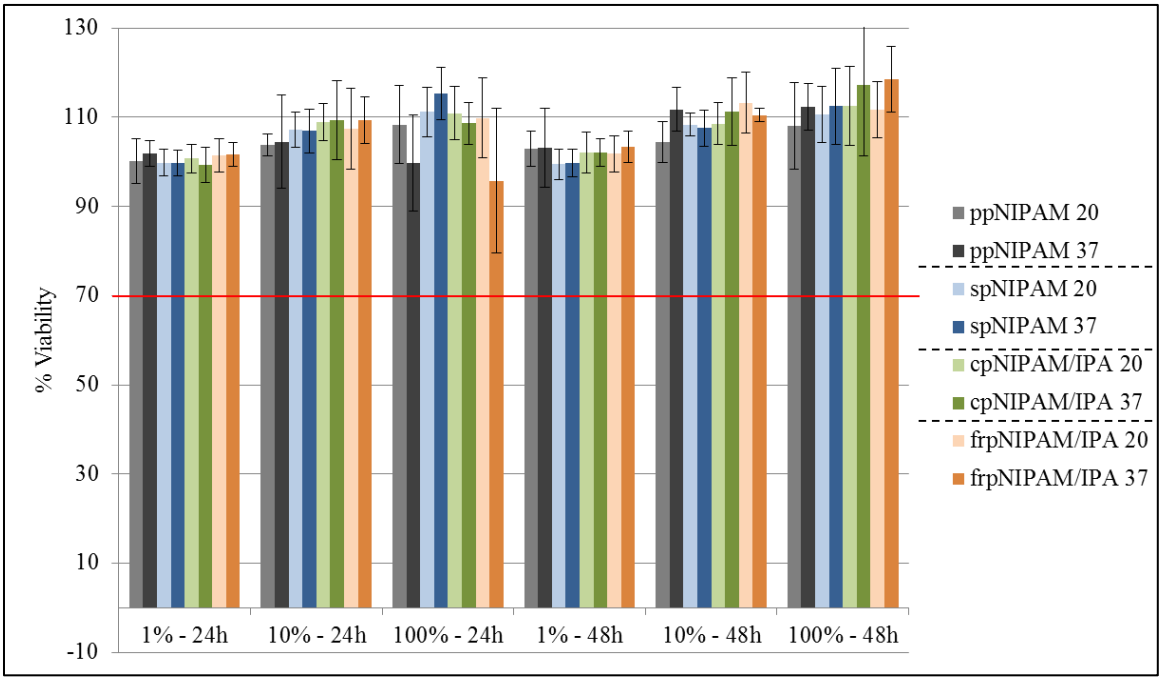

Figure 4.9 MTS assay results for culture of SMCs in the presence of pNIPAM extracts. Red line indicates viability of 70%, below which a compound is considered to be cytotoxic.

All extract concentrations and time points resulted in viabilities of 100% or larger. See Figures A1 and Figure A2 in the Appendix for extract results for Veros and 3T3s.

However, BAECs consistently showed decreased cell viability for all eight types of extracts after 48 hours of exposure at the 100% concentration. Figure 4.10 shows the results for all concentrations, time points, and types of extracts for BAECs. It is clear that after 24 hour exposure, the 1 and 10% extracts do not affect the viability, as the viabilities are all ~100%. The average viabilities drop slightly after 24 hours of exposure to 100% extracts. However, as the assay results are still at or above 80%, they are still considered not cytotoxic. Forty eight hours of exposure at 1 and 10% did not result in a significant drop of viabilities (although the average viabilities are lower than the corresponding viabilities after 24 hours).

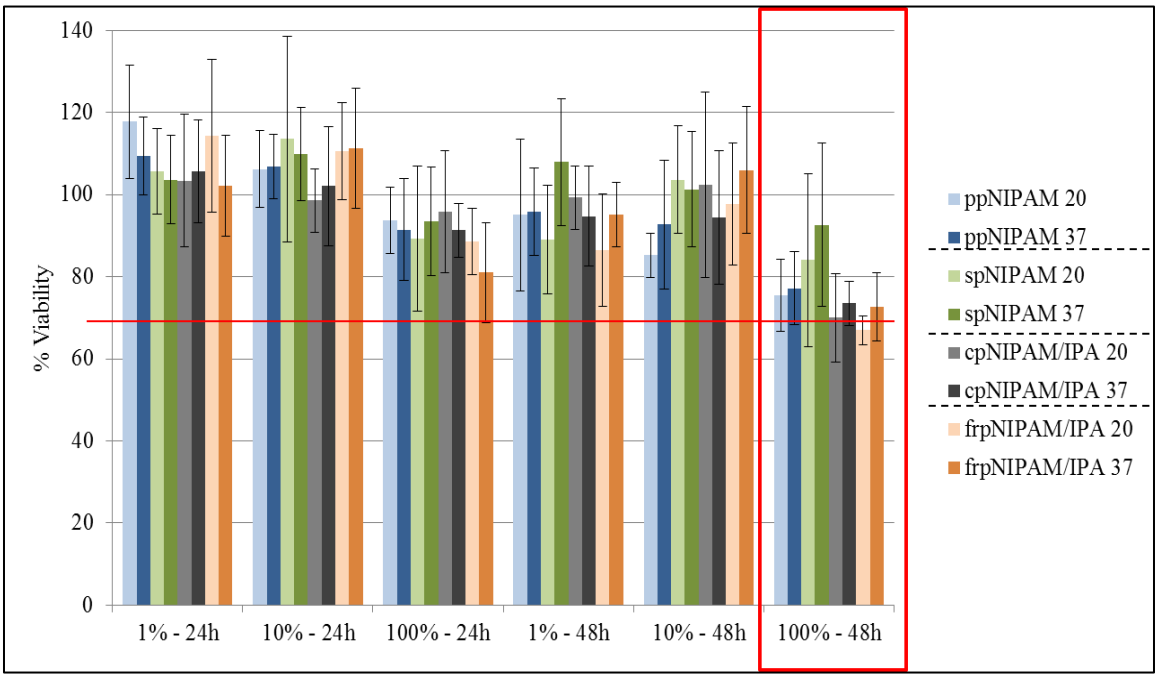

Figure 4.10 MTS assay results for culture of BAECs in the presence of pNIPAM extracts. Red line indicates viability of 70%, below which a compound is considered to be cytotoxic. Red box indicates the only time and concentration for which the viability of BAECs was lowered to ≤ 70% across all pNIPAM coated surfaces. Corresponding figures for Veros, SMCs, and 3T3s can be found in supplemental information.

The only time and concentration for which the viabilities of BAECs were lowered to about (or below 70%) was 100% extracts at 48 hours of exposure (red box in Figure 4.10). None of the other cell types showed similar sensitivity (see Figure 4.9 and Figures A1 and A2 in the Appendix). This result agrees with other published studies, where endothelial cells were found to be more sensitive than epithelial cells when exposed to cytotoxic compounds.[136-138]

Of the four surface types, spNIPAM extracts had the highest average viability at this time point and concentration. This could possibly be explained by the uneven coverage of spNIPAM surfaces. SpNIPAM surfaces had the most uneven coating, with more of the underlying surface exposed (as evidenced by the XPS measurements showed in Table 4.1 and Figure 4.3). Therefore, the substrates likely had the smallest amount of deposited pNIPAM, which could result in smaller amounts of pNIPAM (and other compounds that were involved in the deposition process) transferred to the extracts; therefore, fewer potential toxic effects.

4.3.4.4 Concentration gradients

The higher sensitivity of BAECs was confirmed in concentration gradient experiments. Here, frpNIPAM and cpNIPAM were dissolved in regular cell culture media in concentrations ranging from 0.1 mg/mL to 10 mg/mL. Figure 4.11 shows results for Veros. The results for SMCs and 3T3s can be found in the Appendix (Figures A3 and A4). All these cell types showed average viability of around 90-100%, with small standard deviations for both cpNIPAM and frpNIPAM. BAECs proved to be more sensitive in this test as well.

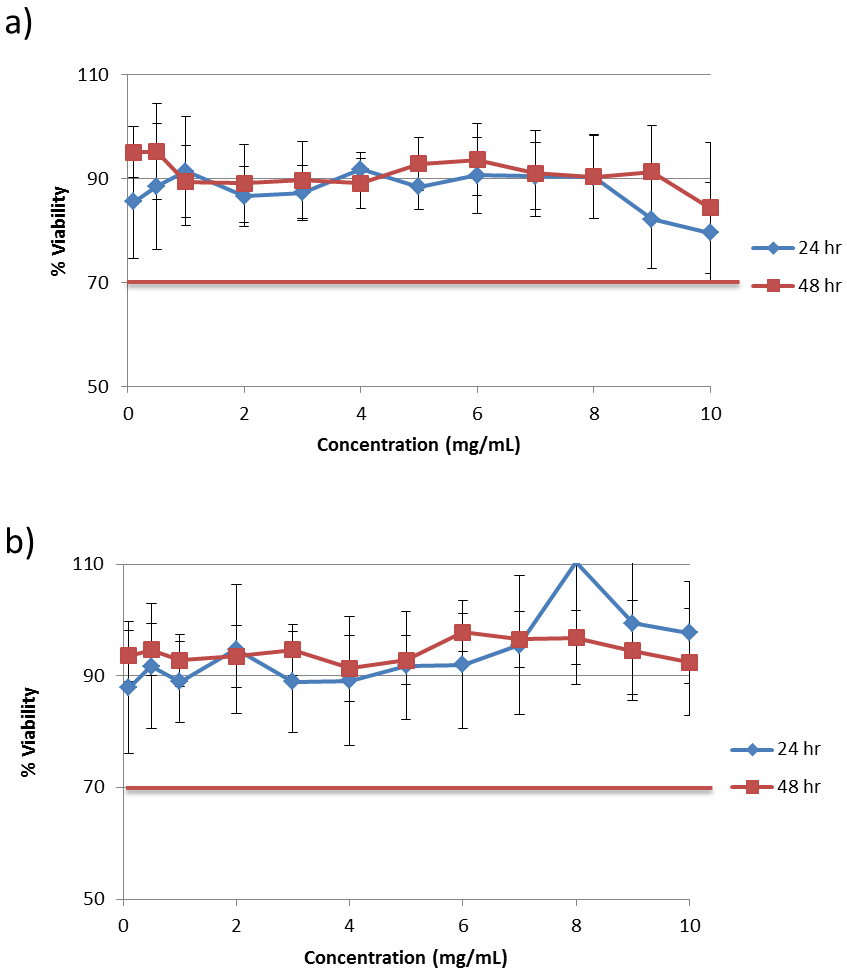

Figure 4.11 MTS assay results for concentration gradient experiments with Veros (a) on cpNIPAM/IPA surfaces, and (b) on frpNIPAM/IPA surfaces. Red line indicates viability of 70%, below which a compound is considered to be cytotoxic.

Figure 4.12 shows the result of concentration gradient experiments for BAECs exposed to cpNIPAM (a) and frpNIPAM (b). Cells exposed to frpNIPAM maintained average viability of 80% for both time points. However, these experiments yielded large standard deviations, with several values for single experiments dropping to or below 70%. CpNIPAM had even larger effect on BAECs. Starting at about 3 mg/mL, the viabilities for both time points (24 and 48 hours) decreased to reach values as low as 20% viability at the concentration of 10 mg/mL. Due to this unexpected result, this experiment

was repeated 6 times (instead of the usual 3), to confirm that there indeed is a trend, and that the result is not due to infected cells or media. All six experiments showed a similar trend, with the viability starting to decrease between 3 and 5 mg/mL. The large standard deviation of the composite graph results from the differences between the single experiments, as the viabilities did vary slightly between the runs.

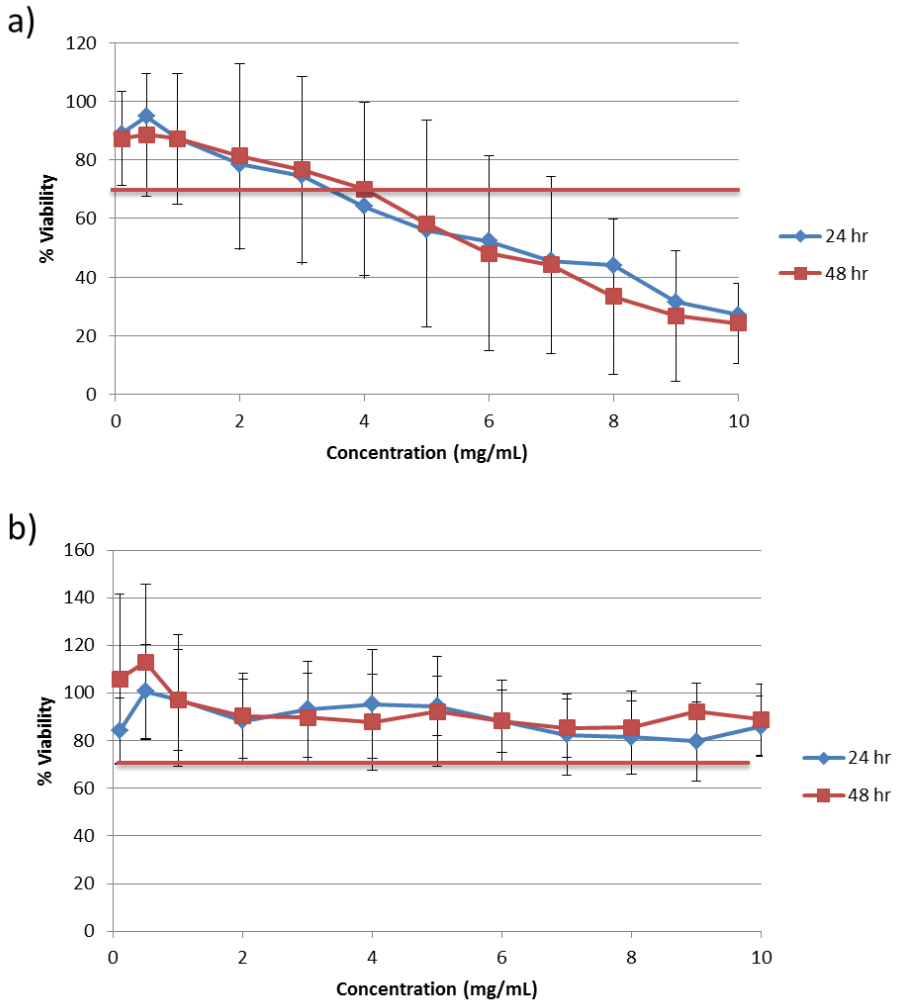

Figure 4.12 MTS assay results for concentration gradient experiments with BAECs (a) on cpNIPAM/IPA surfaces, and (b) on frpNIPAM/IPA surfaces. Red line indicates viability of 70%, below which a compound is considered to be cytotoxic. Corresponding figures for Veros, SMCs, and 3T3s can be found in the Appendix.

This variability is not explained by the presence of bacterial or other contaminants in the cpNIPAM test solution, as no decrease in viability, normal growth, and proliferation were observed in the other three cell types that were exposed to the same test solution. NMR of cpNIPAM was performed to confirm the identity and the extent of polymerization of this compound, which could affect the cytotoxicity (see Figure 4.13).

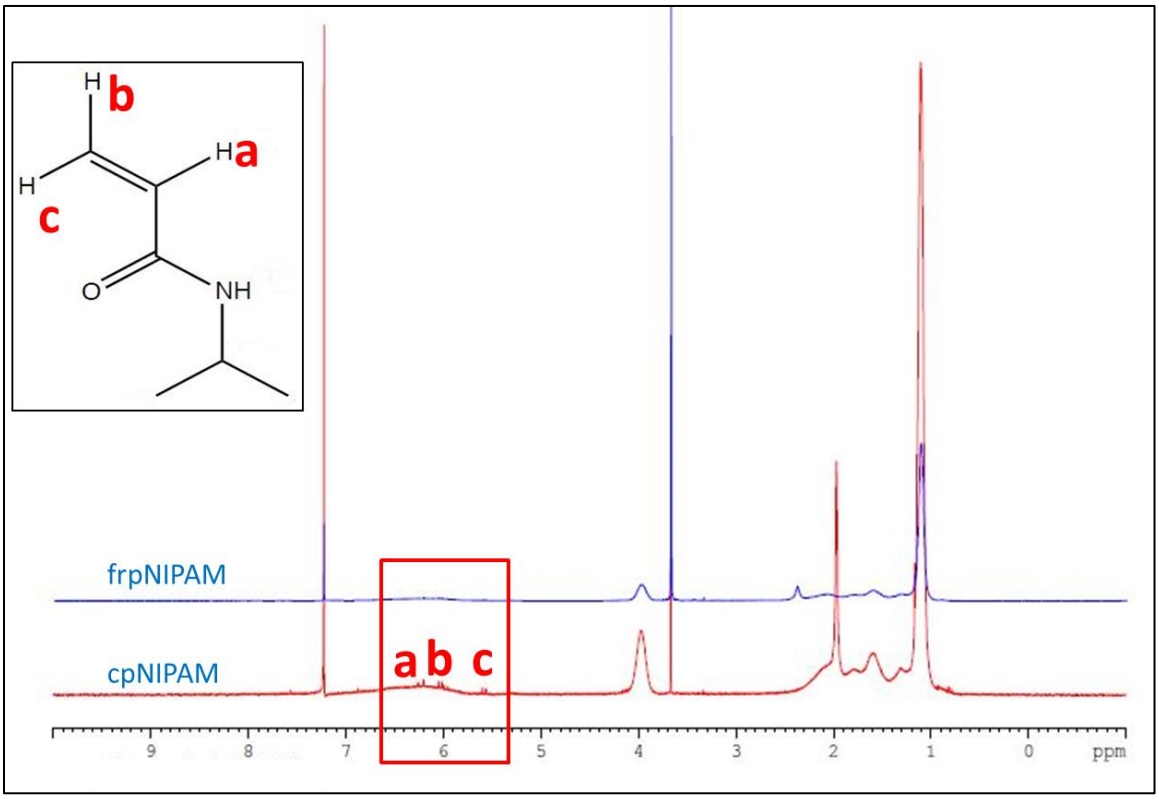

Figure 4.13 NMR spectra of frpNIPAM (top, blue) and cpNIPAM (bottom, red). Red box indicates the peaks corresponding to hydrogens attached to double bonded carbons (indicative of the presence of monomer). Inset shows chemical structure of the NIPAM monomer. Hydrogens bound to alkenes are indicated as “a”, “b”, and “c” in the inset and spectrum.

While confirming the identity of the polymer, the NMR spectrum showed presence of small amount of the monomer. The peaks corresponding to double bonds in the monomer were not visible on the NMR spectrum of frpNIPAM. The presence of small amounts of monomer could explain the results of the concentration gradient

experiment. It would also account for the variability between the six experiments performed with cpNIPAM test solutions, as different amounts of the monomer could end up in the wells, resulting in different cellular toxicity. Since endothelial cells appeared to be most sensitive to the monomer, purification of the polymer before using it with this cell type would be recommended.

4.4 Conclusions

In this chapter, the cytotoxicity of the NIPAM monomer, pNIPAM, and pNIPAM-coated substrates prepared using different polymerization (free radical and plasma polymerization) and deposition (spin coating and plasma polymerization) techniques was evaluated using appropriate cytotoxicity tests (MTS, Live/Dead, plating efficiency). Four different mammalian cell types (endothelial, epithelial, smooth muscle, and fibroblasts) were used for the cytotoxicity testing. The pNIPAM-coated surfaces were evaluated for their thermoresponse and surface chemistry using X-ray photoelectron spectroscopy and goniometry.

We found that while cell viability on pNIPAM surfaces decreases when compared to controls, the viability also seems to be deposition type dependent, with sol gel based pNIPAM surfaces being the least biocompatible. Long term experiments proved that all pNIPAM-coated surfaces were not cytotoxic to the four cell types evaluated in a direct contact test. Plating efficiency experiments also showed no cytotoxicity toward tested cell types. Cellular sensitivity to pNIPAM and to the NIPAM monomer varied, depending on cell type. Endothelial cells consistently showed decreased viability after 48 hours of exposure to pNIPAM extracts and were more sensitive than the other cell lines to impurities in the polymer.

CHAPTER 5: MECHANISM OF CELL DETACHMENT FROM PNIPAM-COATED SURFACES

5.1 Introduction

As described in Chapter 1, the mechanism of cell detachment is the least understood aspect of cell sheet engineering using temperature-responsive surfaces. Only ~ 5% of studies on pNIPAM investigated the detachment mechanism. The most extensive study of the mechanism of cell detachment was performed by Okano et al.[72-74] In their work, a two-step process was proposed, with a first passive phase involving hydration of pNIPAM chains, and second, active phase, involving cellular metabolism. Other groups found that the hydration of pNIPAM chains itself failed to detach fibronectin from fibronectin-preadsorbed pNIPAM-surfaces,[73] and that inhibition of actin polymerization and stabilization of F-actin slowed cell detachment, which indicates that cell detachment may involve actin dynamics.[74]

While many studies agree on the two-step mechanism, there is a dispute about the temperature at which the detachment should be performed. Okano et al. concluded that the best cell detachment was achieved at room temperature with less cell detachment at lower temperatures (4, 10^{o}C)[72] However, a number of studies (including those done by our group) performed successful cell sheet detachment from pNIPAM-grafted surfaces at lower temperatures (4 and 10^{o}C).[27, 45, 46, 78, 79] The Okano group suggests 25^{o}C as the optimal detachment temperature for endothelial cells.[72] Our group found 4^{o}C to provide better detachment for endothelial cells,[27] while Wang et al. found that the highest detachment of fibroblast cells from pNIPAM-coated surfaces was achieved at ~15^{o}C.[80]

There still is insufficient knowledge about the mechanism of cellular detachment from pNIPAM-coated surfaces (how significant cellular metabolism is to the detachment) and about important detachment parameters (such as the temperature). The understanding of the mechanism of cell detachment from pNIPAM and the optimal conditions for the detachment is crucial for developing a quicker and more reliable way of generating tissues using this cell sheet engineering technique.

In this chapter, we investigate the mechanism of cell detachment from pNIPAM-coated surfaces by testing how temperature and presence of an ATP inhibitor affect the detachment. For this purpose, we utilized surface-initiated atom transfer polymerization (ATRP) to synthesize atrpNIPAM surfaces. The reaction conditions were optimized for sufficient cell attachment and detachment. BAECs were used for cell detachment experiments, which were performed with and without sodium azide, an ATP inhibitor.

5.2 Methods

The experiments performed in this chapter follow the procedures outlined in Chapter 2, including surface-initiated atom transfer radical polymerization of NIPAM, (ATRP), XPS, goniometry, and cell culture. BAECs and Vero cells were used for optimization of atrpNIPAM surfaces. BAECs were used for cellular detachment experiments. Experiments with BAECs were performed in regular cell culture media as well as in cell culture media supplemented with 2mM of sodium azide, an ATP inhibitor. For experiments with sodium azide, cells were first cultured at regular cell culture conditions (as described in Chapter 2). One hour before the start of detachment experiments, the regular cell culture media was replaced with media supplemented with

sodium azide. The cells were returned to the incubator. After 1 hour of incubation, cells were removed from the incubator and detachment experiments were started.

Cellular detachment was tested at three different conditions: at 21^{o}C in warm media (RT/WM), at 21^{o}C in cold (refrigerated) media (RT/FM), and at 4^{o}C in cold media (FT/FM). To perform the detachment at 21^{o}C in warm media (RT/WM), cells were removed from the incubator, their media was replaced with warm serum-free media, and they were left at 21^{o}C for up to 60 minutes. To perform the detachment at 21^{o}C in cold media (RT/FM), cells were removed from the incubator, their media was replaced with cold serum-free media, and the detachment was allowed to proceed for 60 minutes. Finally, for the detachment at 4^{o}C, (FT/FM), after removal from the incubator, the media was replaced with cold serum-free media, and cells were allowed to detach for 60 minutes at 4^{o}C. Table 5.1, below, lists all the conditions and their respective abbreviations used for the detachments. Detachment experiments were performed at the three treatment conditions with and without sodium azide.

Table 5.1 Conditions for the detachment experiments used in Chapter 5.

CONDITION	ABBREVIATION USED
20^{o}C (room temperature) in warm media	RT/WM
20^{o}C (room temperature) in cold (refrigerated) media	RT/FM
4^{o}C (refrigerated) in cold (refrigerated) media	FT/FM

5.3 Results and discussion

5.3.1 Surface- initiated atom transfer radical polymerization of NIPAM and surface optimization

There are several different techniques for generating pNIPAM-coated surfaces. These include plasma polymerization, spin-coating, electro-spinning, and electron beam irradiation.[13] These techniques vary in cost, potential applications, and ease of use. For many of them, control of deposited polymer thickness – and therefore their applicability for cellular attachment and detachment – is limited. For the investigation of the mechanism of cell detachment, we chose surface-initiated atom transfer radical polymerization (ATRP). ATRP has the advantage over other techniques (such as plasma polymerization or spin coating) in that it allows control over the degree of polymerization. The polymer thickness is controlled by polymerization time, with longer polymerization times resulting in a thicker polymer layer.[85]

Table 5.2 summarizes the most recent studies using ATRP of NIPAM for cellular attachment and detachment. Although various polymerization techniques and conditions were used, there are a few common conclusions that can be made. In general, there is a limit to the length and density of pNIPAM brushes before cells will not adhere to the surface. Conversely, if the brushes are too short or insufficiently dense, adherent cells will not detach. There appears to be optimal film thickness and density that allow for reversible cell adhesion. Furthermore, the optimal parameters are dependent on the technique and the reagents used for the ATRP of NIPAM.

Table 5.2 Overview of most recent articles employing ATRP of NIPAM.

REFERENCE	POLYMERIZATION TECHNIQUE USED	RESULTING CELL BEHAVIOR
Chen et al, *Acta Biomaterialia*, 2008[76]	ATRP for 24 hours at 4^{o}C + collagen coating	Smooth muscle cells were used. Cells grew on the pNIPAM-collagen coated surfaces and detached from them when the temperature was lowered.
Gunnewiek et al, *Israel Journal of Chemistry*, 2012[139]	ATRP, 30 minutes at room temperature.	Fibroblast cells were used. High density brushes resulted in lower cell attachment. Complete detachment occurred after lowering the temperature. There were fewer cells on PNIPAM surfaces when compared to controls.
Ke et al, *Journal of Applied Polymer Science*, 2010[140]	ATRP at 60°C for 2, 4, 8, and 12 hours.	Fibroblast cells were used. The cells could adhere and grow to some extent on the surfaces. Significant number of cells detached from the surfaces after temperature was lowered.
Kim et al., *Bulletin of Korean Chemical Society*, 2004[141]	ATRP for 2 hours at room temperature.	Fibroblast cells used. Little cell attachment to pNIPAM surfaces.
Li et al, *Colloids and Surfaces B: Biointerfaces*, 2011[142]	ATRP at room temperature for 2 hours. RGD peptide added.	Liver carcinoma cells were used. The thicker the surface, the fewer cells attached. The surfaces grafted with a pNIPAM(25nm)-b-PAA(5-15nm) layer and further decorated with RGD had the best balance between satisfactory cell adhesion and detachment.
Li et al, *Langmuir*, 2008[143]	ATRP at room temperature for 60, 150, and 300 minutes.	Liver carcinoma cells were used. As the surfaces became thicker, the number of cells adhering decreased. For thicknesses between 20 and 45 nm, the cells satisfactorily attached and detached by the temperature switching.
Mizutani, *Biomaterials*, 2008[144]	The reaction proceeded at 25°C for up to 16 hours.	Endothelial cells were used. Thicker layers with high polymer grafted amount had negligible cell adhesion. On surfaces to which cells attached, they detached completely when the temperature was lowered.
Nagase et al, *Journal of Materials Chemistry*, 2012[145]	ATRP for 16 hours AT 25°C.	Endothelial cells, fibroblasts, smooth muscle cells, and skeletal muscle myoblast cells were used. Short brush surfaces showed cell adhesion. However, cells did not detach from short brush surfaces. Cells were unable to adhere to long brush surfaces. Moderate brush lengths showed cell adhesion and detachment.
Tamura et al, *Biomaterials*, 2012[146]	ATRP at room temperature for 16 hours.	Chinese hamster ovary cells were used. The number of adhering cells was found to decrease with increasing amount of grafted pNIPAM.
Sui et al, *Australian Journal of Chemistry*, 2011[147]	ATRP for at room temperature 30 minutes.	Fibroblast cells were used. Lower density brushes had a much higher adhesion with elongated cell morphology, whereas middle and high density brushes displayed progressive decrease of cell density. After decreasing temperature, all cells detached from the lower density brushes.

Table 5.2 (cont.) Overview of most recent articles employing ATRP of NIPAM.

REFERENCE	POLYMERIZATION TECHNIQUE USED	RESULTING CELL BEHAVIOR
Xu et al, *Colloids and Surfaces B: Biointerfaces*, 2011[148]	ATRP at room temperature for 0.5 – 2 hours plus collagen coating.	Fibroblast cells were used. Cells attached. The higher the content of the collagen, the higher the density of the attached cells. Cells detached from the surfaces when the temperature was lowered, however, higher contents of the collagen weakened the interaction between the chains and attached cells and hindered complete cell recovery.
Zhang et al, *Journal of Biomedical Materials Research B: Applied Biomaterials*, 2012[149]	ATRP at 50-55^{o}C for 22 hours.	Fibroblast cells used. Very low cell adhesion and proliferation.
Nagase et al., *Macromolecular Bioscience*, 2011[150]	ATRP at 25^{o}C for 16 hours.	Endothelial cells were used. Dilute pNIPAM brushes showed better cell attachment than dense brushes. Better cell attachment occurred on surfaces with shorter pNIPAM chain length.

For this study, we chose to work with a polymerization technique developed by Professor Lopez's group at the University of New Mexico.[85] The reagents and details of this polymerization method are described in Chapter 2. To obtain cellular attachment and detachment from the synthesized atrpNIPAM substrates, we varied several parameters (see Table 5.3 for the parameters).

Table 5.3 Parameters varied for optimization of atrpNIPAM surfaces.

PARAMETER VARIED	PARAMETER VALUES
Initiation time	6 hours, 18 hours
Dish size for initiation	Small (8 cm in diameter), large (18 cm in diameter)
Initiator concentration	50 µL/50mL; 100 µL/50mL
Polymerization time	5 min, 10 min, 15 min, 30 min

Preliminary studies were performed to determine the optimal polymerization conditions (data not shown). To control the thickness of atrpNIPAM surfaces (the pNIPAM chain length), polymerization time was varied from 5 minutes to 30 minutes. Initiator concentration, initiation time, as well as the size of the dish in which the initiation took place, were varied to obtain different density of the initiator on the surfaces, and therefore, different densities of pNIPAM tethered to the surface. To evaluate the coated surfaces, BAECs and Vero cells were seeded and cultured on them, and detachment experiments were performed.

Initiation time did not seem to affect cellular attachment or detachment. Both time points resulted with similar results. Dish size proved to be important, with cells not attaching to surfaces initiated in the smaller dish (higher pNIPAM density surfaces). There was no significant difference between the two initiator concentrations tested, with the larger concentration resulting in a slightly better attachment of cells. Finally, 30 minutes polymerization time resulted in surfaces that were too thick for attachment of cells. Based on several experiments, atrpNIPAM surfaces that resulted from overnight initiation in the large dish, with 100 μL of initiator/50 mL of toluene, and 15 minutes polymerization time were chosen for further experiments. These parameters resulted in the best attachment and detachment of cells.

Figure 5.1 shows microscopy images of mammalian cells, BAECs on the left and Veros on the right, growing on atrpNIPAM surfaces. The top row shows cells at 37^{o}C, the physiological temperature. The cells are spread and elongated, indicating that they are attached to the surface. After lowering the temperature to below pNIPAM's LCST, the cells started to detach. The bottom row of Figure 5.1 shows cells on atrpNIPAM surfaces

after 2 hours below the LCST. BAECs have rounded morphology, and it appears that most cells have detached from the surface. There is still a large number of Vero cells attached to the surface, although several cells have detached. Since BAECs showed the most reliable attachment and detachment on the atrpNIPAM surfaces, this cell type was used for all remaining experiments.

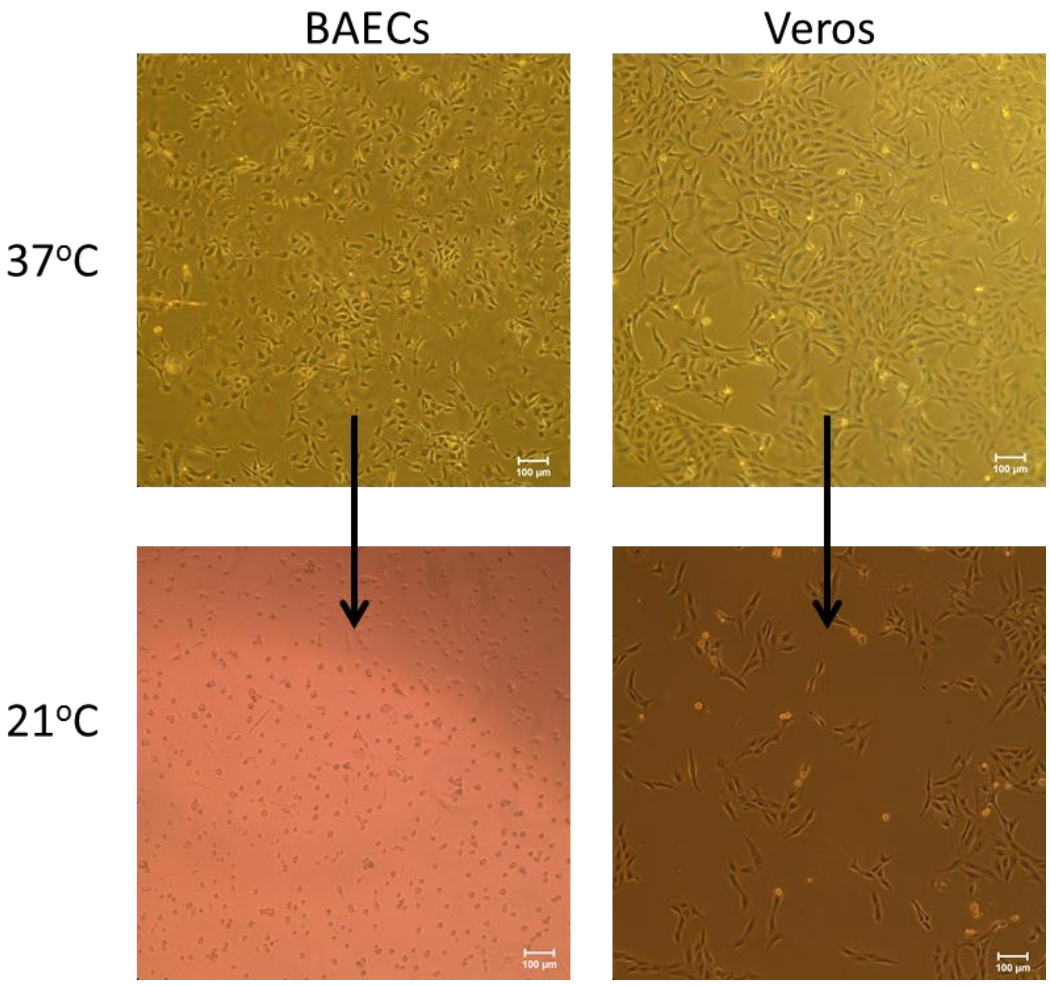

Figure 5.1 BAECs (left) and Veros (right) cultured on atrpNIPAM surfaces at 37°C (top row) and after detachment at 21°C (bottom row). Scale bar is 100 µm.

5.3.2 Surface characterization: goniometry and XPS

The atrpNIPAM surfaces were analyzed as described in previous chapters, using goniometry and XPS data analysis. Figure 5.2 shows the results of inverted bubble contact angle measurements. The measurements were taken at room temperature (20^{o}C) and at body temperature (37^{o}C). Control samples (uncoated Si chips) did not show any thermoresponse, with average values of ~ 54 and 58^{o} at room and body temperature, respectively. The atrpNIPAM surfaces however, showed a large difference between average values at room temperature (48^{o}), and at body temperature (62^{o}), therefore proving that the atrpNIPAM surfaces are thermoresponsive.

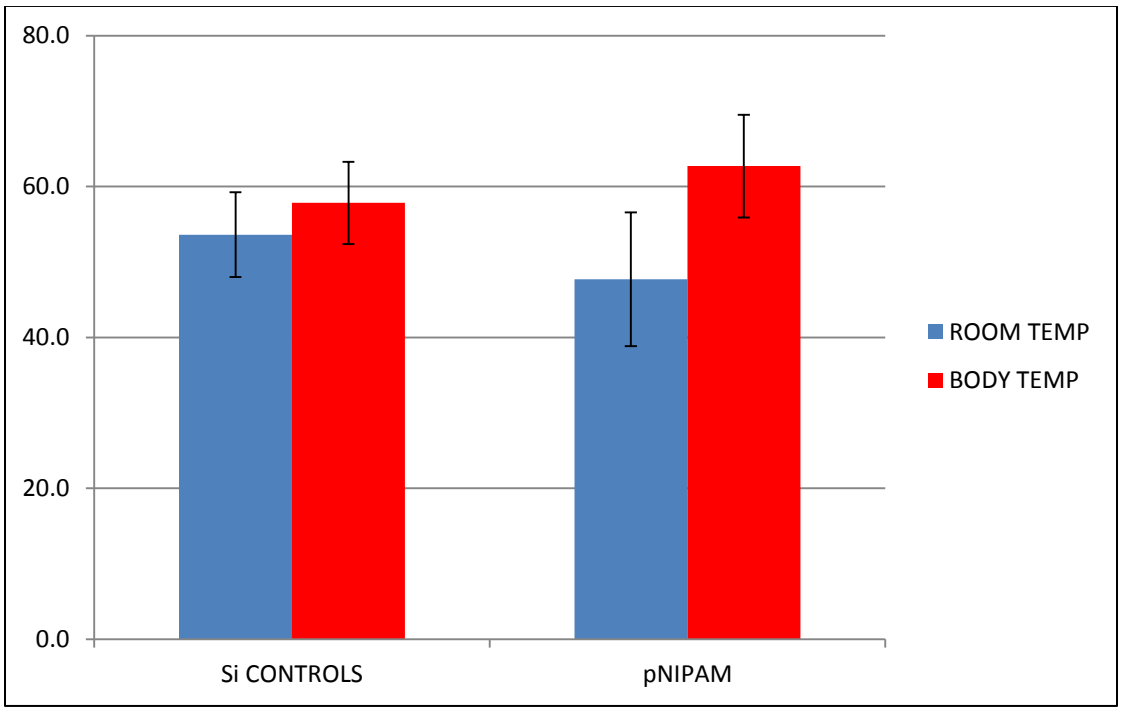

Figure 5.2 Inverted bubble contact angles of atrpNIPAM surfaces measured at room and body temperature in ultrapure water.

To confirm deposition of pNIPAM onto the surfaces, XPS analysis was performed. The survey spectra, (to determine elemental composition of the outer ~100

Angstroms of the sample), and high resolution C1s spectra, (to determine molecular bonding environment), were obtained, and compared to the theoretical composition of pNIPAM-coated surfaces, as calculated by the stoichiometry of the monomer. Figure 5.3 below shows the results of the XPS analysis. Analysis of both the elemental composition (top) and the carbon bonding environment (bottom) shows close adherence to the theoretical composition. In addition, no silicon was detected from the substrate, indicating that the films were pinhole-free. Therefore, XPS analysis shows that pNIPAM was successfully deposited onto the surface, and the coverage was uniform.

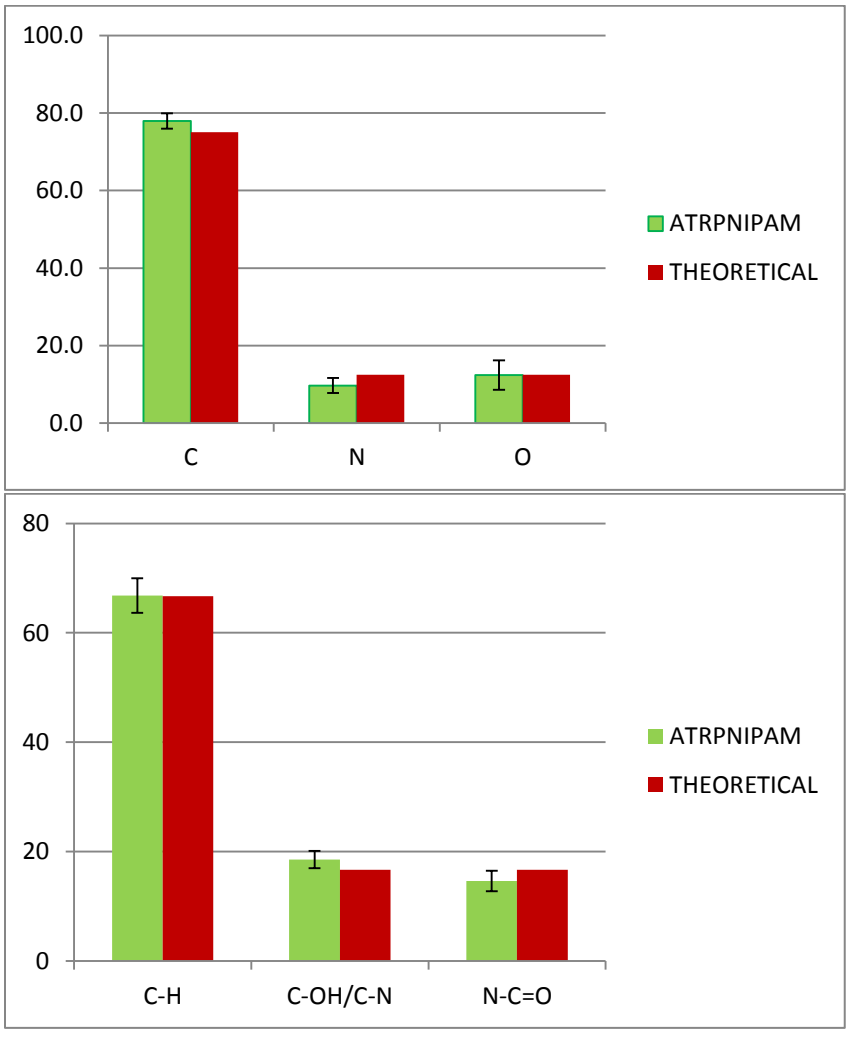

Figure 5.3 Elemental composition (top) and molecular bonding environment (bottom) of atrpNIPAM surfaces from XPS data analysis. N=3 with a standard deviation of ±1.

5.3.3 Cell detachment from atrpNIPAM surfaces

The above described atrpNIPAM surfaces were used to investigate the mechanism of cell detachment. As previously mentioned, all experiments were performed with BAECs, as the surfaces were optimized for attachment and detachment of this type of cell. The detachment experiments were performed with and without sodium azide. Sodium azide is a known inhibitor of cytochrome c oxidase, which is a protein complex in mitochondria, involved in proton transfer that leads to the synthesis of ATP.[151, 152] When sodium azide is present, ATP generation will be inhibited and all metabolic processes that rely on ATP will be disrupted. In this work, we used 2mM of sodium azide, as this amount has been shown to partially inhibit cell metabolic processes without killing the cells.[72] To probe the influence of the temperature on cell detachment from pNIPAM, experiments were performed at three different conditions: at 4^{o}C with cold serum-free media, at 21^{o}C with cold serum-free media, and at 21^{o}C with warm serum-free media. The detachment was observed at each temperature for the duration of 60 minutes. In addition, cell detachment was tracked every 15 minutes to obtain data of detachment versus time.

5.3.3.1 Cell detachment at 4^{o}C (FR/FM)

Detachment of BAECs at 4^{o}C was observed in the presence of sodium azide as well as in regular cell culture media without sodium azide. Figure 5.4, below, shows images of cells growing on atrpNIPAM surfaces at 37^{o}C, right before the detachment started (first row), and 15 minutes and 60 minutes after changing the media to cold serum-free media and putting the cells in 4^{o}C. The left column shows cell unexposed to

sodium azide, while the right column shows cells that have been incubated in media with 2mM of sodium azide for 1 hour before the detachment.

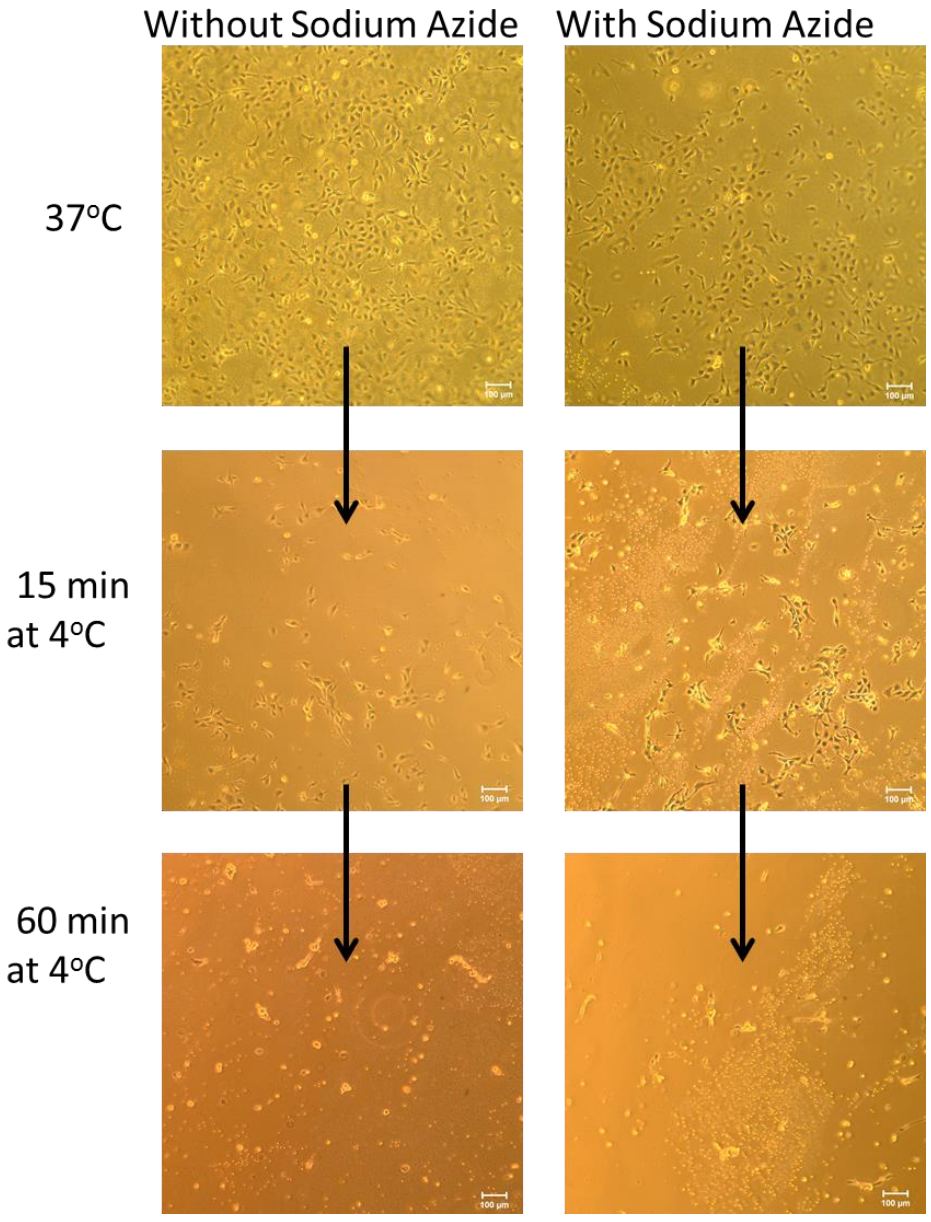

Figure 5.4 BAECs cultured on atrpNIPAM at 37°C (top), and after 15 minutes (middle) and 60 minutes (bottom) at 4°C (FR/FM) without (left column) and with (right column) sodium azide. Scale bar is 100 µm.

It can be seen that the cells were initially elongated and spread on the surfaces. When the temperature was lowered to below pNIPAM's LCST, there were visibly fewer cells on the surface. Even the cells that remained attached also began to detach. These cells were less spread out, and their edges are coming out of focus as they are starting to lift away from the surface. Finally, after 60 minutes, almost all cells are detached (mostly round, out of focus cells visible).

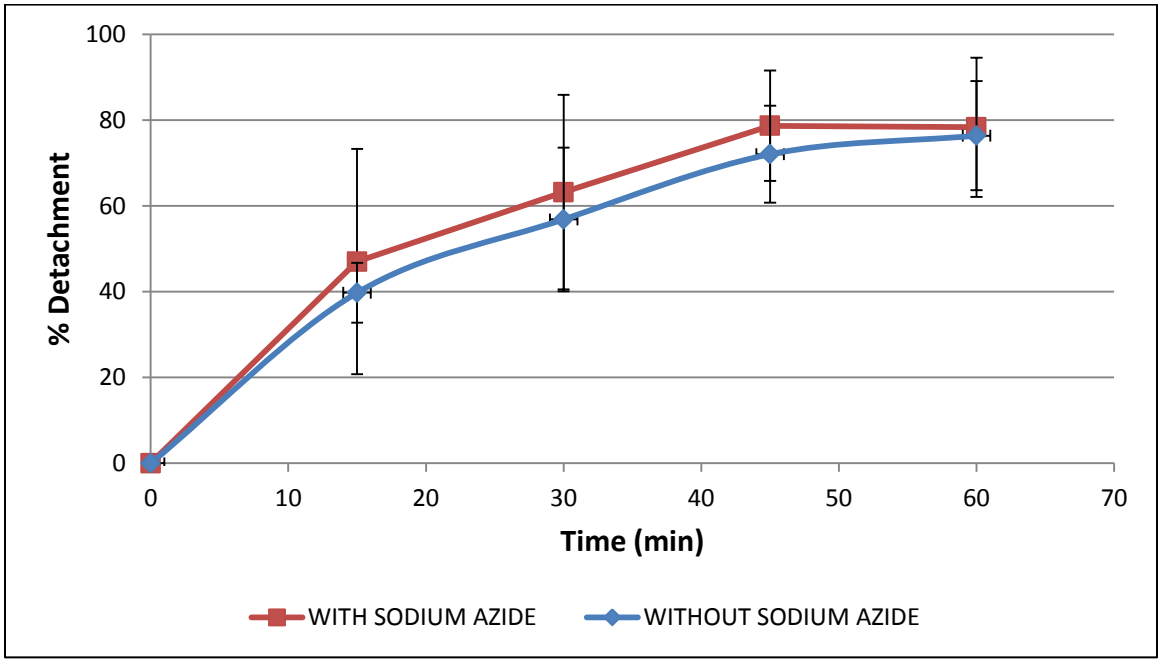

Figure 5.5 Cell detachment at 4^{o}C (FR/FM) in the presence of sodium azide (red line), and without sodium azide (blue line).

The percentage of cells detached for each time point was calculated and graphed. Figure 5.5 shows the results for detachment with sodium azide (red line) and without sodium azide (blue line). Time point zero is the time right before the detachment started, at which point the detachment was 0%. The figure shows that there is no significant difference in cell detachment with the addition of sodium azide. Both conditions result with an initially slower detachment of 40-45% after the first 15 minutes. With time, the

detachment plateaued at 79% after 45 minutes. The initial detachment rates (calculated based on detachment after 15 minutes) are 2.7 %/min for experiments without sodium azide, and 3.1 %/min for experiments with sodium azide.

5.3.3.2 Cell detachment with cold media at 20^{o}C (RT/FM)

The same detachment procedure was followed for experiments in cold media at 20^{o}C. Figure 5.6 shows cells attached to the atrpNIPAM surfaces immediately prior to detachment, and cells detaching after 15 minutes and 60 minutes at 20^{o}C. Similarly to experiments at 4^{o}C in Figure 5.5, the cells exhibit normal, spread morphology before the beginning of detachment. There still are cells attached to the surfaces at the 15 minute time point. After 60 minutes, almost all cells are completely detached.

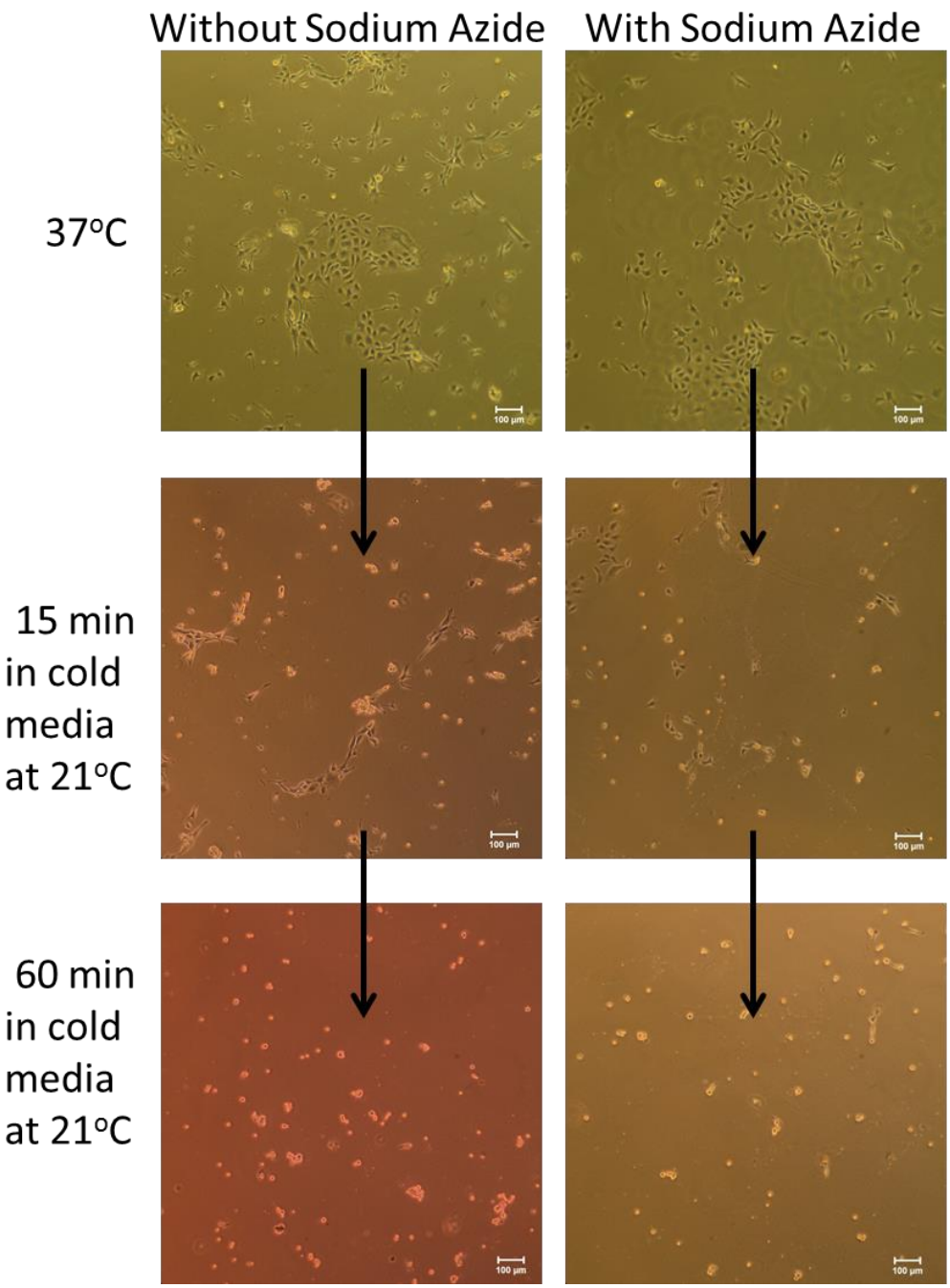

Figure 5.6 BAECs cultured on atrpNIPAM at 37°C (top), and after 15 minutes (middle) and 60 minutes (bottom) in cold media at 20°C (RT/FM) with (left column) and without (right column) sodium azide. Scale bar is 100 µm.

Figure 5.7 shows a graph of percentage detachment versus time. Here, the initial detachment rate is the same for both conditions, with and without sodium azide, with the

value of 4.7 %/min. The number of cells equilibrates at 89% for cells not exposed to sodium azide, and 86% for cells exposed to sodium azide, after 45 minutes of detachment.

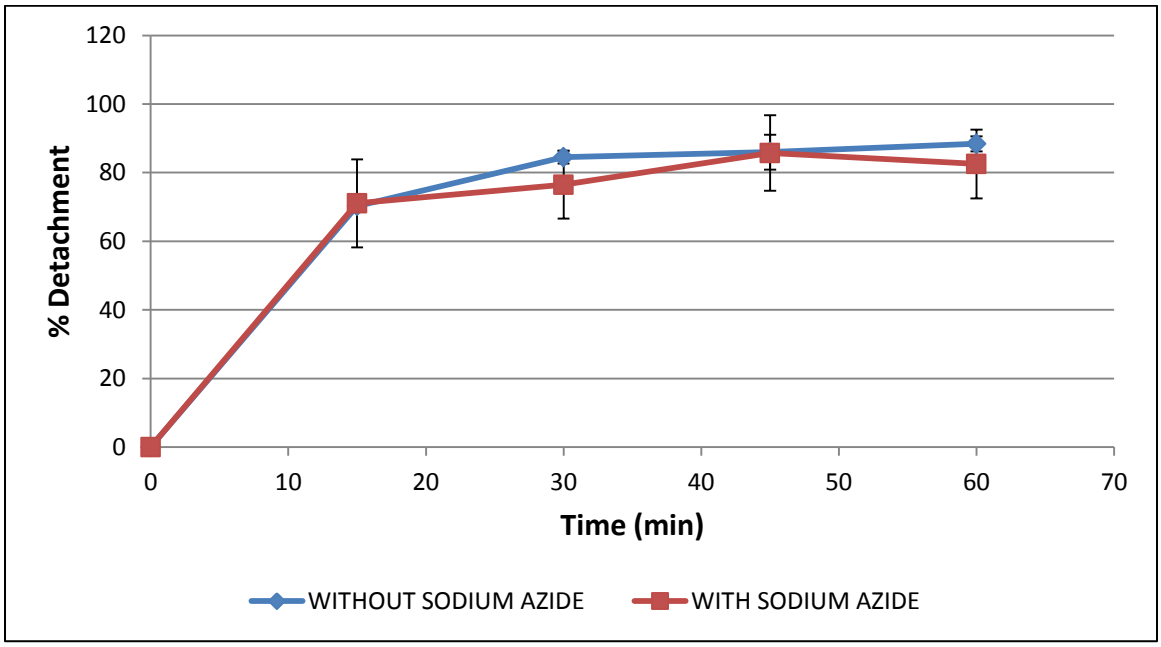

Figure 5.7 Cell detachment in cold media at 20°C (RT/FM) in the presence of sodium azide (red line), and without sodium azide (blue line).

5.3.3.3 Cell detachment with warm media at 20°C (RT/WM)

To further examine the influence of temperature on cell detachment from pNIPAM-coated substrates, we performed another set of detachment experiments at 20°C. For this set of experiments, the regular cell culture media in which cells were growing was replaced with warm (not cold like in previous section) serum-free media. Since the media is not as cold as the media in the previous section, the initial hydration of pNIPAM chains will be smaller than with colder media, and it may affect the detachment.

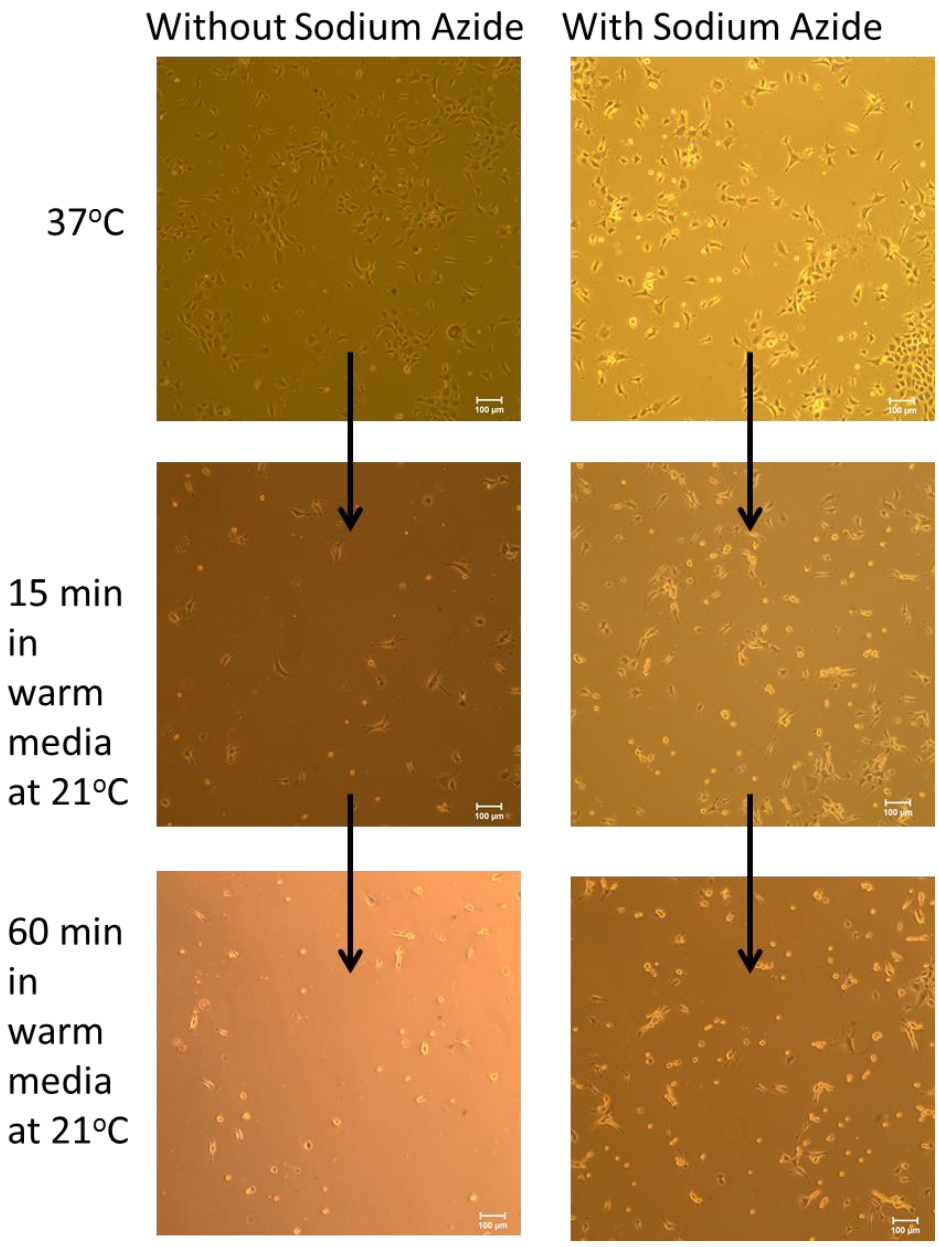

Figure 5.8 BAECs cultured on atrpNIPAM at 37°C (top), and after 15 minutes (middle) and 60 minutes (bottom) in warm media at 20°C (RT/WM) with (left column) and without (right column) sodium azide. Scale bar is 100 µm.

Figure 5.8 shows images of BAECs growing on atrpNIPAM surfaces before and during the detachment in the same manner as shown in the previous sections. Here, we again see elongated and spread cells on atrpNIPAM at 37°C. After 15 minutes under

detachment conditions, a large number of cells have detached from the surface. After 60 minutes, most cells have detached and there are only few left that are still attached to the surface.

The percent detachment in warm media at 20°C for each time point is shown in Figure 5.9. As with the previous results in Figures 5.5 and 5.7, the presence of sodium azide does not significantly affect the percentage of cells detached. For both conditions, the maximum detachment occurred after 45 minutes (87%). The initial percent detachments rates are 3.7 %/min for experiments without sodium azide and 4.3 %/min for the experiments with sodium azide.

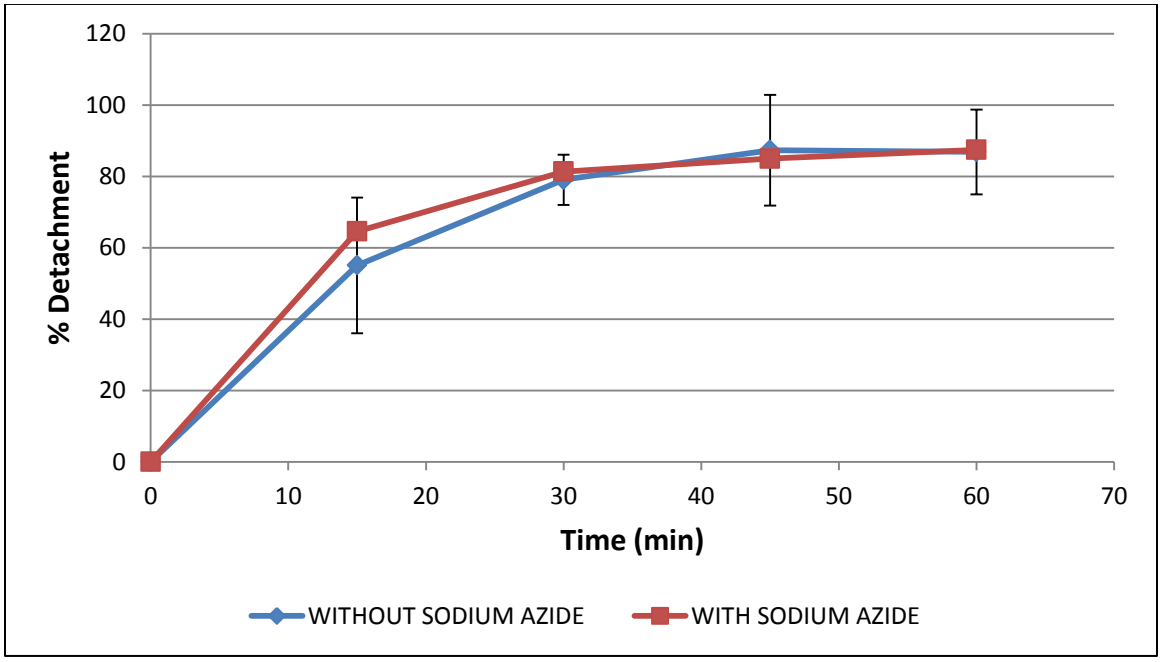

Figure 5.9 Cell detachment in warm media at 20°C (RT/WM) in the presence of sodium azide (red line), and without sodium azide (blue line).

5.3.3.4 Comparison of cell detachment at different temperatures with and without sodium azide

Figures 5.10 and 5.11 compare cell detachment from atrpNIPAM surfaces without sodium azide at the three different conditions (Figure 5.10), and in the presence of sodium azide (Figure 5.11). Table 5.4 compares the initial detachment rates for all detachment conditions.

Table 5.4 Comparison of initial detachment rates at all conditions.

Detachment conditions	Initial detachment rates (%/min)
FT/FM with sodium azide	3.1 ± 1.7
FT/FM without sodium azide	2.7 ± 0.5
RT/FM with sodium azide	4.7 ± 0.9
RT/FM without sodium azide	4.7 ± 0.1
RT/WM with sodium azide	4.3 ± 0.9
RT/WM without sodium azide	3.7 ± 1.3

There appears to be a trend for slower initial detachment at 4^{o}C. In both cases, with and without sodium azide, the average detachment at 4^{o}C is lower than at the other two temperatures, although there is no significant difference between any of the time points for all three conditions. In both cases, with and without sodium azide, the detachment that starts with cold media and continues at room temperature (green line on the graphs) has the fastest initial detachment rate. Thirty minutes after the detachment started, there is no difference between the percentages of cells detached starting in cold media vs warm media at room temperature. The average values for the detachment at 4^{o}C are slightly lower than the ones at the other two conditions.

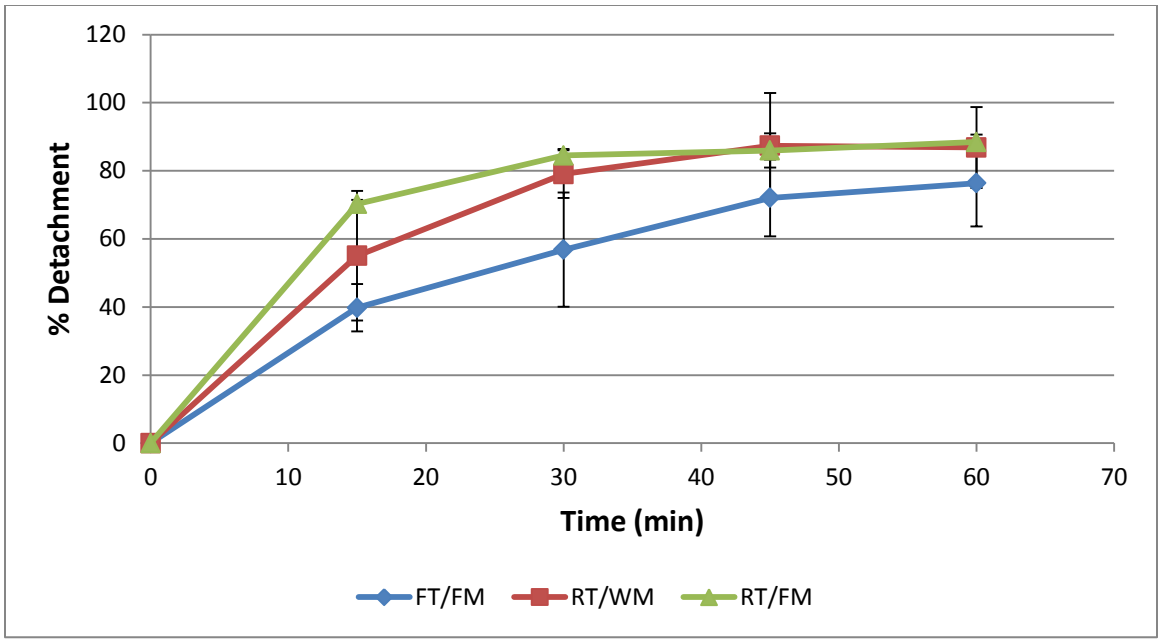

Figure 5.10 Comparison of cell detachment without sodium azide at 4°C (FT/FM), in cold media at 20°C (RT/FM), and in warm media at 20°C (RT/WM).

This trend is the same for detachment in the presence or absence of sodium azide. There is no difference in the final percentage detachment between the three conditions with and without sodium azide. In both cases, cold media at room temperature has the fastest initial detachment, with warm media at room temperature being the second fastest, and the 4°C detachment having slightly smaller values than the other two. Also, in both cases, both detachments at room temperature, in cold and warm media, have almost identical values starting with 30 minutes after the detachment.

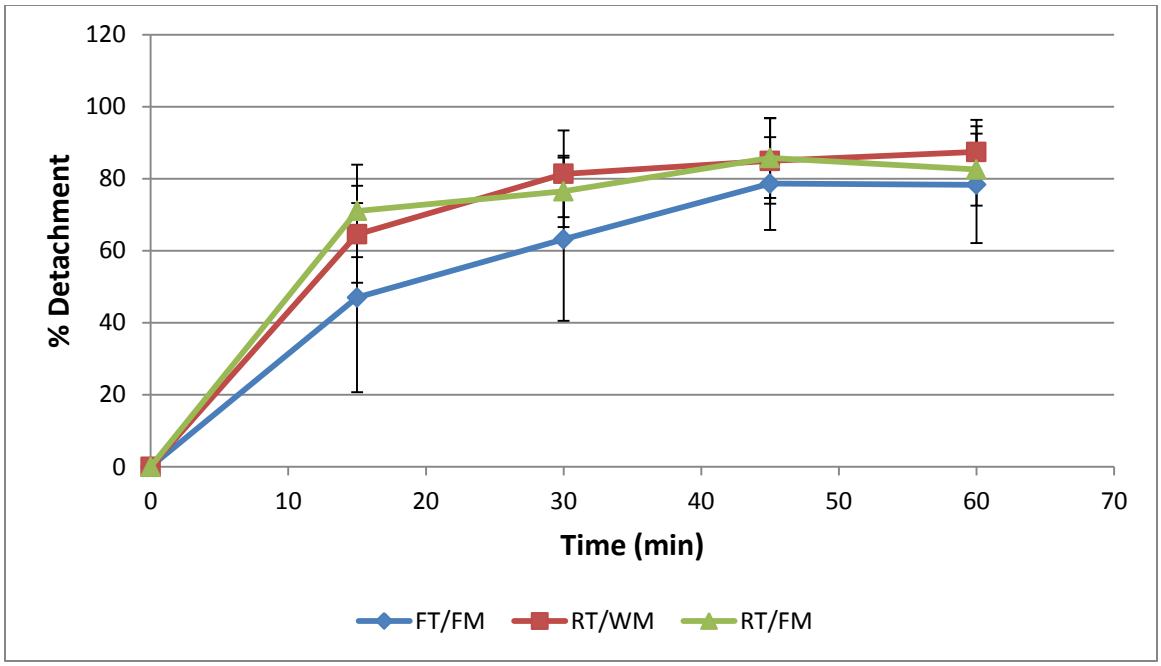

Figure 5.11 Comparison of cell detachment with sodium azide at 4°C (FT/FM), in cold media at 20°C (RT/FM), and in warm media at 20°C (RT/WM).

The observation that there is no difference in cell detachment with the addition of sodium azide indicates that the ATP inhibitor did not influence cellular detachment from pNIPAM. The temperature of the media, however, seems to be an important factor. When the detachment was started with cold media and allowed to occur at room temperature, more cells detached initially than when the detachment was started in warm media. Since pNIPAM chains become more hydrated at lower temperatures, these results suggest that the hydration of pNIPAM chains is the most important factor in the detachment process. These results also suggest that at room temperature, the influence of sodium azide, which inhibits ATP generation and therefore the metabolic activities in the cell, is negligent. Therefore, the proposed active step in the mechanism of cell detachment is not crucial, as previously thought. However, when the detachment was performed at 4°C, the initial detachment occurred more slowly than for detachments at

room temperature. Here, the effects of significantly lower temperature than the cell culture temperature affect the cells enough to slightly lower the initial detachment of cells from pNIPAM. Nonetheless, the hydration of pNIPAM chains is sufficient to cause cell detachment at longer times.

5.4 Conclusions

In this chapter, we investigated the factors that affect the detachment of cells from pNIPAM-coated surfaces. For this investigation, we synthesized and optimized pNIPAM-coated surfaces using surface-initiated atom transfer radical polymerization. We then performed series of detachment experiments in the presence of sodium azide, an ATP inhibitor, and without it, at three different conditions: at 4^{o}C (FT/FM), at 20^{o}C with initially cold media (RT/FM), and at 20^{o}C with initially warm media (RT/WM).

We found that the addition of sodium azide did not affect cellular detachment from pNIPAM, with similar cell detachment trends and percentages from pNIPAM for cell culture with and without sodium azide. The important factor turned out to be the temperature. The best initial detachment was achieved in cells treated with cold media followed by detachment at room temperature, while there was a slightly lower initial detachment at 4^{o}C. If quick initial detachment is important, it would be suggested to perform the detachment at room temperature, starting with cold media. However, if the quick initial detachment is not crucial, the detachment can also be performed at colder temperatures, with similar results. These results imply that the detachment process is predominantly passive where cellular activity is not required. The detachment depends on the rapid hydration of pNIPAM chains. This hydration ruptures the cellular anchors to the film (most likely through the ECM) and causes the cells to detach from the surface.

CHAPTER 6: INVESTIGATION OF PNIPAM/CELL INTERFACE

6.1 Introduction

As stated in Chapter 1, cell sheets generated using stimuli responsive polymers, such as pNIPAM, are being used for tissue engineering. Cells harvested from the patient can be grown on a pNIPAM-coated substrate to form cell sheets, which then can be layered to form a tissue. While a great deal of research is focused on cell sheet engineered from pNIPAM surfaces, there are still several unanswered questions about the nature of cellular detachment from this polymer and about the biocompatibility of pNIPAM surfaces. The NIPAM monomer is cytotoxic, and prior to our work in Chapter 4, it was unclear if pNIPAM was, too. In Chapter 4, we performed a comprehensive study of cytotoxicity of pNIPAM-coated surfaces, and proved that pNIPAM-coated surfaces are not cytotoxic. In this chapter (as well as in Chapter 5) we investigated the mechanism of cell detachment from pNIPAM. While in Chapter 5 we examined the major factors that influence cellular detachment from pNIPAM, in this chapter we are taking a closer look at the pNIPAM-cell interface.

As was reviewed in Chapter 3, several research groups have investigated the behavior of the extracellular matrix (ECM) deposited by the cultured cells on pNIPAM-coated surfaces. Investigations by Kushida et al revealed that BAECs adhered, spread, and deposited fibronectin on pNIPAM surfaces over the time of the culture.[36] Upon lowering the temperature, intact cell sheets detached from the grafted surfaces. Immunostaining of the detached sheets showed that a majority of fibronectin detached with the cell sheets. The area from which the cells detached did not show the presence of fibronectin.[36] Canavan et al. reported that, after detachment with low-temperature

treatment, fibronectin and laminin remained for the most part with the detached cell sheet, although some ECM was left behind ("residual ECM").[39] These results were confirmed by several other studies.

Low-temperature cell sheet detachment using pNIPAM-grafted surfaces is thought to be less destructive than detachment using mechanical scraping or enzymatic digestion. It is known that most of the ECM proteins detach together with the cells during low-temperature cell release from pNIPAM-grafted surfaces.[22, 35, 36, 38, 40] However, it has not been investigated if the detaching cell sheets remove a portion of the pNIPAM from the surfaces, as well. Figure 6.1 shows a schematic of cells detaching from pNIPAM-coated surfaces without pNIPAM (A) and with pNIPAM (B). It is essential to know if any fragments of the polymer are removed with the cells, as small polymer fragment could have cytotoxic effects on the cells. This is especially important if these cells are going to be used for the generation of a tissue used for transplantation.

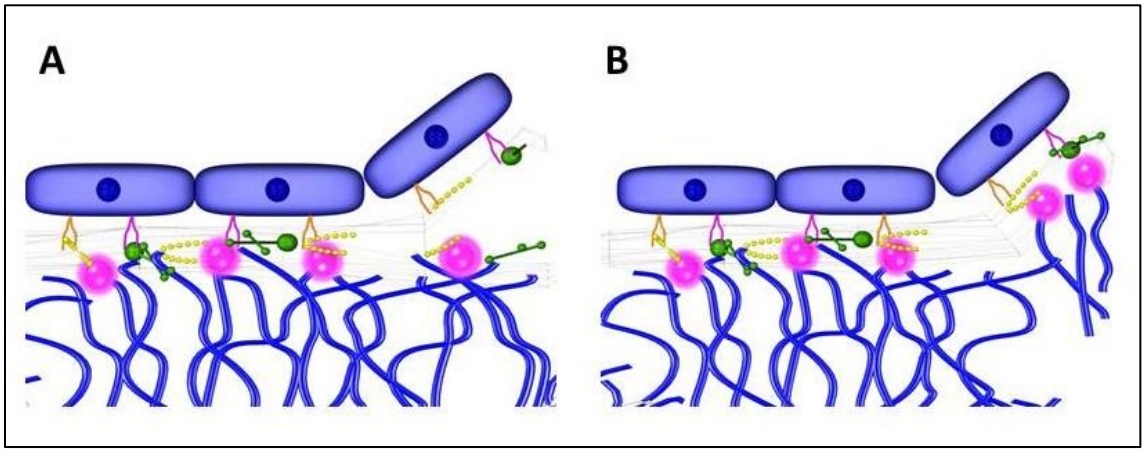

Figure 6.1 Schematic of cells detaching from pNIPAM-coated surfaces without fluorescently labeled pNIPAM (A), or with fragments of pNIPAM (B).

In this chapter, we assessed whether cell sheet detachment from pNIPAM is accompanied by the removal of pNIPAM from the substrate itself (see Figure 6.1 b), as well. As previous work by our group had demonstrated that traditional surface characterization techniques such as XPS and ToF-SIMS are incapable of distinguishing between ECM proteins and pNIPAM, this necessitated the generation of a fluorescently-tagged pNIPAM film for cell culture. [16, 23]

The technique for generating pNIPAM-grafted surfaces described in Chapter 5 was modified to incorporate a fluorescent compound to the reaction vessel. There are several studies reporting the synthesis of fluorescent pNIPAM, employing a number of different fluorescent dyes.[153-156] To our knowledge, none of these studies used the resulting fluorescent pNIPAM for cell adhesion. For this study, 5-acrylamidofluorescein was used. This compound has recently been used in our lab to label of pNIPAM-based microgels using free radical polymerization reaction, resulting in successful generation of fluorescent microgels. The resulting fluorescent pNIPAM surfaces (atrpNIPAM-5AF) were tested for cell attachment and detachment using bovine aortic endothelial cells (BAECs). Using a semipermeable superstrate, the BAEC cell sheets were transferred to a secondary culture dish to assess whether the detachment of cells resulted in any the pNIPAM removal. In addition, the function of the transplanted BAECs was assessed by determining whether they would proliferate and grow on the new secondary substrate.

6.2 Methods

The experiments performed in this chapter follow the procedures outlined in Chapter 2, including surface-initiated atom transfer radical polymerization of NIPAM and 5-acrylamidofluorescein, goniometry, and cell culture. All experiments with cells

were performed on BAECs. Detachment experiments from atrpNIPAM-5AF surfaces were performed as described in Chapter 2, using cold serum-free media and storage at 21^{o}C as the detachment conditions. To determine if there is any pNIPAM removed along with the detaching cells, assisted detachment utilizing a polyvinylidene fluoride (PVDF, Milipore Corporation, Bedford, MA) membrane was performed. To perform the detachment, cell culture media was removed from the wells with cells until only a thin film of media remained on the cells. A PVDF membrane was positioned on the top of the cells and the well plate with cells and PVDF membranes were incubated at 37^{o}C for 30 minutes. After 30 minutes, cold (4^{o}C) serum-free media was added to the wells and the detachment was allowed to proceed for 30 minutes at room temperature. After 30 minutes, the membrane with attached cells was peeled from the substrate and transferred into a new well plate. The cells were then incubated at 37^{o}C with a minimum amount of media for another 30 minutes. After 30 minutes, warm regular cell culture media was added to the well and the PVDF membrane was released from the cells.

6.3 Results and discussion

6.3.1 Synthesis of fluorescent pNIPAM surfaces

To synthesize fluorescent pNIPAM surfaces, the surface-initiated atom transfer polymerization technique used in Chapter 5 to generate pNIPAM films was modified to include 5-acrylamidofluorescein as one of the reagents. After optimizing the concentration of the fluorescent molecule to be used for the reaction (0.5 mol%, 0.1 mol%, and 0.05 mol%), the final atrpNIPAM-5AF surfaces were synthesized with 0.05 mol% of 5-acrylamidofluorescein.

6.3.2 Characterization of atrpNIPAM-5AF surfaces

Figure 6.2 shows a glass cover slip that has been coated with fluorescent atrpNIPAM-5AF using this technique. The white dashed lines have been added to guide the eye to distinguish between the green fluorescence (from the 5-acrylamidofluorescein) on the glass slip against the Petri dish in which the surface was placed (which is not fluorescent, and therefore appears black).

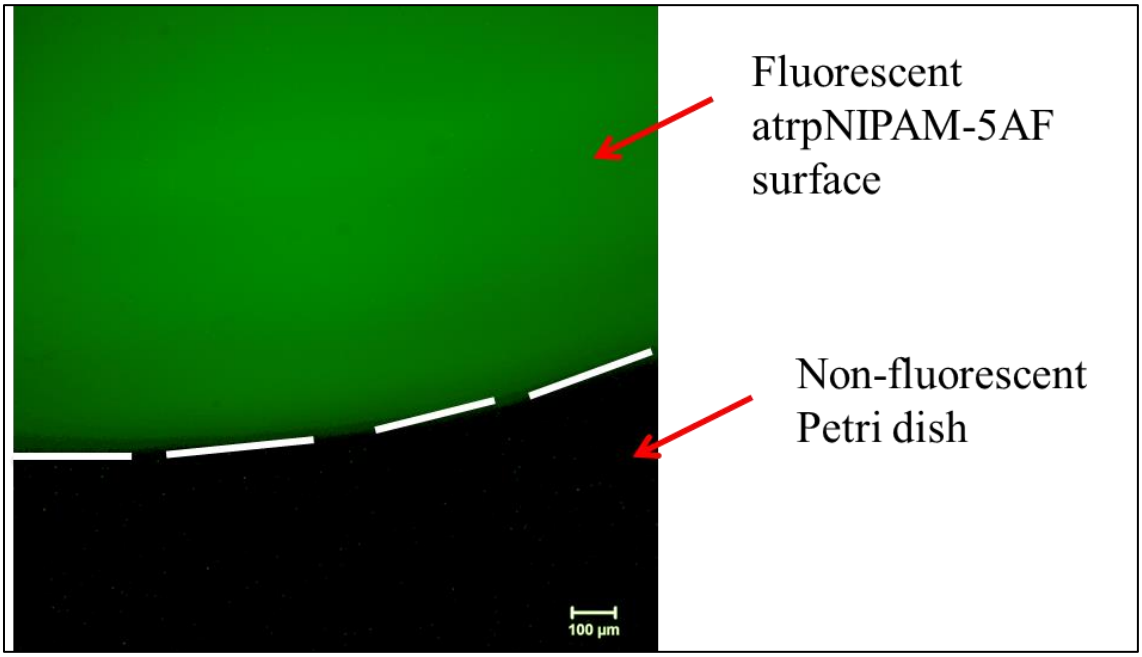

Figure 6.2 Fluorescence microscopy image of an atrpNIPAM-5AF-coated glass cover slip resting in a Petri dish. The fluorescent surface appears in green; the Petri dish does not fluoresce, and appears in black. White dotted lines outline the edge of the coated cover slip. Scale bar is 100 µm.

The thermoresponse of these surfaces was tested using contact angle goniometry. Inverted bubble contact angle measurements were performed at room temperature (20^{o}C) and body temperature (37^{o}C). Figure 6.3 shows the results of these measurements. Controls (uncoated Si chips) showed no thermoresponse. The atrpNIPAM surfaces had an average value of 25^{o} at room temperature, and 30^{o} at body temperature. These values

are lower than the contact angles of pure atrpNIPAM surfaces (~48^{o} at room temperature, and 63^{o} at body temperature). This change in the contact angle is not unexpected, as a new compound was added to the films, altering their resulting chemistry. Most importantly, the fluorescently tagged pNIPAM surfaces retained their thermoresponse, indicating that the films will still be suitable for use to reversibly adhere cells. [As an interesting aside, the thermoresponse was especially visible while taking the measurement, when the relative ease at which the air bubbles stayed on the surface at body temperature was observed, when compared to room temperature.]

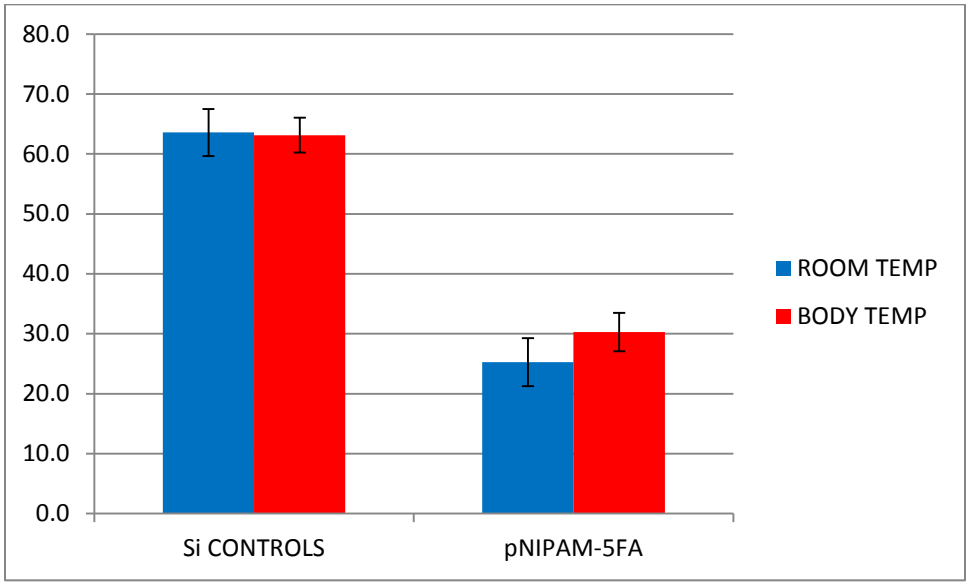

Figure 6.3 Inverted bubble contact angles of atrpNIPAM-5AF-coated surfaces measured at room and body temperature in ultrapure water.

6.3.3 Cell attachment and detachment

The atrpNIPAM-5AF surfaces were tested for cellular attachment and detachment using BAECs. The cells were seeded on the surfaces, and after they reached desired

confluency, they were detached from the surfaces as described in Chapter 2 (in cold serum-free media, at 21^{o}C).

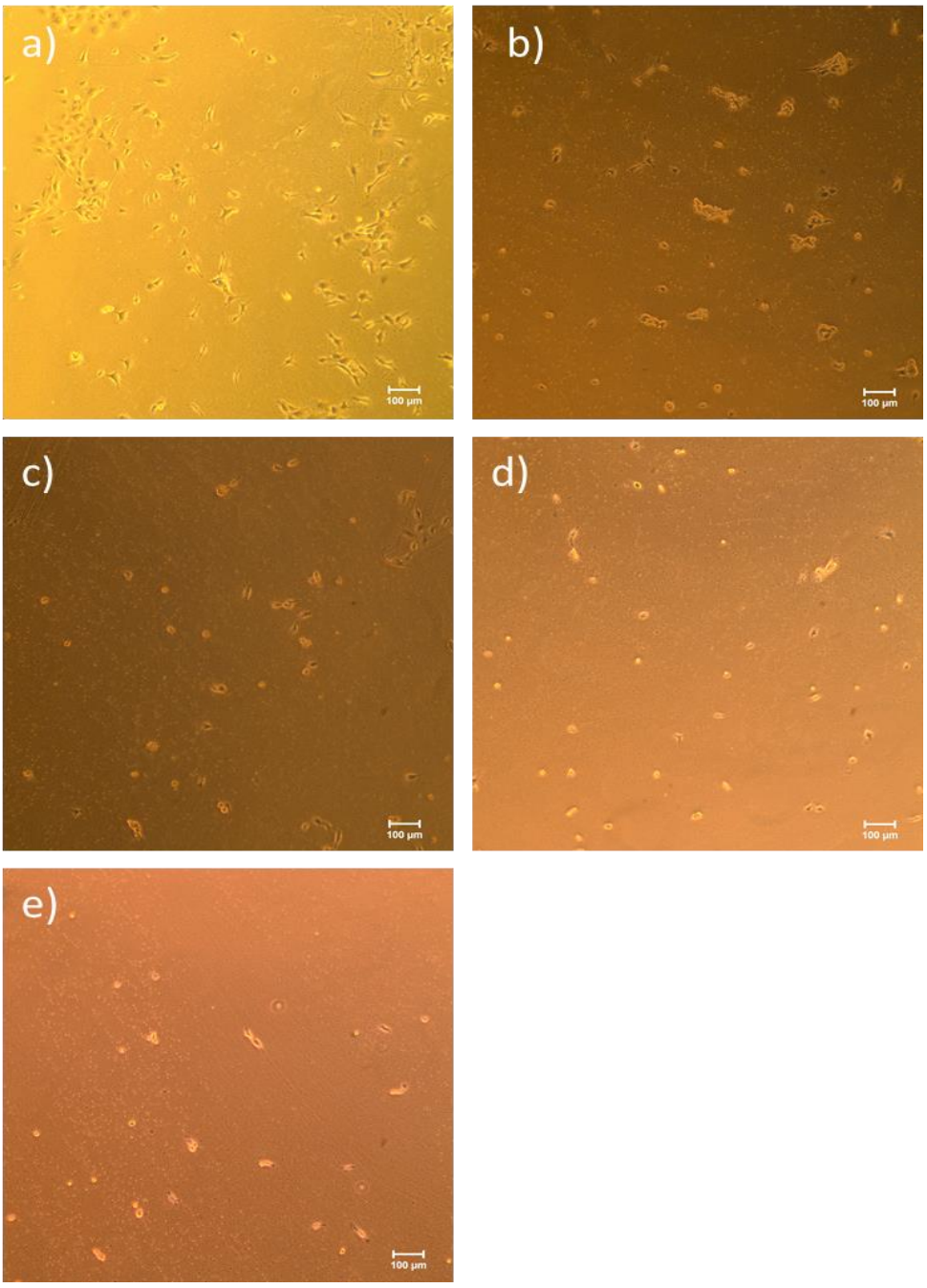

Figure 6.4 Bright phase microscopy of endothelial cells cultured on atrpNIPAM-5AF surfaces during detachment at room temperature after 0 minutes (a), after 15 minutes (b), after 30 minutes (c), after 45 minutes (d), and after 60 minutes (e). Scale bar is 100 µm.

To ensure that the surfaces still behave the same as the unmodified atrpNIPAM surfaces, the detachment was observed over time, at time points of 15 minutes, 30 minutes, 45 minutes, and 60 minutes. Figure 6.4 shows images of cells growing on the atrpNIPAM-5AF surfaces prior to detachment, at 37^{o}C, as well as after 15 minutes (b), 30 minutes (c), 45 minutes (d), and 60 minutes (e) of detachment.

At first, the cells appear spread and attached to the surface, as has previously been observed with this cell type (see Fig 6.4a). After the introduction of the media at low temperature was introduced, the cells became more rounded, and start detaching from the surface (see Fig 6.4b). Almost complete detachment was achieved after 60 minutes (see Fig 6.4e).

Next, the number of detached cells was calculated by counting the cells that remained attached to the surface, and subtracting that number from the number of cells attached to the surface before the detachment was started. The percentage detachment was graphed against the time. Figure 6.5 compares the detachment from atrpNIPAM-AF to the detachment from atrpNIPAM (non-fluorescent surfaces from Chapter 5). Inspection of Figure 6.5 indicates that detachment of BAECs from the fluorescent atrpNIPAM films is almost identical to those cells cultured on non-fluorescent counterparts. For example, the initial rate of deadhesion of cells (indicated by the slope of the linear region of the graph) is 4.2 %/min, which is very similar to the detachment at room temperature from atrpNIPAM (which was 4.7 %/min). In addition, the detachment reaches its maximum after 45 minutes, at 90% of detached cells, which is similar to those detached from non-fluorescent atrpNIPAM. Together, these results indicate that the

presence of the fluorescent tag did not alter the dynamics of how detachment occurs from pNIPAM.

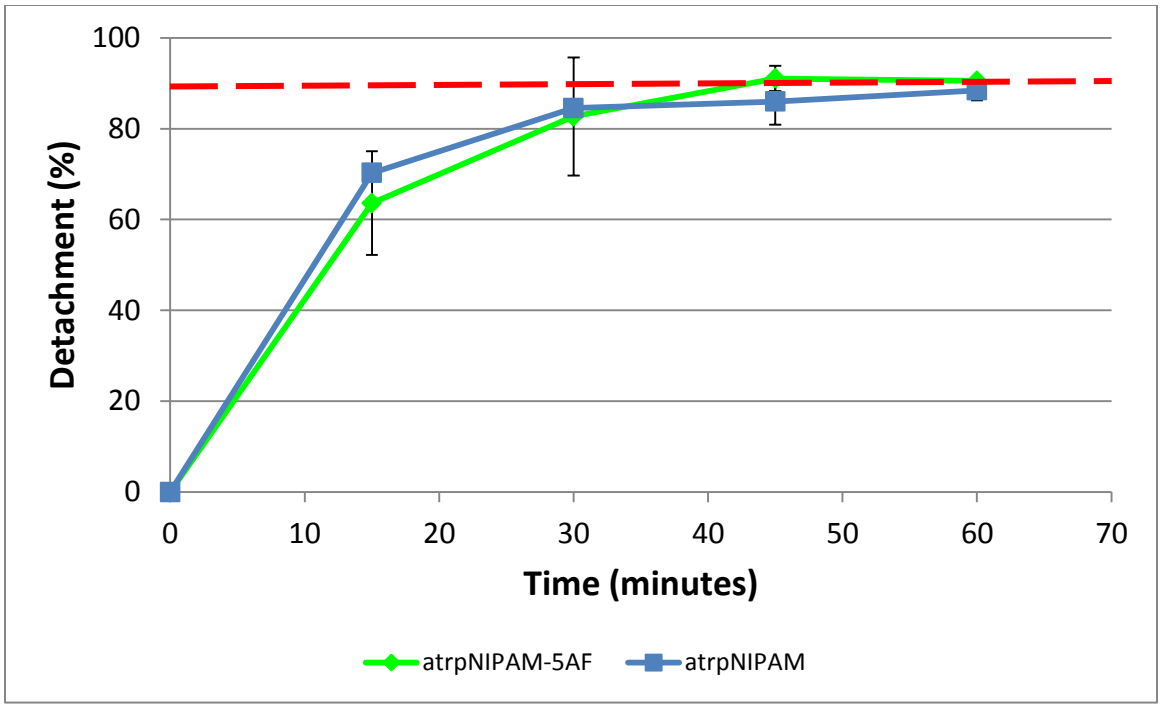

Figure 6.5 Comparison of the detachment of endothelial cells from atrpNIPAM-5AF surfaces (bright green) and atrpNIPAM surfaces (blue). Time points were 15 min, 30 min, 45 min, and 60 min. The red dashed line indicates 90% detachment.

6.3.4 Cellular proliferation and survival after detachment

To test if the cells were still alive and capable of proliferating after detachment, the detached cells were transferred into a new well plate, and were incubated at 37^{o}C to allow them to attach and grow. Figure 6.6 shows a fluorescence microscopy image of an atrpNIPAM-5AF surface during cell culture (a). Figure 6.6 b shows an image of cells growing on this atrpNIPAM-5AF surface. Finally, Figure 6.6 c shows cells that were detached from atrpNIPAM-5AF and seeded in a cell culture flask. The image here shows cells 4 days after the detachment and reseeding. The cells easily attached to the new

flask, and had a normal, elongated and spread morphology identical to BAECs prior to cell detachment. From these results, we can conclude that the functions of the BAECs were not altered, as they did not show any signs of damage resulting from the fluorescently tagged atrpNIPAM-5AF surfaces.

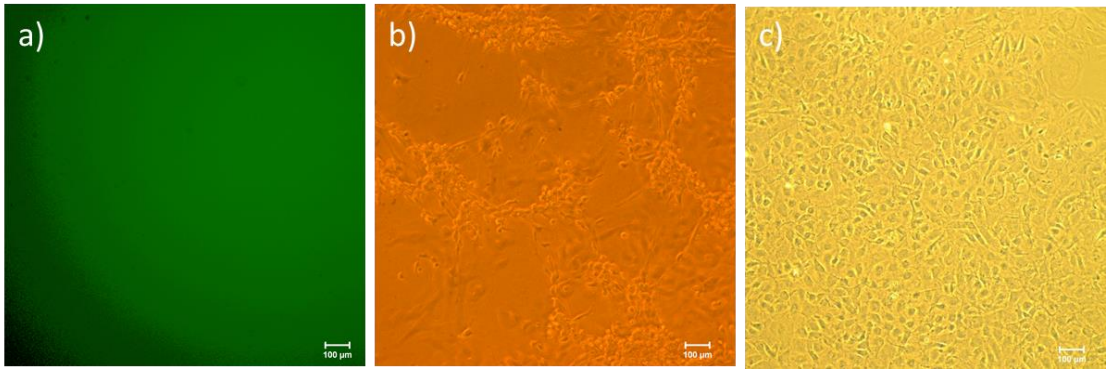

Figure 6.6 Fluorescence microscopy image of atrpNIPAM-5AF surface during cell culture (a); bright phase microscopy of cells growing on the fluorescent surface (b); reseeded endothelial cells growing in a tissue culture flask after detachment from atrpNIPAM-5AF surfaces (c). Scale bar is 100 µm.

6.3.5 Fluorescence study

The final experiment in this study tested whether cells detached from pNIPAM concurrently remove any of the pNIPAM film itself, as well. As with previous experiments, BAECs were seeded on atrpNIPAM-5AF surfaces, and allowed to grow and divide until they reached the desired confluency. Since in this case we used assisted detachment (i.e., "lift-off") with a PVDF membrane superstrate, the cells were allowed to grow to a confluence of ~60-70%. As described in the Methods section of this chapter, the use of the PVDF membrane allows the apical surface of cells to temporarily adhere to the PVDF membrane, during which time they can be transferred to a new (secondary) culture substrate, and allowed to attach. After cell sheet removal using this method, fluorescent images of the atrpNIPAM-5AF surfaces were obtained, to observe whether

there was any visible damage to the surface (e.g., pinholes). Fluorescent images of the cell sheets were also obtained, to determine whether any fluorescence (and therefore the pNIPAM film) had been transferred with the cells during their detachment.

Figure 6.7 shows the results of this experiment. As seen in Figure 6.7a, the atrpNIPAM-5AF surface remains fluorescent and pinhole-free after the detachment process. Careful examination of all surfaces used in this experiment revealed no visible signs of damage to the surface, with all surfaces retaining their fluorescence. Figure 6.7 b shows a fluorescent image of the cells after they were transferred into a new well plate and were allowed to attach. No fluorescence was detected in the wells with the transferred cells, indicating that atrpNIPAM-5AF is not present. Figure 6.7 c shows a bright field microscopy image of the cells one day after the transfer. The cells appear to be adhered to the surface, with normal morphology, indicating that their function has not been altered by the transfer process.

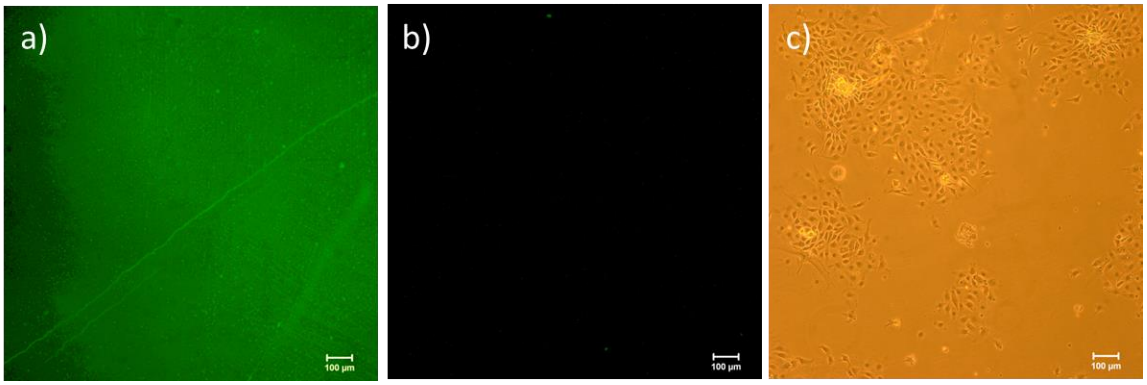

Figure 6.7 Fluorescence microscopy image of atrpNIPAM-5AF surface after cell detachment (a); fluorescence microscopy image (b) and bright field microscopy image (c) of BAECs one day after detachment from atrpNIPAM-5AF surface and subsequent attachment to an uncoated well plate. Scale bar is 100 µm.

6.4 Conclusions

In this chapter, we presented the work we performed to investigate the interface between pNIPAM-coated surfaces and the cells. For this study, we fluorescently tagged pNIPAM-coated surfaces by modifying surfaces developed in the previous chapter (Chapter 5). This was done by adding a fluorescent molecule as an additional reagent for the surface-initiated atom transfer radical polymerization. This novel technique was not previously used for cell culture. The resulting surfaces were tested for cell attachment and detachment, to ensure that they have the same characteristics as the surfaces developed in Chapter 5 (i.e. thermoresponse and similar detachment profile). We then performed cell detachment from these surfaces and checked for fluorescence to see if any of the pNIPAM detached with the cells.

We found that the inclusion of the fluorescent tag in the atrpNIPAM-5AF surfaces did not affect the thermoresponsive and reversibly cell adherent nature of the films, as we observed similar cell attachment and detachment profiles to cells cultured on their non-fluorescent atrpNIPAM counterparts. More importantly, we did not observe fluorescence in the cell sheets after the detachment was performed, while the atrpNIPAM-5AF substrates from which they were obtained retained their fluorescence and appeared pinhole-free. Our results are consistent with previous studies of the ECM and cells after detachment from pNIPAM-coated surfaces that showed that detached cell sheets leave behind some ECM (i.e., “residual ECM”) during the detachment. We therefore conclude that for these pNIPAM films, the cell sheets detach without simultaneously also detaching the underlying pNIPAM film. Together with the results from the previous chapter (Chapter 4 on cytotoxicity), our results indicate that cell sheets obtained by

detachment from pNIPAM films will be suitable for use in engineered tissues (i.e., biocompatible and non-cytotoxic), provided that the pNIPAM films are robust (i.e., grafted, covalently linked, or similar).

CHAPTER 7: CONCLUSIONS AND FUTURE DIRECTIONS

7.1 Conclusions

PNIPAM has become one of the most widely used stimulus-responsive polymers for bioengineering applications due to its ability to release intact biological cells. In fact, to date, over 300 publications exist on the subject of cell release from pNIPAM substrates.

As reviewed in Chapter 3, and summarized by Table A1 in the Appendix, many of these publications investigate the use of pNIPAM films to release biological cells ("cell sheet engineering"). The majority of the papers (approximately 90%) focus on the cell release and its applications, rather than the mechanism of the release. The popularity of the pNIPAM substrate for this purpose and the sheer number of publications in the literature may have led many to certain misunderstandings regarding cell detachment from pNIPAM; namely, that the sole application for which cell release from pNIPAM is used is for tissue engineering, that the mechanism by which cell release is achieved is a well-understood phenomenon, that the potential non-cytotoxicity of pNIPAM is clearly established, or that there is a standard set of procedures that researchers follow to yield predictable release from pNIPAM.

7.1.1 Cytotoxicity of pNIPAM

A comprehensive study of cytotoxicity of pNIPAM and pNIPAM-coated surfaces was described in Chapter 4. We used commercially available pNIPAM as well as pNIPAM synthesized in our laboratory for the tests. These two polymers were used for the investigation of the cytotoxicity of pNIPAM using a concentration gradient test. We also generated four different pNIPAM-coated surfaces for the determination of the

cytotoxicity of pNIPAM-coated surfaces: plasma polymerized pNIPAM (ppNIPAM), spin-coated pNIPAM sol-gel (spNIPAM), spin-coated pNIPAM synthesized via free radical polymerization (frpNIPAM), and spin-coated commercially available pNIPAM (cpNIPAM). These surfaces were extensively tested with extracts and direct contact experiments. The cytotoxicity tests were performed with endothelial, epithelial, fibroblast, and smooth muscle cells.

We found that the NIPAM monomer at 0.5 mg/mL is toxic to all tested cell types, except to fibroblasts at short-term exposure. Endothelial and epithelial cells were the most sensitive to the monomer, while fibroblasts were the most resistant. Although initially the attachment and proliferation of fibroblast and smooth muscle cells was hindered on spNIPAM surfaces, long-term experiments proved that all pNIPAM-coated surfaces were not cytotoxic to the four cell types evaluated in the direct contact test. A plating efficiency assay showed no cytotoxic effects for cells exposed to either form of the polymerized NIPAM; only those cells exposed to the monomer died, which was an expected result. Extract and concentration gradient experiments showed no cytotoxic effects when tested with epithelial, smooth muscle, and fibroblast cells. Endothelial cells showed increased sensitivity to extracts at very high exposures (100% concentration) after 48 hour exposure. Concentration gradient experiments showed that endothelial cells were more sensitive to commercially available pNIPAM, which was likely a result of the presence of residual monomer. These results agree with other published findings, where endothelial cells were found to be more sensitive than epithelial cells.

Since we have demonstrated that cellular sensitivity to pNIPAM varies depending on cell type, we recommend that cytotoxicity testing is performed on cell types

previously unexposed to pNIPAM before using them with this polymer for research. Also, the purity of the polymer is essential, as demonstrated by the concentration gradient experiments. We also found that while cell viability on pNIPAM surfaces decreases when compared to controls, the viability also seems to be deposition type dependent, with sol-gel-based pNIPAM surfaces being the least biocompatible.

7.1.2 Mechanism of cell detachment from pNIPAM

For the investigation of the mechanism of cell detachment from pNIPAM-coated surfaces, we used atrpNIPAM surfaces, which were synthesized using surface-initiated atom transfer radical polymerization (ATRP). This method allowed us to control the polymer film thickness and density on the surface, which are important factors for cell detachment and attachment. The surfaces were optimized for attachment and detachment of endothelial cells. Detachment at various conditions (at 4^{o}C with cold media, room temperature with cold media, and room temperature in warm media) were performed in the presence of sodium azide, and ATP inhibitor, and in the absence of it.

We found that the ATP inhibitor did not affect the detachment of cells at any of the three conditions. Instead, we found that the most important factor impacting cell detachment was the temperature of the media used to initiate the detachment. Our observations therefore support a "passive" mechanism of cell detachment from pNIPAM proposed by Okano et al.[72] However, our findings on inhibition of cellular activity through an ATP inhibitor contradict their proposed "active" step following the passive step.

7.1.3 PNIPAM-cell interface

To further understand the mechanism of cell detachment, we examined the interface between the cells and pNIPAM after the detachment. While it has been previously demonstrated that most of the ECM proteins detach together with the cells during low-temperature cell release from pNIPAM-grafted surfaces,[22, 35, 36, 38, 40] there are no studies investigating if the detaching cell sheets remove a portion of the pNIPAM from the surfaces, as well.

To test this, we synthesized fluorescent pNIPAM surfaces (atrpNIPAM-5AF) by modifying the surface-initiated atom transfer radical polymerization utilized in Chapter 5. The resulting surfaces were tested for cell attachment and detachment, and used to determine if any of the pNIPAM attached to the surface leaves with the cells during the detachment.

Endothelial cells showed a similar attachment and detachment pattern to the one from atrpNIPAM surfaces. There was no visible fluorescence in the cells detached from the fluorescent surfaces. The cells attached and proliferated normally after they were transferred to a new cell culture dish following the detachment. The atrpNIPAM-5AF surfaces appeared to be undamaged after the detachment and retained their fluorescence for the total of 3 weeks. These results indicate that there is no pNIPAM removed with cells during cell detachment. We therefore conclude that for these pNIPAM films, the cell sheets detach without simultaneously also detaching the underlying pNIPAM film. Together with the results from the previous chapter (Chapter 4 on cytotoxicity), our results indicate that cell sheets obtained by detachment from pNIPAM films will be

suitable for use in engineered tissues (i.e., biocompatible and non-cytotoxic), provided that the pNIPAM films are robust (i.e., grafted, covalently linked, or similar).

7.2 Future directions

7.2.1 Investigation of the effect of pNIPAM extracts on bovine aortic endothelial cells

As described in Chapter 4, all of the formulations of pNIPAM we tested were found to be non-cytotoxic to the mammalian cells tested in this study. However, at extremely high concentrations (100% pNIPAM extracts), pNIPAM did negatively impact cell viability. It is therefore important to perform further investigation into the extracts and their cytotoxic effects on bovine aortic endothelial cells. Further experiments with cell attachment and survival in the presence of the extracts would be warranted (LDH assay, LIVE/DEAD assay, plating efficiencies). In addition, the extracts should be characterized via mass spectroscopy to determine their composition and potential cytotoxic components.

7.2.2 Investigation of the effect of commercially available pNIPAM (cpNIPAM) on endothelial cells

In our cytotoxicity study in Chapter 4, we found that the commercially available pNIPAM was cytotoxic to endothelial cells at extremely high polymer concentrations. While we hypothesized that this effect can be attributed to traces of the NIPAM monomer in the polymer powder, it would be advised to further investigate the source of the cytotoxicity. It is possible that shorter pNIPAM chains cause the cytotoxicity. To determine that, a series of experiments is proposed. The commercially available pNIPAM should be further investigated using mass spectroscopy. The polymer would be

first separated into fractions by high performance liquid chromatography. These fractions could then be analyzed by electrospray ionization. In addition to chemical analysis, cpNIPAM would be tested with cells. Endothelial cells and epithelial cells would be seeded on cpNIPAM-coated surfaces, with various concentrations of cpNIPAM (1%, 2%, and 3%). The epithelial cells have shown normal growth and morphology on cpNIPAM surfaces and will be used as negative controls. Cytotoxicity assays such as MTS and LIVE/DEAD would be performed on the cells growing on cpNIPAM surfaces. All results will be analyzed to determine what exactly in the polymer (monomer/short pNIPAM chains/other toxins) affects endothelial cells viability, and if these cytotoxic effects are limited only to endothelial cells.

7.2.3 Determination of cellular activity by staining of actin and talin

As previously mentioned, it was suggested that actin dynamics are important in cell detachment from pNIPAM-coated surfaces.[36, 74] Actin is an intracellular protein that is a major component of cellular cytoskeleton. It is crucial for cellular movement, maintenance of cell shape, and muscle contraction. Actin functions are ATP-dependent, and ATP inhibitors will prevent actin from performing its tasks. Talin, another intracellular protein, connects integrins with actin cytoskeleton at the point of cell adhesion to a surface.[157] Integrins attach cells to the extracellular matrix. Therefore, talin is especially prominent in the points of focal adhesion.

For this study, observation of actin and talin during cell detachment from pNIPAM is proposed. Staining of actin and talin in live cells is proposed to be performed using CellLight Backmam 2.0 reagents (Invitrogen, Grand Island, NY). Actin will be stained red using CellLight Actin – RFP, and talin will be stained green using CellLight

Talin – GFP. Backmam 2.0 reagents contain double stranded DNA insect viruses (baculovirus) coupled with a mammalian promoter. When introduced into the cell, the baculovirus enters the nucleus and the gene of interest with the mammalian promoter is transcribed and expressed, while the viral genes are not recognized by the cell and therefore not transcribed.

Detachment experiments would be performed at room temperature, at $4^{o}C$, and at $4^{o}C$ followed by raising the temperature to room temperature. The cells would be observed during detachment through an inverted light microscope and fixed to obtain a series of images of cells right before the detachment, and during the detachment. The fixed cells would be then imaged using confocal fluorescence microscopy. The results would be compared to same experiments performed in the presence of an ATP inhibitor. These experiments would be repeated with other types of cell (such as fibroblasts and epithelial cells) to determine if the mechanism of cell detachment and its temperature dependency is uniform throughout different cell lines.

7.2.4 Investigation of pNIPAM surfaces and detached cells after detachment

In Chapter 6, we performed an investigation of pNIPAM-cell interface using fluorescent pNIPAM surfaces. While we detected no traces of fluorescent pNIPAM with the detached cells, this study should be followed with a study employing more quantitative and higher resolution detection methods than provided by fluorescence microscopy. Therefore, we are proposing here further investigation into the nature in which the cells detach from atrpNIPAM-5AF surfaces.

In the proposed study, the atrpNIPAM-5AF surfaces would be investigated via atomic force microscopy (AFM). AFM would be performed on the surfaces prior to cell

attachment, as well as after the detachment. AFM is a high-resolution technique, and it can bring more insight into the character of the surfaces than observing them using regular light microscopy. AFM data would give insight into the topography of the surfaces before and after the detachment, and could give understanding if cellular detachment from pNIPAM changes the pNIPAM surfaces in any way. Furthermore, an attempt to quantify the fluorescence present in the detached cells (if there is any) can be made by using fluorescence setting in a plate reader. A plate reader provides quantifiable results with a lower and more reliable detection limit than visual observation of fluorescence.

APPENDIX

Table A1. Published articles incorporating cellular studies and pNIPAM through 2014, as referenced in Chapter 3. The research area and a short description of the findings provided.

RESEARCH AREA	TITLE	AUTHOR	JOURNAL/YEAR	SHORT DESCRIPTION
Review	Poly(*N*-isopropylacrylamide) – Experiment, Theory and Application[19]	Schild, H.G.	*Progress in Polymer Science/1992*	Summary of work done on pNIPAM from 1956 to 1991. Summary of methods of synthesis of pNIPAM, characterization, experimental techniques used to observe the LCST and known applications.
Review	Functional copolymers of *N*-isopropylacrylamide for bioengineering applications[93]	Rzaev, Z.M.O. et al.	*Progress in Polymer Science/2007*	Copolymers of N-isopropylacrylamide, their synthesis, structure, properties and applications in the bioengineering.
Review	Smart thermoresponsive coatings and surfaces for tissue engineering: switching cell-material boundaries[13]	Da Silva R.M.P. et al.	*Trends in Biotechnology/2007*	A review of methods of producing thermoresponsive substrates coated w/pNIPAM for cell sheet engineering. Discusses the effectivenes of the surfaces in cell adhesion and detachment.
Review	Thermosensitive water-soluble copolymers with doubly responsive reversibly interacting entities[12]	Dimitrov, I. et al.	*Progress in Polymer Science/2007*	Thermo-, pH-, magnetic and light sensitive polymers.
Review	Stimuli-responsive polymers and their bioconjugates[11]	Gil, E.S. et al.	*Progress in Polymer Science/2004*	The review discusses temperature-, pH-, glucose-, field-, ionic strength-, and antigen-responsive polymers. About pNIPAM: LCST, comb vs linear pNIPAM hydrogels, random copolymerization, controlling LCST, pNIPAM micelles, temperature responsive surfaces, cell culture.
Review	Stimuli-sensitive hydrogels: ideal carriers for chronobiology and chronotherapy[30]	Peppas, N.A. et al.	*Journal of Biomaterials Science – Polymer Edition/2004*	Temperature- and pH-sensitive hydrogels in chronotherapy. Different types of hydrogels with pNIPAM as one of the copolymer are discussed.
Review	Temperature-sensitive aqueous microgels[94]	Pelton, R.	*Advances in Colloid and Interface Science/2000*	Microgels made of pNIPAM and other polymers, and methods of microgel synthesis. Microgel properties and applications.
Review	Stimuli-responsive interfaces and systems for the control of protein-surface and cell-surface interactions[16]	Cole, M.A. et al.	*Biomaterials/2009*	Energy based and chemical based stimuli responsive systems, emphasis on temperature-responsive surfaces. Described are synthesis, applications, as well as theoretical considerations.
Cell Sheet Engineering	Two-dimensional manipulation of differentiated Madin-Darby canine kidney (MDCK) cell sheets: The noninvasive harvest from temperature-responsive culture dishes and transfer to other surfaces[40]	Kushida, A. et al.	*Journal of Biomedical Materials Research/2001*	MDCK cells on PNIPAM, investigation of the cells after detachment; immunoblotting and anti-FN antibody to examine whether ECM is recovered w/cells; mechanism of cell sheet detachment.
Cell Sheet Engineering	Multilayered mouse preosteoblast MC3T3-E1 sheets harvested from temperature-responsive poly(*N*-isopropylacrylamide-co-acrylamide) grafted culture surface for cell sheet engineering[41]	Wong-In, S. et al.	*Journal of Applied Polymer Science/2013*	pNIPAM-co-acrylamide surfaces prepared by ultraviolet irradiation. Cells were successfully seeded on the surfaces and detached from them.

Cell Sheet Engineering	Rapid cell sheet detachment using spin-coated pNIPAAm films retained on surfaces by an aminopropyltrietoxysilane network[42]	Patel, N.G. et al.	*Acta Biomaterialia/2012*	Spin-coated pNIPAM surfaces with 3-aminopropyltriethoxysilane supported cell adhesion and quick detachment.
Cell Sheet Engineering	Comparison of mesenchymal stem cells released from poly(*N*-isopropylacrylamide) copolymer film and by trypsinization[43]	Yang et al.	*Biomedical Materials/2012*	Mesenchymal stem cells cultured on and detached from pNIPAM-coated surfaces – comparison of cellular characteristics (morphology, immunophenotype and osteogenesis) to cells cultured on glass coverslips.
Cell Sheet Engineering	Rapid cell sheet detachment from alginate semi-interpenetrating nanocomposite hydrogels of pNIPAm and hectorite clay[44]	Wang, T. et al.	*Reactive and Functional Polymers/2011*	Alginate-pNIPAM hydrogels. Fibroblasts, human lung adenocarcinoma epithelial cells, and human cervical cancer cells were cultured and detached. Cell sheets were reseeded and proliferated.
Cell Sheet Engineering	Effect of protein and cell behavior on pattern-grafted thermoresponsive polymer[45]	Chen, G. P., et al.	*Journal of Biomedical Materials Research/1998*	Copolymer (pNIPAM-co-acrylic acid) coupled with azidoaniline in a specific pattern used for selective cell detachment in serum-free media (mouse fibroblast STO cells).
Cell Sheet Engineering	Patterned immobilization of thermoresponsive polymer[46]	Ito, Y. et al.	*Langmuir/1997*	pNIPAM copolymerized with acrylic acid coupled with azidoaniline, patterned and used with mouse fibroblast STO cells for selective detaching of cells.
Cell Sheet Engineering	Transplantable urothelial cell sheets harvested noninvasively from temperature-responsive culture surfaces by reducing temperature[158]	Shiroyanagi, Y. et al.	*Tissue Engineering/2003*	Transplantable urothelial cell sheets recovered from pNIPAM surfaces; useful in urinary tract tissue engineering.
Cell Sheet Engineering	Repair of impaired myocardium by means of implantation of engineered autologous myoblast sheets[48]	Memon, I. A. et al.	*Journal of Thoracic and Cardiovascular Surgery/2005*	Skeletal myoblast sheets engineered on pNIPAM surfaces used to repair impaired myocardium in rats.
Cell Sheet Engineering	The effects of cell culture parameters on cell release kinetics from thermoresponsive surfaces[27]	Reed, J.A. et al.	*Journal of Applied Biomaterials and Biomechanics/2008*	Study of optimal conditions for cell detachment from pNIPAM-coated surfaces (plasma polymerization and spin-coating, SFM, DPBS, DPBS followed by SFM, and MWS).
Cell Sheet Engineering	Bioengineered chondrocyte sheets may be potentially useful for the treatment of partial thickness defects of articular cartilage[49]	Kaneshiro, N. et al.	*Biochemical and Biophysical Research Communications/2006*	Cell sheets were detached from pNIPAM-coated surfaces using a PVDF membrane. The generated tissues were examined in vivo and ex vivo.
Cell Sheet Engineering	Functional bioengineered corneal epithelial sheet grafts from corneal stem cells expanded ex vivo on a temperature-responsive cell culture surface[26]	Nishida, K. et al.	*Transplantation/2004*	pNIPAM surfaces + limbal corneal endothelial stem cells; characterization of cells after detachment; corneal surface reconstruction in rabbits (transplantation).
Cell Sheet Engineering	Corneal reconstruction with tissue-engineered cell sheets composed of autologous oral mucosal epithelium[50]	Nishida, K. et al.	*New England Journal of Medicine/2004*	pNIPAM surfaces + autologous oral mucosal epithelial cells; transplanted to denuded corneal surfaces (eyes).
Cell Sheet Engineering	Functional human corneal endothelial cell sheets harvested from temperature-responsive culture surfaces[159]	Sumide, T. et al.	*FASEB Journal/2005*	Fabricating human corneal endothelial cell sheets on pNIPAM for ocular surgery and repair. Scanning electron microscopy, cell immunofluorescence staining etc. of recovered cell sheets.
Cell Sheet Engineering	Fabrication of pulsatile cardiac tissue grafts using a novel 3-dimensional cell sheet manipulation	Shimizu, T. et al.	*Circulation Research/2002*	Layering cardiomyocyte sheets recovered from pNIPAM surfaces; transplanted into subcutaneous tissue of nude

	technique and temperature-responsive cell culture surfaces[52]			rats (functioning pulsatile grafts).
Extracellular Matrix	Cell sheet detachment affects the extracellular matrix: A surface science study comparing thermal liftoff, enzymatic, and mechanical methods[22]	Canavan, H. E. et al.	*Journal of Biomedical Materials Research Part A/2005*	How different ways of detaching cells affect the extracellular matrix (ECM).
Extracellular Matrix	Comparison of native extracellular matrix with adsorbed protein films using secondary ion mass spectrometry[35]	Canavan, H. E. et al.	*Langmuir/2007*	ECM and fibronectin after low-temperature liftoff from pNIPAM surfaces (XPS, PCA, ToF-SIMS).
Extracellular Matrix	Decrease in culture temperature releases monolayer endothelial cell sheets together with deposited fibronectin matrix from temperature-responsive culture surfaces[36]	Kushida, A. et al.	*Journal of Biomedical Materials Research/1999*	Endothelial cells + pNIPAM, immunoblotting, immunofluorescence; focus on fibronectin deposition and recovery (how much detaches w/cells, how much stays on the surface).
Extracellular Matrix	A plasma-deposited surface for cell sheet engineering: Advantages over mechanical dissociation of cells[160]	Canavan, H. E. et al.	*Plasma Processes and Polymers/2006*	Analysis of the mechanical dissociation of cells; pNIPAM used to compare surfaces after enzymatic, T-liftoff and mechanical dissociation of cells.
Extracellular Matrix	Structural characterization of bioengineered human corneal endothelial cell sheets fabricated on temperature-responsive culture dishes[38]	Ide, T. et al.	*Biomaterials/2006*	Human corneal endothelial cells detachment form pNIPAM; checking ECM proteins (type IV collagen and fibronectin); corneal regenerative medicine.
Extracellular Matrix	Surface characterization of the extracellular matrix remaining after cell detachment from a thermoresponsive polymer[23]	Canavan, H. E. et al.	*Langmuir/2005*	Surface characterization of ECM after cell detachment from pNIPAM surfaces. Looking at laminin, fibronectin and collagen (XPS, PCA, ToF-SIMS, immunostaining)
Extracellular Matrix	Two-dimensional manipulation of differentiated Madin-Darby canine kidney (MDCK) cell sheets: The noninvasive harvest from temperature-responsive culture dishes and transfer to other surfaces[40]	Kushida, A. et al.	*Journal of Biomedical Materials Research/2001*	MDCK cells on PNIPAM, investigation of the cells after detachment; immunoblotting and anti-fibronectin antibody to examine whether ECM is recovered w/cells; mechanism of cell sheet detachment
Controlling Cell Attachment and Detachment	The effects of cell culture parameters on cell release kinetics from thermoresponsive surfaces[27]	Reed, J.A. et al.	*Journal of Applied Biomaterials and Biomechanics/2008*	Study of optimal conditions for cell detachment from pNIPAM-coated surfaces (plasma polymerization and spin-coating, SFM, DPBS, DPBS followed by SFM, and MWS).
Controlling Cell Attachment and Detachment	Rapid cell sheet detachment from poly(N-isopropylacrylamide)-grafted porous cell culture membranes[95]	Kwon, O. H. et al.	*Journal of Biomedical Materials Research/2000*	pNIPAM on porous membranes with cells for fast detachment (to accelerate cell detachment).
Controlling Cell Attachment and Detachment	Copolymerization of 2-carboxyisopropylacrylamide with N-isopropylacrylamide accelerates cell detachment from grafted surfaces by reducing temperature[97]	Ebara, M. et al.	*Biomacromolecules/2003*	Accelerating cell detachment by using p(IPAAM-co-CIPAAm) grafted dishes. Introduction of CIPAAm into PIPAAm chains accelerates cell detachment.
Controlling Cell Attachment and Detachment	Ultrathin poly(N-isopropylacrylamide) grafted layer on polystyrene surfaces for cell adhesion/detachment control[82]	Akiyama, Y. et al.	*Langmuir/2004*	pNIPAM surfaces for cell attachment/detachment: importance of the thickness of pNIPAM layer. Correlation of the thickness of pNIPAM layers and cell attachment and detachment.
Controlling Cell Attachment and	Inhibition of protein adsorption and cell adhesion on PNIPAAm-grafted polyurethane surface: effect	Zhao, T.L. et al.	*Colloids and Surfaces B – Biointerfaces/2011*	Investigation of the effects of molecular weight of surface grafted pNIPAM on cell attachment and protein

Detachment	of graft molecular weight[98]			adsorption.
Controlling Cell Attachment and Detachment	Cell attachment and detachment on micropattern-immobilized poly(N-isopropylacrylamide) with gelatin[99]	Liu, H. C. et al.	*Lab on a Chip/2002*	pNIPAM copolymerized with acrylic acid coupled with azidoaniline and w/gelatin for enhanced cell attachment (mouse fibroblast STO cells).
Controlling Cell Attachment and Detachment	Poly(N-isopropylacrylamide) (PNIPAM)-grafted gelatin as thermoresponsive three-dimensional artificial extracellular matrix: molecular and formulation parameters vs. cell proliferation potential[100]	Ohya, S. et al.	*Journal of Biomaterials Science-Polymer Edition/2005*	pNIPAM-gelatin +cells - what composition works best for cell proliferation.
Controlling Cell Attachment and Detachment	Poly(N-isopropylacrylamide) (PNIPAM)-grafted gelatin hydrogel surfaces: interrelationship between microscopic structure and mechanical property of surface regions and cell adhesiveness[101]	Ohya, S. et al.	*Biomaterials/2005*	pNIPAM-gelatin hydrogels; interrelationship between elastic modulus and cell adhesion.
Controlling Cell Attachment and Detachment	Poly(N-isopropylacrylamide)-grafted gelatin as a thermoresponsive cell-adhesive, mold-releasable material for shape-engineered tissues[102]	Matsuda, T.	*Journal of Biomaterials Science-Polymer Edition/2004*	pNIPAM-gelatin used for fabrication of a tubular endothelial cell construct; shape tissue engineering.
Controlling Cell Attachment and Detachment	System-engineered cartilage using poly(N-isopropylacrylamide)-grafted gelatin as in situ-formable scaffold: In vivo performance[103]	Ibusuki, S. et al.	*Tissue Engineering/2003*	pNIPAM grafted gelatin + engineered cartilage; precultured tissue for transplantation; chondrocyte transplantation into rabbits' knees.
Controlling Cell Attachment and Detachment	Thermoresponsive artificial extracellular matrix: N-isopropylacrylamide-graft-copolymerized gelatin[104]	Morikawa, N. et al.	*Journal of Biomaterials Science-Polymer Edition/2002*	pNIPAM and gelatin as a thermoresponsive artificial ECM. Cell detachment and the ratio of pNIPAM-gelatin to pNIPAM.
Controlling Cell Attachment and Detachment	Bio-functionalized thermoresponsive interfaces facilitating cell adhesion and proliferation[105]	Hatakeyama, H. et al.	*Biomaterials/2006*	NIPAM copolymerized w/CIPAAm, surfaces co-immobilized w/cell adhesive peptide (RGDS), and cell growth factor insulin to enhance cell adhesion and proliferation (bovine carotid artery endothelial cells); detachment achieved.
Controlling Cell Attachment and Detachment	Switching the conformational behavior of poly(*N*-isopropyl acrylamide)[106]	Rimmer, S. et al.	*Polymer International/2009*	Review of using luminescence spectroscopy in the study of conformational behavior of pNIPAM.
Hydrogels (Review)	Switching the conformational behavior of poly(*N*-isopropyl acrylamide)[106]	Rimmer, S. et al.	*Polymer International/2009*	Review of using luminescence spectroscopy in the study of conformational behavior of pNIPAM.
Hydrogels	Poly(N-isopropylacrylamide) (PNIPAM)-grafted gelatin hydrogel surfaces: interrelationship between microscopic structure and mechanical property of surface regions and cell adhesiveness[101]	Ohya, S. et al.	*Biomaterials/2005*	pNIPAM-gelatin hydrogels; interrelationship between elastic modulus and cell adhesion.
Hydrogels	Thermo-responsive PNiAAm-g-PEG films for controlled cell detachment[107]	Schmaljohan n, D. et al.	*Biomacromolecules/4/6/2003*	pNIPAM hydrogels and mouse fibroblasts (study of cell detachment). Suitable as cell carriers.
Hydrogels	Thermo-responsive peptide-modified hydrogels for tissue regeneration[108]	Stile, R. A. et al.	*Biomacromolecules/2001*	P(NIPAM-co-Aac) hydrogels for studying cell-material interactions in 3D. Could be used as injectable scaffolds for tissue engineering applications. Cell used: Rat calvarial osteoblasts.
Hydrogels	Novel thermally reversible hydrogel as detachable	von Recum,	*Journal of Biomedical*	(CCMS-IPAAm) copolymer hydrogel and cell

	cell culture substrate[109]	H. A. et al.	*Materials Research/1998*	attachment/detachment (bovine endothelium and human retinal pigmented epithelium).
Hydrogels	Thermoresponsive nanocomposite hydrogels with cell-releasing behavior[110]	Hou Y et al.	*Biomaterials/2008*	pNIPAM nanocomposite hydrogels and detachment of mouse smooth muscle precursor cells.
Hydrogels	Control of cell cultivation and cell sheet detachment on the surface of polymer/clay nanocomposite hydrogels[111]	Haraguchi, K. et al.	*Biomacromolecules/2006*	Thermo-sensitive pNIPAM-NC gels as soft, wet substratum for cell attachment and detachment. Cells used: human hepatoma cells, human dermal fibroblasts, human umbilical vein endothelial cells.
Spheroids	A Novel Method to Prepare Multicellular Spheroids from Varied Cell-Types[116]	Yamazaki, M. et al.	*Biotechnology and Bioengineering/1995*	Preparing multicellular spheroids from different cell types using pNIPAM surfaces (pNIPAM conjugated w/collagen) 23 cell types.
Spheroids	Rearrangement of Esophageal-Carcinoma Cells and Stromal Fibroblasts in a Multicellular Spheroid[113]	Shima, I. et al.	*International Journal of Oncology/1995*	Hetero-multicellular spheroids developed using a collagen-conjugated pNIPAM.
Spheroids	Cell-Culture on a Thermoresponsive Polymer Surface[114]	Takezawa, T. et al.	*Bio-Technology/1990*	pNIPAM + collagen w/fibroblasts; detached cells formed a spheroid.
Spheroids	Morphological and Immuno-Cytochemical Characterization of a Hetero-Spheroid Composed of Fibroblasts and Hepatocytes[115]	Takezawa, T. et al.	*Journal of cell science/1992*	Preparing of heterospheroids using pNIPAM surfaces. Using rat parenchymal hepatocytes and human dermal fibroblasts. Histological and immuno-cytochemical observations of spheroids.
Spheroids	A Novel Method to Prepare Multicellular Spheroids from Varied Cell-Types[116]	Yamazaki, M. et al.	*Biotechnology and Bioengineering/1995*	Preparing multicellular spheroids from different cell types using pNIPAM surfaces (pNIPAM conjugated w/collagen) 23 cell types.
Spheroids	Size-Regulation and Biochemical Activities of the Multicellular Spheroid Composed of Rat-Liver Cells[117]	Endoh, K. et al.	*Research Communications in Chemical Pathology and Pharmacology/1994*	Obtaining vital spheroids composed of rat liver cells using pNIPAM; formation of intended size spheroids.
Spheroids	Thermoreversible hydrogel for in situ generation and release of HepG2 spheroids[118]	Wang, D. et al.	*Biomacromolecules/2011*	Generation of cell spheroids in temperature-responsive hydrogel scaffold, followed by liquefying the scaffold and releasing the generated spheroids.
Spheroids (Review)	A strategy for the development of tissue engineering scaffolds that regulate cell behavior[53]	Takezawa, T.	*Biomaterials/2003*	Review of development of ideal cellular scaffolds, also generation of spheroids using temperature-responsive surfaces.
Pattern and Shape Engineering	Effect of protein and cell behavior on pattern-grafted thermoresponsive polymer[45]	Chen, G. P. et al.	*Journal of Biomedical Materials Research/1998*	Copolymer (pNIPAM-co-acrylic acid) coupled with azidoaniline in a specific pattern used for selective cell detachment in serum-free media (mouse fibroblast STO cells).
Pattern and Shape Engineering	Patterned immobilization of thermoresponsive polymer[46]	Ito, Y. et al.	*Langmuir/1997*	pNIPAM copolymerized with acrylic acid coupled with azidoaniline, patterned and used with mouse fibroblast STO cells for selective detaching of cells.
Pattern and Shape Engineering	Poly(N-isopropylacrylamide)-grafted gelatin as a thermoresponsive cell-adhesive, mold-releasable material for shape-engineered tissues[102]	Matsuda, T.	*Journal of Biomaterials Science-Polymer Edition/2004*	pNIPAM-gelatin used for fabrication of a tubular endothelial cell construct; shape tissue engineering.

Pattern and Shape Engineering	Nanofabrication for micropatterned cell arrays by combining electron beam-irradiated polymer grafting and localized laser ablation[119]	Yamato, M. et al.	*Journal of Biomedical Materials Research Part A/2003*	pNIPAM and rat hepatocytes for patterned cell adhesion. Surfaces prepared by combining electron beam irradiation and localized laser ablation + adsorption of fibronectin.
Pattern and Shape Engineering	Novel cell patterning using microheater-controlled thermoresponsive plasma films[120]	Cheng, X. H. et al.	*Journal of Biomedical Materials Research Part A/2004*	Microheaters and a poly(N-isopropyl acrylamide) (pNIPAM) themoresponsive coating. This thermoresponsive coating is created by a radio frequency NIPAM plasma.
Pattern and Shape Engineering	Creation of designed shape cell sheets that are noninvasively harvested and moved onto another surface[25]	Hirose, M. et al.	*Biomacromolecules/2000*	Creating shaped cell sheets using PIPAAM and PDMAAm as cell adhesive and cell nonadhesive domains.
Pattern and Shape Engineering	Novel approach for achieving double-layered cell sheets co-culture: overlaying endothelial cell sheets onto monolayer hepatocytes utilizing temperature-responsive culture dishes[121]	Harimoto, M. et al.	*Journal of Biomedical Materials Research/2002*	Square patterning w/pNIPAM and PDMAAm; liver tissue engineering; human aortic endothelial cells double layered w/rat hepatocytes.
Pattern and Shape Engineering	Temperature-responsive surface for novel co-culture systems of hepatocytes with endothelial cells: 2-D patterned and double layered co-cultures[122]	Hirose, M. et al.	*Yonsei Medical Journal/41/6/2000*	Co-culture of hepatocytes w/ endothelial cells (a 2-D patterned co-culture and a double-layered co-culture) using pNIPAM surface.
Tissue Transplantation	Repair of impaired myocardium by means of implantation of engineered autologous myoblast sheets[48]	Memon, I. A. et al.	*Journal of Thoracic and Cardiovascular Surgery/2005*	Skeletal myoblast sheets engineered on pNIPAM surfaces used to repair impaired myocardium in rats.
Tissue Transplantation	Bioengineered chondrocyte sheets may be potentially useful for the treatment of partial thickness defects of articular cartilage[49]	Kaneshiro, N. et al.	*Biochemical and Biophysical Research Communications/2006*	Cell sheets were detached from pNIPAM-coated surfaces using a PVDF membrane. The generated tissues were examined in vivo and ex vivo.
Tissue Transplantation	Functional bioengineered corneal epithelial sheet grafts from corneal stem cells expanded ex vivo on a temperature-responsive cell culture surface[26]	Nishida, K. et al.	*Transplantation/2004*	pNIPAM surfaces +limbal corneal endothelial stem cells; characterization of cells after detachment; corneal surface reconstruction in rabbits.
Tissue Transplantation	Corneal reconstruction with tissue-engineered cell sheets composed of autologous oral mucosal epithelium[50]	Nishida, K. et al.	*New England Journal of Medicine/2004*	pNIPAM surfaces + autologous oral mucosal epithelial cells; transplanted to denuded corneal surfaces (eyes).
Tissue Transplantation	Functional human corneal endothelial cell sheets harvested from temperature-responsive culture surfaces[159]	Sumide, T. et al.	*FASEB Journal/2005*	Fabricating human corneal endothelial cell sheets on pNIPAM for ocular surgery and repair. Scanning electron microscopy, cell immunofluorescence staining etc. of recovered cell sheets.
Tissue Transplantation	Fabrication of pulsatile cardiac tissue grafts using a novel 3-dimensional cell sheet manipulation technique and temperature-responsive cell culture surfaces.[52]	Shimizu, T. et al.	*Circulation Research/2002*	Layering cardiomyocyte sheets recovered from pNIPAM surfaces; transplanted into subcutaneous tissue of nude rats (functioning pulsatile grafts).
Tissue Transplantation	System-engineered cartilage using poly(N-isopropylacrylamide)-grafted gelatin as in situ-formable scaffold: In vivo performance[103]	Ibusuki, S. et al.	*Tissue Engineering/2003*	pNIPAM grafted gelatin + engineered cartilage; precultured tissue for transplantation; chondrocyte transplantation into rabbits' knees.
Other Uses of	Red blood cell deformability as a predictor of	Dondorp,	*American Journal of*	Red blood cell deformability was measured using a laser

pNIPAM with Cells	anemia in severe falciparum malaria[123]	A.M. et al.	*Tropical Medicine and Hygiene/1999*	diffraction technique.
Other Uses of pNIPAM with Cells	Type-specific separation of animal cells in aqueous two-phase systems using antibody conjugates with temperature-sensitive polymers[127]	Kumar, A. et al.	*Biotechnology and Bioengineering/2001*	NIPAM copolymerized with monoclonal antibodies for specific separation of animal cells (human acute myeloid leukemia cells and human T lymphoma cells).
Other Uses of pNIPAM with Cells	Reversible cell deformation by a polymeric actuator[125]	Pelah, A. et al.	*Journal of the American Chemical Society/2007*	Study of cell deformation. Obtaining deformation of red blood cells using pNIPAM gel (by stretching and compression).
Other Uses of pNIPAM with Cells	Polymeric actuators for biological applications[124]	Pelah, A. et al.	*Chemphyschem/2007*	Deformation of red blood cells using pNIPAM gels; pNIPAM as actuator for stretching and compressing cells and tissues using volume changes; tool for studying the effects induces by physical forces.
Other Uses of pNIPAM with Cells	Adhesion behavior of monocytes, macrophages and foreign body giant cells on poly (N-isopropylacrylamide) temperature-responsive surfaces[126]	Collier, T. O. et al.	*Journal of Biomedical Materials Research/2002*	Investigating monocytes and macrophage adhesion and foreign body giant cell formation on pNIPAM surfaces; allows investigation of the adhesive behavior of adherent inflammatory cells.
Bioadhesion and Bioadsorption	Modifying stainless steel surfaces with responsive polymers: effect of PS-PAA and PNIPAAM on cell adhesion and oil removal[128]	Callewaert, M. et al.	*Journal of Adhesion Science and Technology/2005*	Treating stainless steel surfaces w/pNIPAM: reduction of yeast cell adhesion and facilitated removal of oil soil.
Bioadhesion and Bioadsorption	Bacterial adsorption to thermoresponsive polymer surfaces[129]	Cunliffe D, et al.	*Biotechnology Letters/2000*	pNIPAM co-polymers and bacterial adsorption (Listeria monocytogenes).
Bioadhesion and Bioadsorption	Surface-grafted, environmentally sensitive polymers for biofilm release[130]	Ista, L. K. et al.	*Applied and Environmental Microbiology/1999*	Controlling biofouling release using pNIPAM.
Bioadhesion and Bioadsorption	Grafted thermo- and pH responsive co-polymers: Surface-properties and bacterial adsorption[131]	Alarcon C.D.L., et al.	*International Journal of Pharmaceutics/2005*	pNIPAM and bacterial adsorption; generating synthetic polymers that control attachment of prokaryotic cells to surfaces.
Manipulation of Microorganisms	Concentrating aqueous dispersions of Staphylococcus Epidermidis bacteria by swelling of thermosensitive poly [(N-isopropylacrylamide)-co-(acrylic acid)] hydrogels[132]	Champ S, et al.	*Macromolecular Chemistry And Physics/2000*	Hydrogels w pNIPAM as a bioseparation device based on size exclusion of bacteria.
Manipulation of Microorganisms	In situ formation of a gel microbead for indirect laser micromanipulation of microorganisms[133]	Ichikawa, A. et al.	*Applied Physics Letters/87/19/2005*	pNIPAM gel microbead for indirect laser manipulation of microorganisms.
Manipulation of Microorganisms	Affinity selection of target cells from cell surface displayed libraries: a novel procedure using thermo-responsive magnetic nanoparticles[134]	Furukawa, H. et al.	*Applied Microbiology and Biotechnology/2003*	Magnetic nanoparticles w/pNIPAM for affinity selection of target yeast cells from cell surface display library.
Manipulation of Microorganisms	Effect of matrix elasticity on affinity binding and release of bioparticles. Elution of bound cells by temperature-induced shrinkage of the smart macroporous hydrogel[135]	Galaev, I. Y. et al.	*Langmuir/2007*	Macroporous pNIPAM hydrogels; the effect of mechanical deformation on the retention of specifically bound bioparticles (bacterial, yeast cells and antibody-labeled inclusion bodies).

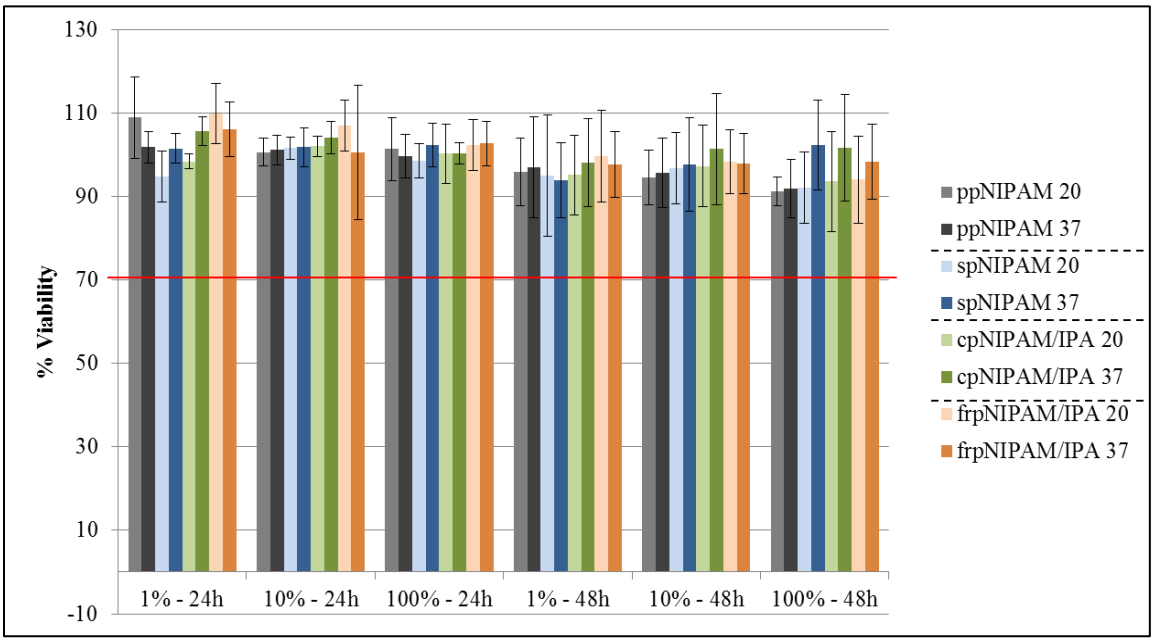

Figure A1. MTS assay results for culture of Veros in the presence of pNIPAM extracts. Red line indicates viability of 70%, below which a compound is considered to be cytotoxic. These results are supplementary information provided for the cytotoxicity study presented in Chapter 4, section 4.3.4.3, Figures 4.9 and 4.10.

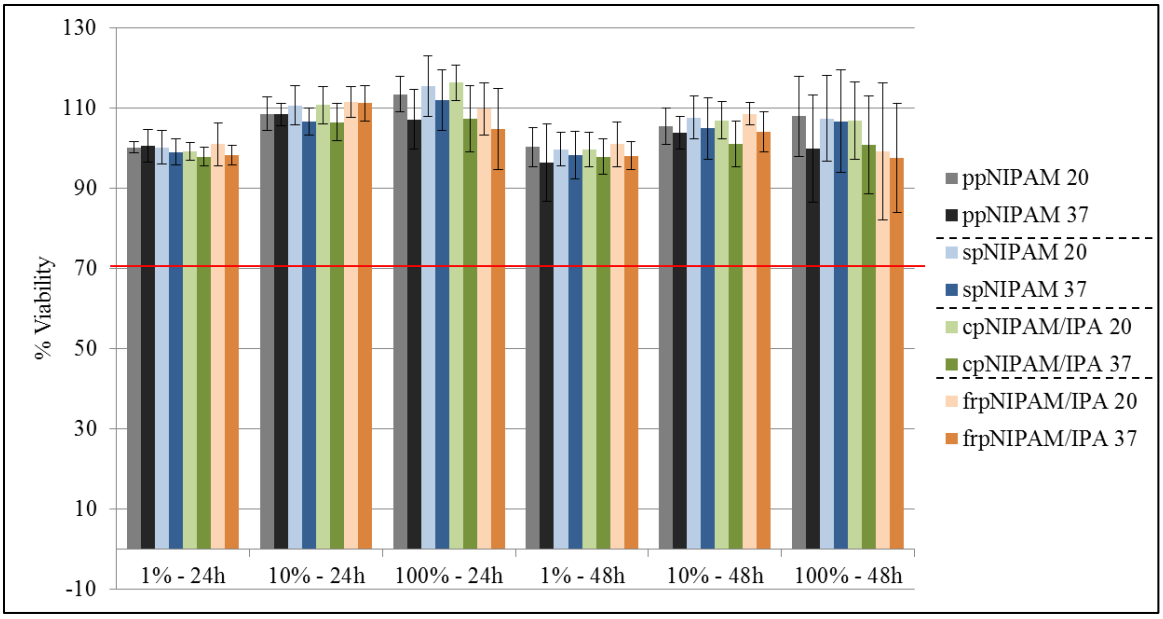

Figure A2. MTS assay results for culture of 3T3s in the presence of pNIPAM extracts. Red line indicates viability of 70%, below which a compound is considered to be cytotoxic. These results are supplementary information provided for the cytotoxicity study presented in Chapter 4, section 4.3.4.3, Figures 4.9 and 4.10.

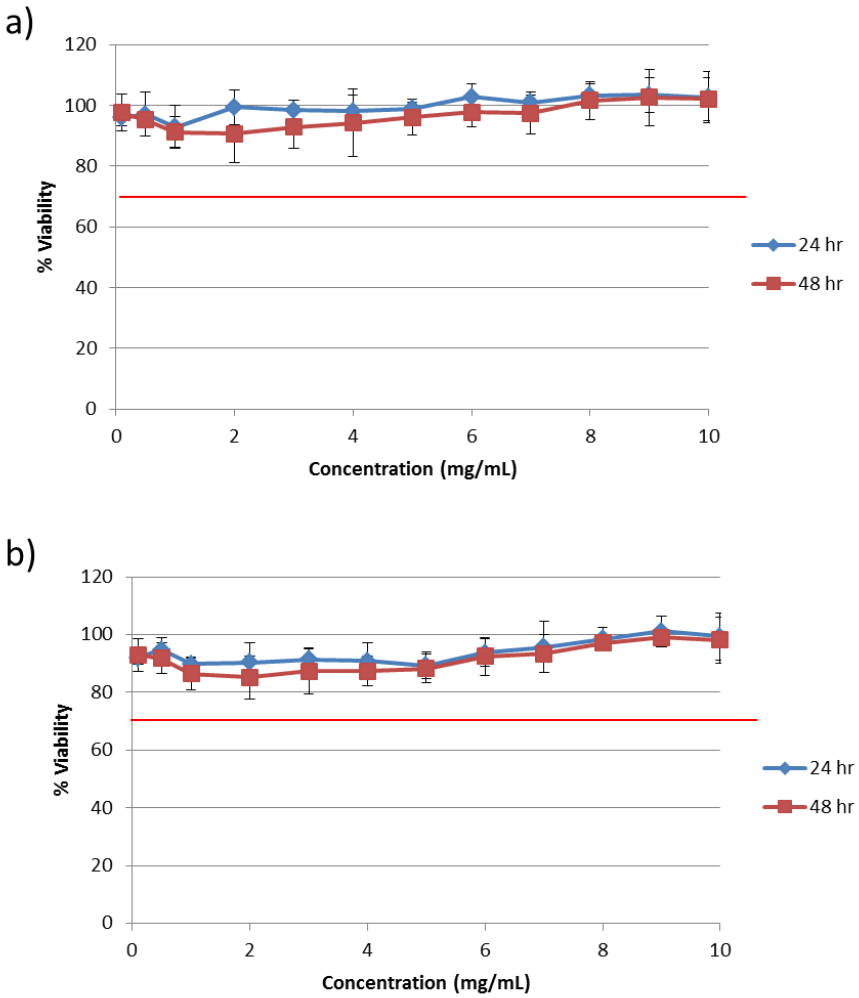

Figure A3. MTS assay results for concentration gradient experiments with SMCs (a) on cpNIPAM/IPA surfaces, and (b) on frpNIPAM/IPA surfaces. Red line indicates viability of 70%, below which a compound is considered to be cytotoxic. These results are supplementary information provided for the cytotoxicity study presented in Chapter 4, section 4.3.4.4, Figures 4.11 and 4.12.

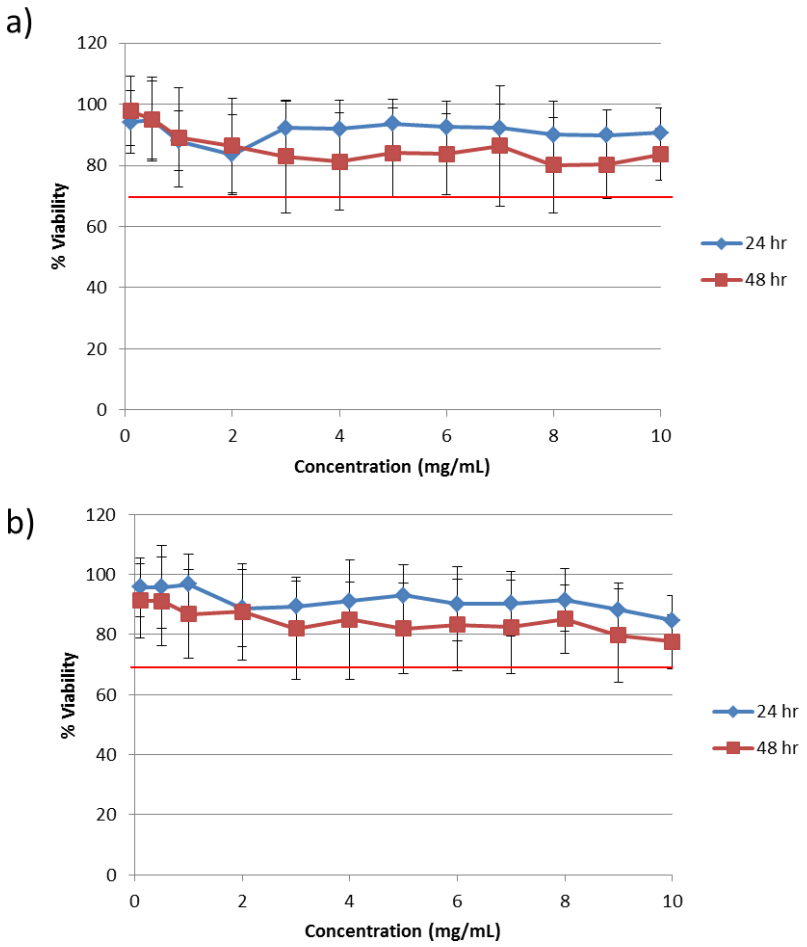

Figure A4. MTS assay results for concentration gradient experiments with 3T3s (a) on cpNIPAM/IPA surfaces, and (b) on frpNIPAM/IPA surfaces. Red line indicates viability of 70%, below which a compound is considered to be cytotoxic. These results are supplementary information provided for the cytotoxicity study presented in Chapter 4, section 4.3.4.4, Figures 4.11 and 4.12.

REFERENCES

1. Go, A.S., et al., *Heart disease and stroke statistics-2014 update: A report from the american heart association.* Circulation, 2014. **129**: p. E28-E292.
2. *Burn injury facts & statistics for the U.S.* [cited 2014 Jan. 24]; Available from: http://www.resource4burninjury.com/topics/facts.html.
3. Nerem, R.M. and D. Seliktar, *Vascular tissue engineering.* Annual Review of Biomedical Engineering, 2001. **3**: p. 225-243.
4. Weinberg, C.B. and E. Bell, *A blood-vessel model constructed from collagen and cultured vascular cells.* Science, 1986. **231**(4736): p. 397-400.
5. Niklason, L.E., et al., *Functional arteries grown in vitro.* Science, 1999. **284**(5413): p. 489-493.
6. Niklason, L.E., *Medical technology - Replacement arteries made to order.* Science, 1999. **286**(5444): p. 1493-1494.
7. Lantz, G.C., et al., *Small intestinal submucosa as a vascular graft: a review.* Journal of investigative surgery : the official journal of the Academy of Surgical Research, 1993. **6**(3): p. 297-310.
8. Yang, J., et al., *Cell sheet engineering: Recreating tissues without biodegradable scaffolds.* Biomaterials, 2005. **26**(33): p. 6415-6422.
9. Yang, J., et al., *Reconstruction of functional tissues with cell sheet engineering.* Biomaterials, 2007. **28**(34): p. 5033-5043.
10. Cabane, E., et al., *Stimuli-responsive polymers and their applications in nanomedicine.* Biointerphases, 2012. **7**(1-4).

11. Gil, E.S. and S.A. Hudson, *Stimuli-reponsive polymers and their bioconjugates.* Progress in Polymer Science, 2004. **29**(12): p. 1173-1222.

12. Dimitrov, I., et al., *Thermosensitive water-soluble copolymers with doubly responsive reversibly interacting entities.* Progress in Polymer Science, 2007. **32**(11): p. 1275-1343.

13. Da Silva, R.M.P., J.F. Mano, and R.L. Reis, *Smart thermoresponsive coatings and surfaces for tissue engineering: switching cell-material boundaries.* Trends in Biotechnology, 2007. **25**(12): p. 577-583.

14. Crespy, D. and R.N. Rossi, *Temperature-responsive polymers with LCST in the physiological range and their applications in textiles.* Polymer International, 2007. **56**(12): p. 1461-1468.

15. Roy, I. and M.N. Gupta, *Smart polymeric materials: Emerging biochemical applications.* Chemistry & Biology, 2003. **10**(12): p. 1161-1171.

16. Cole, M.A., et al., *Stimuli-responsive interfaces and systems for the control of protein-surface and cell-surface interactions.* Biomaterials, 2009. **30**(9): p. 1827-1850.

17. Cooperstein, M.A. and H.E. Canavan, *Biological cell detachment from poly(N-isopropyl acrylamide) and its applications.* Langmuir, 2010. **26**(11): p. 7695-7707.

18. Seuring, J. and S. Agarwal, *Polymers with upper critical solution temperature in aqueous solution.* Macromolecular Rapid Communications, 2012. **33**(22): p. 1898-1920.

19. Schild, H.G., *Poly (N-isopropylacrylamide) - Experiment, theory and application.* Progress in Polymer Science, 1992. **17**(2): p. 163-249.

20. Okano, T., et al., *Temperature-responsive poly(N-isopropylacrylamide) as a modulator for alteration of hydrophilic hydrophobic surface-properties to control activation inactivation of platelets.* Journal of Controlled Release, 1995. **36**(1-2): p. 125-133.

21. Okano, T., et al., *A novel recovery-system for cultured cells using plasma-treated polystyrene dishes grafted with poly(N-isopropylacrylamide).* Journal of Biomedical Materials Research, 1993. **27**(10): p. 1243-1251.

22. Canavan, H.E., et al., *Cell sheet detachment affects the extracellular matrix: A surface science study comparing thermal lift-off, enzymatic and mechanical methods.* J. Biomed. Mater. Res., 2005. **75A**(1): p. 1-13.

23. Canavan, H.E., et al., *Surface characterization of the extracellular matrix remaining after cell detachment from a thermoresponsive polymer.* Langmuir, 2005. **21** (5): p. 1949-1955.

24. Shimizu, T., et al., *Cell sheet engineering for myocardial tissue reconstruction.* Biomaterials, 2003. **24**(13): p. 2309-2316.

25. Hirose, M., et al., *Creation of designed shape cell sheets that are noninvasively harvested and moved onto another surface.* Biomacromolecules, 2000. **1**(3): p. 377-381.

26. Nishida, K., et al., *Functional bioengineered corneal epithelial sheet grafts from corneal stem cells expanded ex vivo on a temperature-responsieve cell culture surface.* Transplantation, 2004. **77**(3): p. 379-385.

27. Reed, J.A., et al., *The effects of cell culture parameters on cell release kinetics from thermoresponsive surfaces.* Journal of Applied Biomaterials and Biomechanics, 2008. **6**(2): p. 81-88.

28. Liu, B.H. and J.L. Hu, *The application of temperature-sensitive hydrogels to textiles: A review of chinese and Japanese investigations.* Fibres & Textiles in Eastern Europe, 2005. **13**(6): p. 45-49.

29. Nakayama, M. and T. Okano, *Intelligent thermoresponsive polymeric micelles for targeted drug delivery.* Journal of Drug Delivery Science and Technology, 2006. **16**(1): p. 35-44.

30. Peppas, N.A. and W. Leobandung, *Stimuli-sensitive hydrogels: ideal carriers for chronobiology and chronotherapy.* Journal of Biomaterials Science-Polymer Edition, 2004. **15**(2): p. 125-144.

31. Qiu, Y. and K. Park, *Environment-sensitive hydrogels for drug delivery.* Advanced Drug Delivery Reviews, 2001. **53**(3): p. 321-339.

32. Stayton, P.S., et al., *Control of protein-ligand recognition using a stimuli-responsive polymer.* Nature, 1995. **378**(6556): p. 472-474.

33. El-Mohdy, H.L.A. and A. Safrany, *Preparation of fast response superabsorbent hydrogels by radiation polymerization and crosslinking of N-isopropylacrylamide in solution.* Radiation Physics and Chemistry, 2008. **77**(3): p. 273-279.

34. Canavan, H.E., et al., *Cell sheet detachment affects the extracellular matrix: A surface science study comparing thermal liftoff, enzymatic, and mechanical methods.* Journal of Biomedical Materials Research Part A, 2005. **75A**(1): p. 1-13.

35. Canavan, H.E., et al., *Comparison of native extracellular matrix with adsorbed protein films using secondary ion mass spectrometry.* Langmuir, 2007. **23**(1): p. 50-56.

36. Kushida, A., et al., *Decrease in culture temperature releases monolayer endothelial cell sheets together with deposited fibronectin matrix from temperature-responsive culture surfaces.* Journal of Biomedical Materials Research, 1999. **45**(4): p. 355-362.

37. Canavan, H.E., et al., *A plasma-deposited surface for cell sheet engineering: Advantages over mechanical dissociation of cells.* Plasma Processes and Polymers, 2006. **3**(6-7): p. 516-523.

38. Ide, T., et al., *Structural characterization of bioengineered human corneal endothelial cell sheets fabricated on temperature-responsive culture dishes.* Biomaterials, 2006. **27**(4): p. 607-614.

39. Canavan, H.E., et al., *Surface characterization of the extracellular matrix remaining after cell detachment from a thermoresponsive polymer.* Langmuir, 2005. **21**(5): p. 1949-1955.

40. Kushida, A., et al., *Two-dimensional manipulation of differentiated Madin-Darby canine kidney (MDCK) cell sheets: The noninvasive harvest from temperature-responsive culture dishes and transfer to other surfaces.* Journal of Biomedical Materials Research, 2001. **54**(1): p. 37-46.

41. Wong-In, S., et al., *Multilayered mouse preosteoblast MC3T3-E1 sheets harvested from temperature-responsive poly(N-isopropylacrylamide-co-*

acrylamide) grafted culture surface for cell sheet engineering. Journal of Applied Polymer Science, 2013. **129**(5): p. 3061-3069.

42. Patel, N.G., et al., *Rapid cell sheet detachment using spin-coated pNIPAAm films retained on surfaces by an aminopropyltriethoxysilane network.* Acta Biomaterialia, 2012. **8**(7): p. 2559-2567.

43. Yang, L., et al., *Comparison of mesenchymal stem cells released from poly(N-isopropylacrylamide) copolymer film and by trypsinization.* Biomedical Materials, 2012. **7**(3).

44. Wang, T., et al., *Rapid cell sheet detachment from alginate semi-interpenetrating nanocomposite hydrogels of PNIPAm and hectorite clay.* Reactive & Functional Polymers, 2011. **71**(4): p. 447-454.

45. Chen, G.P., Y. Imanishi, and Y. Ito, *Effect of protein and cell behavior on pattern-grafted thermoresponsive polymer.* Journal of Biomedical Materials Research, 1998. **42**(1): p. 38-44.

46. Ito, Y., et al., *Patterned immobilization of thermoresponsive polymer.* Langmuir, 1997. **13**(10): p. 2756-2759.

47. Shiroyanagi, Y., et al., *Transplantable urothelial cell sheets harvested noninvasively from temperature-responsive culture surfaces by reducing temperature.* Tissue Engineering, 2003. **9**(5): p. 1005-1012.

48. Memon, I.A., et al., *Repair of impaired myocardium by means of implantation of engineered autologous myoblast sheets.* Journal of Thoracic and Cardiovascular Surgery, 2005. **130**(5): p. 1333-1341.

49. Kaneshiro, N., et al., *Bioengineered chondrocyte sheets may be potentially useful for the treatment of partial thickness defects of articular cartilage.* Biochemical and Biophysical Research Communications, 2006. **349**(2): p. 723-731.

50. Nishida, K., et al., *Corneal reconstruction with tissue-engineered cell sheets composed of autologous oral mucosal epithelium.* New England Journal of Medicine, 2004. **351**(12): p. 1187-1196.

51. Sumide, T., et al., *Functional human corneal endothelial cell sheets harvested from temperature-responsive culture surfaces.* Faseb Journal, 2005. **19**(14): p. 392-+.

52. Shimizu, T., et al., *Fabrication of pulsatile cardiac tissue grafts using a novel 3-dimensional cell sheet manipulation technique and temperature-responsive cell culture surfaces.* Circulation Research, 2002. **90**(3): p. E40-E48.

53. Takezawa, T., *A strategy for the development of tissue engineering scaffolds that regulate cell behavior.* Biomaterials, 2003. **24**(13): p. 2267-2275.

54. Vihola, H., et al., *Cytotoxicity of thermoresponsive polymers poly(N-isopropylacrylamide), poly(N-vinylcaprolactam) and amphiphilically modified poly(N-vinylcaprolactam).* Biomaterials, 2005. **26**: p. 3055-3064.

55. Panayiotou, M. and R. Freitag, *Influence of the synthesis conditions and ionic additives on the swelling behaviour of thermo-responsive polyalkylacrylamide hydrogels.* Polymer, 2005. **46**(18): p. 6777-6785.

56. Wadajkar, A.S., et al., *Cytotoxic evaluation of N-isopropylacrylamide monomers and temperature-sensitive poly(N-isopropylacrylamide) nanoparticles.* Journal of Nanoparticle Research, 2009. **11**(6): p. 1375-1382.

57. Naha, P.C., et al., *Intracellular localisation, geno- and cytotoxic response of polyN-isopropylacrylamide (PNIPAM) nanoparticles to human keratinocyte (HaCaT) and colon cells (SW 480).* Toxicology Letters, 2010. **198**(2): p. 134-143.

58. Xu, F.J., et al., *Comb-shaped conjugates comprising hydroxypropyl cellulose backbones and low-molecular-weight poly(N-isopropylacryamide) side chains for smart hydrogels: Synthesis, characterization, and biomedical applications.* Bioconjugate Chemistry, 2010. **21**(3): p. 456-464.

59. Mortisen, D., et al., *Tailoring thermoreversible hyaluronan hydrogels by "click" chemistry and RAFT polymerization for cell and drug therapy.* Biomacromolecules, 2010. **11**(5): p. 1261-1272.

60. Li, Y.Y., et al., *Fluorescent, thermo-responsive biotin-P(NIPAAm-co-NDAPM)-b-PCL micelles for cell-tracking and drug delivery.* Nanotechnology, 2007. **18**(50): p. 1-8.

61. *International Organization for Standardization (2009), Biological evaluation of medical devices - Part 5: Tests for in vitro cytotoxicity; ISO 10993-5; Geneva, Switzerland.* p. 1-34.

62. *N-isopropylacrylamide.* MSDS No. 91139 [Online]; Acros Organics: Geel, Belgium; June, 20, 2009, http://www.acros.com/DesktopModules/Acros_Search_Results/Acros_Search_Results.aspx?search_type=CatalogSearch&SearchString=N-isopropylacrylamide (accessed January 20, 2013).

63. Abraham, T.N., et al., *A novel thermoresponsive graft copolymer containing phosphorylated HEMA for generating detachable cell layers.* Journal of Applied Polymer Science. **115**(1): p. 52-62.

64. Chastek, T.T., et al., *Polyglycol-templated synthesis of poly(N-isopropyl acrylamide) microgels with improved biocompatibility.* Colloid and Polymer Science, 2010. **288**(1): p. 105-114.

65. Joseph, N., et al., *A cytocompatible poly(N-isopropylacrylamide-co-glycidylmethacrylate) coated surface as new substrate for corneal tissue engineering.* Journal of Bioactive and Compatible Polymers, 2010. **25**(1): p. 58-74.

66. Meenach, S.A., et al., *Biocompatibility analysis of magnetic hydrogel nanocomposites based on poly(N-isopropylacrylamide) and iron oxide.* Journal of Biomedical Materials Research Part A, 2009. **91A**(3): p. 903-909.

67. Bisht, H.S., et al., *Temperature-controlled properties of DNA complexes with poly(ethylenimine)-graft-poly(N-isopropylacrylamide).* Biomacromolecules, 2006. **7**: p. 1169-1178.

68. Fan, L., et al., *pH-sensitive podophyllotoxin carrier for cancer cells specific delivery.* Polymer Composites, 2010. **31**(1): p. 51-59.

69. Ma, Z.W., et al., *Thermally responsive injectable hydrogel incorporating methacrylate-polylactide for hydrolytic lability.* Biomacromolecules, 2010. **11**(7): p. 1873-1881.

70. Feil, H., et al., *Effect of Comonomer Hydrophilicity and Ionization on the Lower Critical Solution Temperature of N-Isopropylacrylamide Copolymers.* Macromolecules, 1993. **26**(10): p. 2496-2500.

71. Gad, S.C., ed. *In Vitro Toxicology*. 2nd ed. 2000, Taylor & Francis: New York.

72. Okano, T., et al., *Mechanism of cell detachment from temperature-modulated, hydrophilic-hydrophobic polymer surfaces.* Biomaterials, 1995. **16**(4): p. 297-303.

73. Yamato, M., et al., *Release of adsorbed fibronectin from temperature-responsive culture surfaces requires cellular activity.* Biomaterials, 2000. **21**(10): p. 981-986.

74. Yamato, M., et al., *Signal transduction and cytoskeletal reorganization are required for cell detachment from cell culture surfaces grafted with a temperature-responsive polymer.* Journal of Biomedical Materials Research, 1999. **44**(1): p. 44-52.

75. von Recum, H., et al., *Growth factor and matrix molecules preserve cell function on thermally responsive culture surfaces.* Tissue Engineering, 1999. **5**(3): p. 251-265.

76. Chen, B.Y., et al., *Engineering cell de-adhesion dynamics on thermoresponsive poly(N-isopropylacrylamide).* Acta Biomaterialia, 2008. **4**(2): p. 218-229.

77. Okano, T., et al., *A novel recovery system for cultured cells using plasma-treated polystyrene dishes grafted with poly(N-isopropylacrylamide).* J. Biomed. Mater. Res., 1993(27): p. 1243-1251.

78. Kenda-Ropson, N., S. Lenglois, and A.O.A. Miller, *Microsupport with two-dimensional geometry (2D-MS) - 4. Temperature-induced detachment of*

anchorage-dependent CHO-K1 cells from cryoresponsive MicroHex (R) (CryoHex). Cytotechnology, 2002. **39**(3): p. 163-170.

79. Moran, M.T., et al., *Intact endothelial cell sheet harvesting from thermoresponsive surfaces coated with cell adhesion promoters.* Journal of the Royal Society Interface, 2007. **4**: p. 1151-1157.
80. Wang, L.S., et al., *Fabrication and characterization of nanostructured and thermosensitive polymer membranes for wound healing and cell grafting.* Advanced Functional Materials, 2006. **16**(9): p. 1171-1178.
81. Cooperstein, M.A. and H.E. Canavan, *Assessment of cytotoxicity of N-isopropyl acrylamide and poly(N-isopropyl acrylamide)-coated surfaces.* Biointerphases, 2013. **8**(19).
82. Akiyama, Y., et al., *Ultrathin poly(N-isopropylacrylamide) grafted layer on polystyrene surfaces for cell adhesion/detachment control.* Langmuir, 2004. **20**(13): p. 5506-5511.
83. Lucero, A.E., et al., *Fabrication and characterization of thermoresponsive films deposited by an RF plasma reactor.* Plasma Processes and Polymers, 2010. **7**(12): p. 992-1000.
84. Reed, J.A., et al., *A low-cost, rapid deposition method for "smart" films: Applications in mammalian cell release.* Acs Applied Materials & Interfaces, 2010. **2**(4): p. 1048-1051.
85. Andrzejewski, B.P., *Bioadhesion to model thermally responsive surfaces.* PhD Thesis, University of New Mexico, 2009.

86. Pan, Y.V., et al., *Plasma polymerized N-isopropylacrylamide: Synthesis and characterization of a smart thermally responsive coating.* Biomacromolecules, 2001. **2**(1): p. 32-36.

87. Bluestein, B.M., J.A. Reed, and H.E. Canavan, *Effect of deposition method and storage conditions on the cytotoxicity and biocompatibility of pNIPAM films. Submitted to Surface and Interface Analysis.*

88. Vickerman, J.C. and I.S. Gilmore, eds. *Surface analysis - The principal techniques*. 2 ed. 2009, John Wiley & Sons, Ltd.

89. *CellTiter 96 Aqueous One Solution Cell Proliferation Assay.* Technical Bulletin. Promega. http://www.promega.com/resources/protocols/technical-bulletins/0/celltiter-96-aqueous-one-solution-cell-proliferation-assay-system-protocol/.

90. *LIVE/DEAD Viability/Cytotoxicity Kit for mammalian cells.* Invitrogen. http://tools.invitrogen.com/content/sfs/manuals/mp03224.pdf.

91. Ham, R.G. and T.T. Puck, *Quantitative colonial growth of isolated mammalian cells.* Methods in Enzymology, 1962. **5**: p. 90-119.

92. Nahapetian, A.T., J.N. Thomas, and W.G. Thilly, *Optimization of environment for high-density vero cell-culture-effect of dissolved oxygen and nutrient supply on cell growth and changes in metabolites.* Journal of Cell Science, 1986. **81**: p. 65-103.

93. Rzaev, Z.M.O., S. Dincer, and E. Piskin, *Functional copolymers of N-isopropylacrylamide for bioengineering applications.* Progress in Polymer Science, 2007. **32**(5): p. 534-595.

94. Pelton, R., *Temperature-sensitive aqueous microgels.* Advances in Colloid and Interface Science, 2000. **85**(1): p. 1-33.

95. Kwon, O.H., et al., *Rapid cell sheet detachment from poly(N-isopropylacrylamide)-grafted porous cell culture membranes.* Journal of Biomedical Materials Research, 2000. **50**(1): p. 82-89.

96. Reed, J.A., *Assessment of the biocompatibility, stability, and suitability of novel thermoresponsive films for the rapid generation of cellular constructs. PhD Dissertation*, in *Chemical Engineering*. 2011, University of New Mexico: Albuquerque.

97. Ebara, M., et al., *Copolymerization of 2-carboxyisopropylacrylamide with N-isopropylacrylamide accelerates cell detachment from grafted surfaces by reducing temperature.* Biomacromolecules, 2003. **4**(2): p. 344-349.

98. Zhao, T.L., et al., *Inhibition of protein adsorption and cell adhesion on PNIPAAm-grafted polyurethane surface: Effect of graft molecular weight.* Colloids and Surfaces B-Biointerfaces, 2011. **85**(1): p. 26-31.

99. Liu, H.C. and Y. Ito, *Cell attachment and detachment on micropattern-immobilized poly(N-isopropylacrylamide) with gelatin.* Lab on a Chip, 2002. **2**(3): p. 175-178.

100. Ohya, S. and T. Matsuda, *Poly(N-isopropylacrylamide) (PNIPAM)-grafted gelatin as thermoresponsive three-dimensional artificial extracellular matrix: molecular and formulation parameters vs. cell proliferation potential.* Journal of Biomaterials Science-Polymer Edition, 2005. **16**(7): p. 809-827.

101. Ohya, S., S. Kidoaki, and T. Matsuda, *Poly(N-isopropylacrylamide) (PNIPAM)-grafted gelatin hydrogel surfaces: interrelationship between microscopic structure and mechanical property of surface regions and cell adhesiveness.* Biomaterials, 2005. **26**(16): p. 3105-3111.

102. Matsuda, T., *Poly(N-isopropylacrylamide)-grafted gelatin as a thermoresponsive cell-adhesive, mold-releasable material for shape-engineered tissues.* Journal of Biomaterials Science-Polymer Edition, 2004. **15**(7): p. 947-955.

103. Ibusuki, S., Y. Iwamoto, and T. Matsuda, *System-engineered cartilage using poly(N-isopropylacrylamide)-grafted gelatin as in situ-formable scaffold: In vivo performance.* Tissue Engineering, 2003. **9**(6): p. 1133-1142.

104. Morikawa, N. and T. Matsuda, *Thermoresponsive artificial extracellular matrix: N-isopropylacrylamide-graft-copolymerized gelatin.* Journal of Biomaterials Science-Polymer Edition, 2002. **13**(2): p. 167-183.

105. Hatakeyama, H., et al., *Bio-functionalized thermoresponsive interfaces facilitating cell adhesion and proliferation.* Biomaterials, 2006. **27**(29): p. 5069-5078.

106. Rimmer, S., I. Soutar, and L. Swanson, *Switching the conformational behaviour of poly(N-isopropyl acrylamide).* Polymer International, 2009. **58**(3): p. 273-278.

107. Schmaljohann, D., et al., *Thermo-responsive PNiAAm-g-PEG films for controlled cell detachment.* Biomacromolecules, 2003. **4**(6): p. 1733-1739.

108. Stile, R.A. and K.E. Healy, *Thermo-responsive peptide-modified hydrogels for tissue regeneration.* Biomacromolecules, 2001. **2**(1): p. 185-194.

109. von Recum, H.A., et al., *Novel Thermally Reversible Hydrogel as Detachable Cell Culture Substrate.* J. Biomed. Mater. Resear., 1998. **40**(4): p. 631-639.

110. Hou, Y., et al., *Thermoresponsive nanocomposite hydrogels with cell-releasing behavior.* Biomaterials, 2008. **29**(22): p. 3175-3184.

111. Haraguchi, K., T. Takehisa, and M. Ebato, *Control of cell cultivation and cell sheet detachment on the surface of polymer/clay nanocomposite hydrogels.* Biomacromolecules, 2006. **7**(11): p. 3267-3275.

112. Yamazaki, M., et al., *A novel method to prepare size-regulated spheroids composed of human dermal fibroblasts.* Biotechnology and Bioengineering, 1994. **44**(1): p. 38-44.

113. Shima, I., et al., *Rearrangement of esophageal-carcinoma cells and stromal fibroblasts in a multicellular spheroid.* International Journal of Oncology, 1995. **7**(4): p. 795-800.

114. Takezawa, T., Y. Mori, and K. Yoshizato, *Cell-culture on a thermoresponsive polymer surface.* Bio-Technology, 1990. **8**(9): p. 854-856.

115. Takezawa, T., et al., *Morphological and immuno-cytochemical characterization of a hetero-spheroid composed of fibroblasts and hepatocytes.* Journal of Cell Science, 1992. **101**: p. 495-501.

116. Yamazaki, M., et al., *A novel method to prepare multicellular spheroids from varied cell-types.* Biotechnology and Bioengineering, 1995. **48**(1): p. 17-24.

117. Endoh, K., et al., *Size-regulation and biochemical activities of the multicellular spheroid composed of rat-liver cells.* Research Communications in Chemical Pathology and Pharmacology, 1994. **83**(3): p. 317-327.

118. Wang, D., et al., *Thermoreversible hydrogel for in situ generation and release of HepG2 spheroids.* Biomacromolecules, 2011. **12**(3): p. 578-584.

119. Yamato, M., et al., *Nanofabrication for micropatterned cell arrays by combining electron beam-irradiated polymer grafting and localized laser ablation.* Journal of Biomedical Materials Research Part A, 2003. **67A**(4): p. 1065-1071.

120. Cheng, X.H., et al., *Novel cell patterning using microheater-controlled thermoresponsive plasma films.* Journal of Biomedical Materials Research Part A, 2004. **70A**(2): p. 159-168.

121. Harimoto, M., et al., *Novel approach for achieving double-layered cell sheets co-culture: overlaying endothelial cell sheets onto monolayer hepatocytes utilizing temperature-responsive culture dishes.* Journal of Biomedical Materials Research, 2002. **62**(3): p. 464-470.

122. Hirose, M., et al., *Temperature-responsive surface for novel co-culture systems of hepatocytes with endothelial cells: 2-D patterned and double layered co-cultures.* Yonsei Medical Journal, 2000. **41**(6): p. 803-813.

123. Dondorp, A.M., et al., *Red blood cell deformability as a predictor of anemia in severe falciparum malaria.* American Journal of Tropical Medicine and Hygiene, 1999. **60**(5): p. 733-737.

124. Pelah, A. and T.M. Jovin, *Polymeric actuators for biological applications.* Chemphyschem, 2007. **8**(12): p. 1757-1760.

125. Pelah, A., R. Seemann, and T.M. Jovin, *Reversible cell deformation by a polymeric actuator.* Journal of the American Chemical Society, 2007. **129**(3): p. 468-469.

126. Collier, T.O., et al., *Adhesion behavior of monocytes, macrophages and foreign body giant cells on poly (N-isopropylacrylamide) temperature-responsive surfaces.* Journal of Biomedical Materials Research, 2002. **59**(1): p. 136-143.

127. Kumar, A., et al., *Type-specific separation of animal cells in aqueous two-phase systems using antibody conjugates with temperature-sensitive polymers.* Biotechnology and Bioengineering, 2001. **75**(5): p. 570-580.

128. Callewaert, M., P.G. Rouxhet, and L. Boulange-Petermann, *Modifying stainless steel surfaces with responsive polymers: effect of PS-PAA and PNIPAAM on cell adhesion and oil removal.* Journal of Adhesion Science and Technology, 2005. **19**(9): p. 765-781.

129. Cunliffe, D., et al., *Bacterial adsorption to thermoresponsive polymer surfaces.* Biotechnology Letters, 2000. **22**(2): p. 141-145.

130. Ista, L.K., V.H. Perez-Luna, and G.P. Lopez, *Surface-grafted, environmentally sensitive polymers for biofilm release.* Applied and Environmental Microbiology, 1999. **65**(4): p. 1603-1609.

131. Alarcon, C.D.L., et al., *Grafted thermo- and pH responsive co-polymers: Surface-properties and bacterial adsorption.* International Journal of Pharmaceutics, 2005. **295**(1-2): p. 77-91.

132. Champ, S., W. Xue, and M.B. Huglin, *Concentrating aqueous dispersions of Staphylococcus Epidermidis bacteria by swelling of thermosensitive poly [(N-isopropylacrylamide)-co-(acrylic acid)] hydrogels.* Macromolecular Chemistry and Physics, 2000. **201**(17): p. 2505-2509.

133. Ichikawa, A., et al., *In situ formation of a gel microbead for indirect laser micromanipulation of microorganisms.* Applied Physics Letters, 2005. **87**(19).

134. Furukawa, H., et al., *Affinity selection of target cells from cell surface displayed libraries: a novel procedure using thermo-responsive magnetic nanoparticles.* Applied Microbiology and Biotechnology, 2003. **62**(5-6): p. 478-483.

135. Galaev, I.Y., et al., *Effect of matrix elasticity on affinity binding and release of bioparticles. Elution of bound cells by temperature-induced shrinkage of the smart macroporous hydrogel.* Langmuir, 2007. **23**(1): p. 35-40.

136. Kiss, L., et al., *Kinetic analysis of the toxicity of pharmaceutical excipients cremophor EL and RH40 on endothelial and epithelial cells.* J Pharm Sci, 2013.

137. Szabo, S., et al., *Cellular approach to cytoprotection - conditional or no protection by prostaglandins (PG) and sulfhydryls (SH) against ethanol-induced or HCL-induced injury to isolated mucous, parietal and chief cells and cultured endothelial-cells.* Gastroenterology, 1988. **94**(5): p. A451.

138. Szabo, S., et al., *Protection by prostaglandins (PG) and sulfhydryls (SH) against ethanol-induced endothelial injury in vitro and in vivo.* Gastroenterology 1987. **92**: p. A381.

139. Gunnewiek, M.K., et al., *Controlled surface initiated polymerization of N-isopropylacrylamide from polycaprolactone substrates for regulating cell attachment and detachment.* Israel Journal of Chemistry, 2012. **52**(3-4): p. 339-346.

140. Ke, Z., et al., *Thermoresponsive surface prepared by atom transfer radical polymerization directly from poly(vinylidene fluoride) for control of cell adhesion and detachment.* Journal of Applied Polymer Science, 2010. **115**(2): p. 976-980.

141. Kim, D.J., et al., *Formation of thermoresponsive surfaces by surface-initiated, aqueous atom-transfer radical polymerization of N-isopropylacrylamide: Application to cell culture.* Bulletin of the Korean Chemical Society, 2004. **25**(11): p. 1629-1630.

142. Li, L., J. Wu, and C. Gao, *Gradient immobilization of a cell adhesion RGD peptide on thermal responsive surface for regulating cell adhesion and detachment.* Colloids and Surfaces B-Biointerfaces, 2011. **85**(1): p. 12-18.

143. Li, L., et al., *Fabrication of thermoresponsive polymer gradients for study of cell adhesion and detachment.* Langmuir, 2008. **24**(23): p. 13632-13639.

144. Mizutani, A., et al., *Preparation of thermoresponsive polymer brush surfaces and their interaction with cells.* Biomaterials, 2008. **29**(13): p. 2073-2081.

145. Nagase, K., et al., *Dynamically cell separating thermo-functional biointerfaces with densely packed polymer brushes.* Journal of Materials Chemistry, 2012. **22**(37): p. 19514-19522.

146. Tamura, A., et al., *Simultaneous enhancement of cell proliferation and thermally induced harvest efficiency based on temperature-responsive cationic copolymer-grafted microcarriers.* Biomacromolecules, 2012. **13**(6): p. 1765-1773.

147. Sui, X., et al., *Stability and cell adhesion properties of poly(N-isopropylacrylamide) brushes with variable grafting densities.* Australian Journal of Chemistry, 2011. **64**(9): p. 1259-1266.

148. Xu, F.J., et al., *Thermoresponsive poly(N-isopropyl acrylamide)-grafted polycaprolactone films with surface immobilization of collagen.* Colloids and Surfaces B-Biointerfaces, 2011. **85**(1): p. 40-47.

149. Zhang, C., et al., *Surface chemical immobilization of parylene C with thermosensitive block copolymer brushes based on N-isopropylacrylamide and N-tert-butylacrylamide: Synthesis, characterization, and cell adhesion/detachment.* Journal of Biomedical Materials Research Part B-Applied Biomaterials, 2012. **100B**(1): p. 217-229.

150. Nagase, K., et al., *Thermo-responsive polymer brushes as intelligent biointerfaces: Preparation via ATRP and characterization.* Macromolecular Bioscience, 2011. **11**(3): p. 400-409.

151. Yonetani, T. and G.S. Ray, *Studies on cytochrome oxidase. 6. Kinetics of aerobic oxidation of ferrocytochrome c by cytochrome oxidase.* Journal of Biological Chemistry, 1965. **240**(8): p. 3392-&.

152. Palmieri, F. and Klingenb.M, *Inhibition of respiration under control of azide uptake by mitochondria.* European Journal of Biochemistry, 1967. **1**(4): p. 439-&.

153. Ottaviani, M.F., et al., *Phase separation of poly(N-isopropylacrylamide) in mixtures of water and methanol: A spectroscopic study of the phase-transition process with a polymer tagged with a fluorescent dye and a spin label.* Helvetica Chimica Acta, 2001. **84**(9): p. 2476-2492.

154. Matsumura, Y. and K. Iwai, *Synthesis and thermo-responsive behavior of fluorescent labeled microgel particles based on poly(N-isopropylacrylamide) and its related polymers.* Polymer, 2005. **46**(23): p. 10027-10034.

155. Matsumura, Y. and A. Katoh, *Synthesis of 2,3-dimorpholino-6-aminoquinoxaline derivatives and application to a new intramolecular fluorescent probe.* Journal of Luminescence, 2008. **128**(4): p. 625-630.

156. Laurenti, M., et al., *Interpenetrated PNIPAM-Polythiophene Microgels for Nitro Aromatic Compound Detection.* Langmuir, 2009. **25**(16): p. 9579-9584.

157. Morgan, J.R., et al., *A role for talin in presynaptic function.* Journal of Cell Biology, 2004. **167**(1): p. 43-50.

158. Shiroyanagi, Y., et al., *Transplantable urothelial cell sheets harvested noninvasively from temperature-responsive culture surfaces by reducing temperature.* Tissue Eng., 2003. **9**(5): p. 1005-1012.

159. Sumide, T., et al., *Functional human corneal endothelial cell sheets harvested from temperature-responsive culture surfaces.* Faseb Journal, 2005. **19**(14): p. 392-+.

160. Canavan, H.E., et al., *A plasma-deposited surface for cell sheet engineering: Advantages over mechanical dissociation of cells.* Plasma Processes and Polymers, 2006. **3**(6-7): p. 516–523.